Developing a tool set to investigate antimicrobial mode of action in a phytopathogen

André Soibelmann Glock Lorenzoni

university of groningen

Developing a tool set to investigate antimicrobial mode of action in a phytopathogen

Phd thesis

to obtain the degree of PhD at the
University of Groningen
on the authority of the
Rector Magnificus prof. E. Sterken
and in accordance with
the decision by the College of Deans.

This thesis will be defended in public on

Monday 25 February 2019 at 11.00 hours

by

André Soibelmann Glock Lorenzoni

born on 18 July 1990
in Porto Alegre, RS, Brazil

Research was funded by:
NWO grant 729.004.005
CNPq grant 246986/2013-1
University of Groningen
GBB.

Cover: Stephanie D. Jurburg
Layout: Lovebird design.
www.lovebird-design.com

Printing: Eikon +

ISBN (print): 978-94-034-1424-9

Supervisors

Prof. D.J. Scheffers
Prof. A.J.M. Driessen

Assessment Committee

Prof. J. Kok
Prof. I.J. van der Klei
Prof. L. Hamoen

Contents

Chapter 1 — Introduction **7**

Chapter 2 — Discovery and investigations on the antimicrobial mode of action of the Au(I) compound 7b-BF_4 **39**

Chapter 3 — Investigations on the mode of action of the antimicrobial compounds BC1 and T9A **65**

Appendix 1 — Investigations on the mode of action of alkyl gallates against *Xanthomonas citri* **89**

Chapter 4 — *Xanthomonas citri* MinC oscillates from pole to pole to ensure proper cell division and shape **97**

Chapter 5 — Summary **127**

Acknowledgments **140**

Chapter 1 — Introduction

André S. G. Lorenzoni and Dirk-Jan Scheffers

Department of Molecular Microbiology, Groningen Biomolecular Sciences and Biotechnology Institute, University of Groningen, Groningen, Netherlands

Abstract

The discovery and use of antibiotics has had a huge impact on human, animal health, and agricultural production, but has come at the expense of the rapid rise of antibiotic resistant bacteria. In agriculture, pathogenic bacteria do not only pose a problem for animals, but also for plant crops. Currently, few substances are available to treat plant infections, and those substances do not generally target specific bacteria. This limitation encourages farmers to use the same substances for extended periods of time and in higher concentrations, stimulating the development of resistance against these substances, resulting in their accumulation in the environment. During the course of evolution, plants, bacteria, and fungi have developed a massive arsenal of antibacterial compounds for their own defenses. Many of these compounds have been shown to target bacterial cell division proteins and/or disrupt the bacterial membrane. In this chapter, the use of some of these natural products and derivatives to control bacterial infections of plants will be discussed, using citrus canker, which impacts on global citriculture, as a model.

1. Introduction

The discovery and use of antibiotics has had a huge impact on human, animal health, and agricultural production, but has come at the expense of the rapid rise of antibiotic resistant bacteria. In agriculture, pathogenic bacteria do not only pose a problem for animals, but also for plant crops. There are three main measures to control plant diseases (*1*). Firstly, one of the most practical and important methods to control diseases is the eradication, or prevention of inoculum. This can be achieved via quarantine, or eradication of contaminated plants (*2*), or destruction of contaminated seeds (*1*), as well as other methods that prevent the causal agent to infect a plant and cause a disease. In the second place, a very effective way of disease managing is the usage of genetically resistant plants. If resistant plants are available this can be a low cost measure of control (*1*). However, the process of developing resistant plants is slow and may take over a decade, additionally, the durability of the resistance is an important aspect and it can only be evaluated retrospectively (*1*). The third measure, that will be the focused of this review, is the chemical control of diseases with antimicrobial agents (*1*). This is usually the alternative adopted when a pathogen is present in a cropping area or in its neighborhood. This has proved to be an effective strategy to control plant diseases, especially when combined with the previous two methods (*3*).

Most antimicrobial compounds discovered so far are natural compounds. The main strategy used to discover new antibiotics during the twentieth century was to screen for natural products with antimicrobial activity (*4*). However, there is an increasing concern of antibiotic resistance and speculations that the antibiotic pipeline is drying out (*5, 6*). Recently, the screens for natural products have been extended using new strategies with the use of improved cultivation methods and (meta-)genome-wide bioinformatics analyses. Nichols *et al.* (*7*) developed an isolation chip that allows to cultivate and isolate previously uncultivable organisms. This chip led to the discovery of Teixobactin (*8*). This compound is able to kill human pathogens such as *Staphylococcus aureus* and *Mycobacterium tuberculosis* and, so far, no resistance development has been detected in a laboratory environment. Teixobactin kills Gram-positive bacteria by binding to the peptidoglycan precursors lipid II and lipid III, a mode of action different from any other antibiotic

currently used to treat infections (8). Hover *et al.* (9) have developed a culture independent approach to prospect antimicrobial compounds, based on the hypothesis that the Asp-X-Asp-Gly calcium-binding motif is an indicative of bacterial encoded antibiotics with diverse mode of actions. Using degenerate PCR primers to amplify bacterial gene clusters encoding calcium binding motifs from environmental DNA, clusters were amplified, further identified and sequenced, and selected gene clusters were inserted in a host to express the genetic product (9). This approach led to the discovery of Malacidin A, which is active against Gram-positive organisms by binding to lipid II precursors in a calcium dependent manner (9).

Despite the recent discoveries of drugs targeting Gram-positive bacteria, no new class of antibiotics against Gram-negatives has been identified since 1968, when quinolones were introduced (10). There have been trials to repurpose or to modify drugs in order to target Gram-negative bacteria, though none of them resulted in a viable antimicrobial yet (11, 12). Drugs targeting gram negative bacteria are considered the highest priority for research according to the World Health Organization (13), and as will be discussed in the next section, the most important bacterial plant infections are caused by Gram-negative organisms, such as citrus canker, fire blight, bacterial speck of tomato, bacterial wilt of tobacco, and bacterial rice blight (14).

2. Important bacterial plant pathogens and control measures

2.1. *Pseudomonas syringae*

There are several *Pseudomonas syringae* pathovars, that combined are among the most important bacterial plant pathogens (14). With a few specific exceptions, such as kiwifruit, hazelnut and stone fruits, there are no economic data on crop loss caused by *P. syringae* (3). *P. syringae* species includes over 30 pathovars classified according to their different hosts, while *P. syringae* pv. *syringae* is often used to describe strains with a broader host range (15).

The three main measures to control plant diseases are applied in the control of *P. syringae (3)*. Contaminated seeds are one of the main means of spreading the bacteria, and limiting the circulation of contaminated

seeds or the treatment of seeds with antibiotics such as streptomycin, kasugamycin, and oxytetracycline can reduce the disease caused by *P. syringae (16–18)*. Induction of systemic acquired resistance is also a practice that can be used to control infections by *P. syringae*. In this case a compound induces the plant to produce an immune response that renders the plant resistant to the pathogen. Salicylic acid is a common inducer for systemic acquired resistance and can be used against *P. syringae* strains, including copper resistant ones (19, 20).

P. syringae pathovars *phaseolicola* and *tomato* were among the firsts organisms to have their virulence genes cloned, opening up the research in molecular biology of virulence over 30 years ago (21).

2.2. *Erwinia amylovora*

Erwinia amylovora is the causal agent of fire blight, a disease that affects pear, apple, quince and other rosaceous trees (22, 23). This disease was first reported in North America, already by the end of the of the 18th century (22, 24). About 100 years after its first description, the causative agent was identified as a bacterium, making *Erwinia* the first phytopathogen described (22, 24). Nevertheless, *it* was only fully sequenced in 2010 (25). During the 20th century fire blight spread to New Zeeland, Western Europe, and the Middle East. In areas where the pathogen has not been detected, such as Japan and Australia, quarantine and eradication methods are used to prevent the introduction of the pathogen (24). In areas where the pathogen is endemic there are several approaches to control the disease.

Streptomycin, oxytetracycline, and copper are used in North America to prevent or reduce the disease in infected plants (26). However, those measures are faced with criticism since use of antibiotics contributes to the emergence of resistance against this compounds (26, 27). *E. amylovora* infects blossoming trees, and managing the disease at this stage is crucial to prevent large amounts of inoculum spreading to other trees via bees or rain (28, 29). Once the bacteria are present in the blossom they can undergo up to 10 doublings a day in favorable temperature conditions. During the blossom blight phase sprays with streptomycin and oxytetracycline are most effective (28). At this stage the disease can also be managed through pruning of infected parts (28, 30). However, the pruning tools are also a vector via which the bacteria can spread,

therefore they should be dipped in bleach or ethanol solutions during the process (30).

Combining different methods in the management of the disease is also possible. *Pseudomonas fluorescens* strain *A506* is available as an antagonistic strain to help control fire blight, this strain is resistant against streptomycin and oxytetracycline and is able to reduce fire blight infection when applied before E. *amylovora* is detected (31). Trees with limited sensitivity to the pathogen are available, but the commercial cultivation of those trees is limited by fruit quality and storability (32).

2.3. Xanthomonads

The genus *Xantohomonas* includes species that infects nearly all major groups of higher plants. The economic importance of this disease varies from very destructive to negligible (33). The genus has a remarkable host diversity and a contrasting phenotypic uniformity, that have led to numerous discussions over the nomenclature of its members (34, 35). Here we will briefly mention some of the most important pathovars, and use *Xanthomonas citri* subsp. *citri* as a model for the remainder of this review.

One of the most destructive pathogens in this genus is *Xanthomonas oryzae* pv. *oryzae*, the causal agent of bacterial blight of rice, one of the most important diseases of rice (36). Unlike *E. amylovora* and *P. syringae, X. orizae pv. oryzae* cannot be efficiently managed with copper or antibiotics (36). This is maybe because the pathogen is highly variable in terms of sensitivity to those compounds (36). Using resistant cultivars of rice has been the major method to manage the disease (36).

Xanthomonas axonopodis pv. *manihotis* is the causal agent of the bacterial blight of cassava, the staple food of nearly 600 million people (14, 37). This disease is mostly managed with inoculum prevention and eradication of contaminated crops (38). Resistant strains are also a possibility, and they are more effective when combined with culturing practices. When cassava is planted before a rainy season the conditions are more favorable to the pathogen. However, if the plants starts to grow in a dryer season, the growth is slower and plants accumulate more pectin and cellulose, and become more resistant to bacterial blight (37).

Xanthomonas citri subsp. *citri* (Xac), previously known as *X. axonopodis* pv. *citri* and *X. campestris* pv. *citri* (39, 40), can infect nearly all citrus

Figure 1: *Xanthomonas citri* subsp. *citri* on citrus plant (Rio Claro, Brazil, 2016).

species and is a major threat to the orange industry (2). Xac causes citrus canker, and the most effective way to control the disease is to eradicate infected trees. However, since the pathogen can infect the trees before being detected and is very difficult to detect all infected trees in a given area (41), an effective eradication requires all the trees in a radius of 30m from the infected tree to be eradicated as well, or the cutting of the entire block when the incidence of infection is over a 0.5% (42). Despite being effective in keeping the incidence of citrus canker to less than 1 in 1 million trees in areas under threat (43); the eradication policy in the Brazilian state of São Paulo, the biggest orange producer in the world, led to the cut of 5.4 million between 1999 and 2010, when a strict eradication policy was in effect (F. Behlau, personal communication).

Nowadays, citrus canker in São Paulo is managed by cutting only the symptomatic trees and spraying copper in a radius of at least 30 meters of the infected plant (44). Similar measures were already used in Florida, Argentina and other Brazilian states where citrus canker is endemic and incidence levels are higher (45, 46).

Table 1: Bacterial pathogens, respective diseases, and available field antimicrobials.

Pathogen	Disease (affected plants)	Antimicrobial compounds
X. citri subsp. *Citri* (Xac)	Citrus Canker (orange, grapefruit and nearly all other citrus species (2))	Copper (46, 47) Streptomycin (51)
X. oryzae pv. *oryzae*	Bacterial blight (rice (36))	Not available[1]
Xanthomonas axonopodis pv. *vesicatoria*	Bacterial spot (tomato (20) and pepper (52))	Copper (52)
P. syringae pv. *syringae*	Bacterial leaf spot (green pumpkin (18)) Blossom blight (kiwifruit (53)) Apical necrosis (mango (54)) Brown spot (snap beans and dry beans (55))	Copper (55) Streptomycin Oxytetracycline (18)
P. syringae pv. phaseolicola	Halo blight (common bean and nearly all *Phaseoleae* plant tribe (16, 56))	Copper Streptomycin (56) Kasugamycin (16)
P. *syringae* pv. *glycinea*	Bacterial blight (soybean (57–59))	Not available[1]
P. *syringae* pv. *tomato*	Bacterial speck (tomato (20))	Copper Streptomycin (20, 60)
E. amylovora	Fire blight (pear, apple, quince, plum, cherry, and other rosaceous trees (23))	Copper Streptomycin Oxytetracycline (26)
Dickeya chrysanthemi	Bacterial Leaf Blight (aglaonema (61))	Copper (61)

[1]To our knowledge there is no viable antimicrobial compound available to control this pathogen in the field.

Copper is the only antimicrobial agent used against Xac in most of areas of citriculture and its widespread use has led to the development of resistant strains in Argentina and the Reunion and Mauritius Islands, France (47, 48). This resistance is mostly plasmid borne, and plasmids can be transferred within different species of the same genus (46, 47), which is alarming considering that copper is probably the most common antimicrobial used in the field to control bacterial phytopathogens (**Table 1**). In addition, whereas antibiotics are inactivated in the soil (49), copper is stable and accumulates. High amounts of copper in the soil have a negative impact on bacterial richness and distribution in the soil (50).

In general, antimicrobial compounds currently used against bacterial phytopathogens are limited to copper, streptomycin, and oxytetracycline.

Against all these compounds, resistance has been reported, requiring that they are used in higher amounts with limited effectivity. Therefore, there is a need for new compounds to control bacterial plant diseases. One way to prevent bacterial species to infect plant hosts is to prevent them to undergo cell division, an essential process for bacterial proliferation and viability. For this reason, we will review in the next section how the cell division machinery, the divisome, works and how it can be a target for novel antimicrobial compounds, using Xac as a model.

3. The divisome and tools available for its study

The divisome is the machinery required for cell division, consisting of many conserved proteins that share little to no homology with eukaryotic proteins and are essential for cell growth, multiplication, and pathogenicity (62). This makes cell division (proteins) a unique target for antimicrobials. Cell division has primarily been studied in *Escherichia coli* and *Bacillus subtilis* (63). However, due to the economic importance of Xac there have been recent efforts to further characterize the divisome in this organism (64–67), that had its genome fully sequenced 16 years ago (68). In this section we will focus on the divisome from Xac. Recent advances made towards the understanding of the divisome of Xac have also resulted in tools that can be used to study the mode of action of antimicrobials.

FtsZ is perhaps the most important piece in the cell division machinery. Present in nearly all bacteria, this protein is a tubulin homologue GTPase that can polymerize to form the so-called Z-ring (63, 69). The Z-ring is a ring like structure, usually assembled at midcell, that constricts the membrane to form 2 daughter cells (63). FtsZ consists of 4 functional regions, a globular tubulin-like core, a C-terminal linker amino acid stretch, a conserved C-terminal tail region of 8 to 9 amino acids, followed by a C-terminal variable region of 4–10 amino acids (69, 70). The globular tubulin-like core contains the active site for GTP hydrolysis and is involved in the formation of dimers and higher order polymers; the C-terminal tail is involved in the interaction with membrane associated proteins of the divisome, that are necessary to anchor the Z-ring in the plasma membrane, such as FtsA and ZipA; the C-terminal variable region mediates lateral interactions between FtsZ polymers; and the C-terminal linker serves as a link between the core

domain and the membrane associated domain and is also essential for the coordination of cell wall synthesis at the division site (*69*, *71*, *72*).

FtsZ from Xac shares over 96% identity with FtsZ from *X. campestris* pv. *campestris* and *X. oryzae* pv. *oryzae*. The differences are in amino acids that constitute the C-terminal linker and amino acid changes in this domain of FtsZ do not cause functional alterations as long as the length remains unchanged (*73*). Therefore it is plausible that inhibitors of Xac FtsZ also inhibit FtsZ from other *Xanthomonads*.

In rod-shaped bacteria, the Z-ring is assembled at midcell, controlled by the so-called Min system. This machinery has been well studied in model organisms such as *E. coli* and *B. subtilis*, but was only recently studied in Xac (*65*). In *E. coli*, the Min system is composed of 3 proteins, MinC, MinD, and MinE (*74*). MinD is recruited to the membrane and forms copolymers with MinC inhibiting FtsZ activity (*75*). MinE forms an oscillating ring that disassembles MinCD copolymers, this dynamic process results in oscillation of the MinCD proteins with a higher concentration of MinCD at the cell poles as a net result. The relative absence of MinCD at midcell allows FtsZ to polymerize and assemble the Z-ring (*75*). In *B. subtilis,* MinE is absent and instead of a dynamic oscillation there is a static gradient of MinCD with again a higher concentration at the cell poles, mediated by DivIVA and MinJ proteins (*75*). Since both DivIVA and MinJ are absent in Xac, we are not going to discuss them in detail in this review.

The divisome is also linked with the chromosome segregation machinery, in order to avoid constriction over the nucleoid, which would result in DNA damage. This ensures that both daughter cells have the same genetic material. This phenomenon is called nucleoid occlusion and is mediated by different proteins in various bacteria, which bind to DNA and use different methods to prevent FtsZ polymerization in their vicinity (*76*). Interestingly, in *E. coli*, the min system also plays a role in chromosome segregation, because MinD binds to DNA and recruits it to the cell poles (*77*). However, this system seem to vary among species and Xac has a chromosome segregation factor absent in *E. coli*, called *parB* (*65*). The function of *parB* was already investigated in *Caulobacter crescentus*, an alphaproteobacteria that does not has a Min system and its divisome localization is controlled by its chromosome segregation machinery (*78*).

In *C. crescentus* ParB acts as a chromosome partitioning protein, it colocalizes with the origin of replication at the cell pole (*78*). During a cell division event, the population of ParB splits and while one part remains static at one pole, the other part moves to the other cell pole together with the nucleoid of the future daughter cell (*78*). Divisome midcell positioning is mediated by MipZ, a protein that interacts with ParB and inhibits FtsZ activity, which avoids constriction over a nucleoid and drives the Z-ring to midcell (*78*). Xac is somewhere 'in the middle' between *E. coli* and *C. crescentus,* as it both possesses a Min system composed of MinCDE, as well as ParB.

3.1. Chromosome segregation and the development of genetic tools in Xac

15 years ago, shortly after the genome was sequenced, open reading frames of Xac were expressed in *E. coli* for structural proteomic studies (*79*). A protocol for protein fingerprinting by 2-D gel electrophoresis and RNA expression assays was developed as well (*67*). The negative impact Xac causes on citrus economy stimulated further interest in studying Xac chromosome segregation and cell division, since they are nice targets for antimicrobials (*80*). Martins *et al. (80)* developed an expression system in Xac that lead to the characterization of FtsZ-stabilizing factor ZapA, originally identified in *B. subtilis* (*81*). Xac *zapA* was fused with *gfp* and integrated in the α-amylase gene (*amy*) of Xac. The disruption of *amy* impaired Xac ability to degrade starch, but did not alter pathogenicity, making it possible to use this locus for other genetic integrations to study their effect on Xac biology and pathogenicity (*80*).

Ucci *et al.* (*65*) used this expression system to express an open reading frame encoding for a *parB* homologue in Xac, initially in amy under control of a xylose-inducible promoter. Later they investigated ParB function in Xac by expressing the fusion ParB-GFP under the control of its native promoter. They observed a polar localization of ParB-GFP, and time lapse fluorescent microscopy observations showed that the ParB-GFP signal splits and one of them moves to the other pole of the cell before cellular constriction, in an asymmetric manner. Simultaneous DNA staining with 4′,6-diamidino-2-phenylindole (DAPI, DNA binding fluorophore) revealed that ParB-GFP colocalizes with the edges of nucleoids and is directly involved in chromosome segregation in Xac, in a

similar manner exhibited by *C. crescentus* (*65*, *82*). Although parB could not be deleted directly (*65*), a later study showed that it was possible to delete *parB* gene after introduction of a separate copy *of* parB under control of the arabinose promoter (*83*). Subsequent depletion of ParB revealed that the lack of *parB* caused a retardation in cell division, but there were no increase in filaments or anucleate cells, and the strain was still able to colonize citrus leaves (*83*).

3.1.1. Xac Min system and cell wall synthesis

Xac possesses a full complement of the Min system, consisting of the MinCDE proteins. We have recently investigated this system by inactivating out the *minC* gene and also expressing and visualizing GFP-MinC integrated in the *amy* locus of the genome (*64*). This showed that, as in other bacteria that contain MinE, MinC oscillates (*64*, *84*). The deletion of *minC* did not disrupt the ability of Xac to infect citrus, but resulted in a branching phenotype depending on the growth medium used and most likely linked to gluconeogenic growth. Fluorescent D-amino acid analogues that label sites of peptidoglycan synthesis (*85*, *86*), allowed us to further study the cell growth and branching of Xac. Xac exhibits a peptidoglycan incorporation pattern similar to the one observed for *E. coli* (*64*, *85*), with strong synthesis at cell division sites, which was correlated with GFP-ZapA fluorescence. This correlation was lost when *minC* was deleted (*64*).

3.1.2. Fluorescent reporters as tools to study Xac division inhibitors

The observations of subcellular localization of GFP fusions and/or fluorophores enables to not only expand the knowledge available about cell biology of organisms but also to use those tools to investigate the mode of action of antimicrobial compounds. The expression system developed by Martins *et al. (80)* was also used in the characterization of virulence genes in Xac (*87*). Liu *et al. (88)* inserted another expression system in Xac to express enhanced green fluorescent protein (EGFP) in order to visualize the propagation and localization of Xac *in planta.*

The Xac strain expressing GFP-ZapA was used as a reporter strain when investigating alkyl gallates, this compounds have been used as food additives (*89*), but also showed antimicrobial activity with

potential inhibitory effect on cell division (*11*). Xac expressing GFP-ZapA exhibits a clear midcell localization that can be easily detected with fluorescent light microscopy, alterations in this localization pattern are an indication of cell division disruption. However, it is also important to point out that the subcellular localization pattern can be disrupted by membrane potential (*90*) or other artifacts (*91*) leading to false positives. Recently, the same strain has been used to study the effects of acetylated alkyl gallates (*92*) and other antimicrobials (**Chapter 3**) on Xac cell division.

3.2. Xac FtsZ as a target for antimicrobials

FtsZ is the most researched cell division protein as a target for antimicrobials as inhibition of FtsZ would effectively block division (*93*). There is only one substance discovered so far that has been shown to inhibit cell division directly without interacting with FtsZ (*94*). Thus, nearly all cell division inhibitors can be characterized with FtsZ assays *in vitro*, and most reviews about cell division inhibitors focus largely on FtsZ inhibitors (*95–97*).

In Xac, the disruption of GFP-ZapA rings by various antimicrobials suggested that these compounds interfere with FtsZ function. Initially, the effect of alkyl gallates on cell division was further investigated with assays using the cell division protein FtsZ from *B. subtilis (98)*. Alkyl gallates have antimicrobial activity against gram positives and selective activity on gram negatives, being ineffective against *E. coli* and *Pseudomonas aeruginosa*, but effective against *Salmonella choleraesuis* and Xac (*11*, *99*). FtsZ from *B. subtilis* can be investigated *in vitro* using sedimentation, light scattering, and GTP hydrolysis assays (*100*). This way Król *et al. (98)* could show that FtsZ is a direct target of alkyl gallates, that some of the alkyl gallates bind to FtsZ with high affinity and inhibit GTPase and polymerization activity. However, the alkyl gallates also have a membrane permeabilizing activity which could already disrupt subcellular localization of some cell division proteins (*90*, *98*).

FtsZ from Xac is poorly characterized. To our knowledge, there has been one report on expression and purification of FtsZ from Xac, using a C-terminal his tag (*101*), and one report on FtsZ from *X. oryzae* pv. *oryzae*, also with C-terminal his tag (*102*). Activity of C-terminally his-tagged Xac FtsZ was only characterized using light scattering at

350nm as a measure for polymerization (*101*), whereas *X. oryzae* FtsZ activity was only determined using a GTP hydrolysis assay (*102*). This, combined with the effects that buffers have on FtsZ behavior, makes it impossible to compare the results for these two FtsZs which share 97% sequence identity. Interestingly, Ha *et al.* (*101*) designed single stranded DNA aptamers with high binding affinity for Xac FtsZ. The aptamers showed a higher affinity for FtsZ from Xac than for FtsZ from *B. anthracis*, and they were able to inactivate 50% of cells (MIC_{50}) with about 115µM (*101*). However, there are no data about whether those aptamers could prevent or treat Xac infections *in planta*, or whether they had selective antimicrobial activity *in vivo* (*101*).

In our lab we have purified native FtsZ from Xac (*103*). Below we discus methods to study FtsZ and their applicability to Xac FtsZ.

3.3. FtsZ assays *in vitro* and caveats

FtsZ activity can be measured by either monitoring GTP hydrolysis, which is linked to FtsZ polymerization, or by measuring FtsZ polymerization and depolymerization (*100, 104*). Other assays done with FtsZ involve protein-protein interactions (*100, 105*).

3.3.1. GTPase assay:

The GTPase activity of FtsZ was first detected using radiolabelled GTP (*106, 107*), which has since been replaced by a malachite green-phosphomolybdate assay, which provided an easier way to detect phosphate release as a measure of GTP hydrolysis (*108*). Various buffer conditions have been used for FtsZ GTPase measurements in the literature, which is important as buffer composition strongly influences FtsZ activity (*98, 100, 106–109*). The GTP hydrolysis can also be tested indirectly in an enzyme coupled assay using lactate dehydrogenase and pyruvate kinase (*110*). This system regenerates GTP from GDP while consuming NADH which is measured via absorbance at 340nm (*109, 110*). This method reduces the effects of GTP depletion and GDP accumulation on the rate of reaction and enables an easy detection of GTPase activity (*109, 110*).

Compound-induced, aspecific, protein aggregation is a problem when screening for inhibitors. Feng *et al.* (*111*) randomly selected 298 molecules and shown that 19% of them shown an inhibitory effect

on β-lactamase at 30µM. For all these molecules the inhibitory effect was attenuated in the presence of 0.1% Triton X-100 (Tx100) (*111*). This means these compounds are not specific inhibitors of β-lactamase but rather cause the protein to aggregate, leading to a false positive result in a β-lactamase inhibition test (*111*). Feng & Shoichet (*112*) suggested the addition of 0.01% Tx100 to detect false positives in screenings. The lower concentration of Tx100 is better tolerated by the enzyme, while it still counters protein aggregation. Anderson *et al.* (*109*) tested the effect of the addition of 0.01% triton X-100 in FtsZ GTPase assays, in combination with the previously reported FtsZ inhibitors totarol (*113*), zantrin Z1 and zantrin Z3 (*108*), dichamanetin (*114*), and PC190723 (*115*). This showed that totarol, dichamanetin and zantrin Z1 no longer inhibited FtsZ GTPase activity in the presence of 0.01% triton X-100, indicating that the inhibitory effect is likely to be caused by the formation of aggregates (*109*). In fact, when when FtsZ incubated with totarol was previously centrifuged before the assay and supernatant was used, no activity was observed (*109*). Zantrin Z3 inhibits GTPase activity of FtsZ and its activity was not changed in the presence of triton X-100 (*109*). PC190723 was reported to inhibit FtsZ GTPase activity, and that FtsZ is a target for PC190723 was evident from the fact that PC190723 resistant mutants exclusively mapped as point mutations in *ftsZ* (*115*). Anderson *et al.* (*109*) found no inhibition of PC190723 in *Staphylococcus aureus* FtsZ, but rather an increased GTPase activity caused by PC190723. An increase in GTPase activity caused by PC190723 was also observed by Elsen *et al.* (*116*).

We have purified native Xac and detected a consistent GTP turnover independent of Xac FtsZ concentration — which was striking as normally GTP hydrolysis only starts when the FtsZ concentration has reached a certain threshold. Both the malachite green and the coupled GTP regeneration assay work with Xac FtsZ. These assays allowed us to study the effect of alkyl-gallates on Xac FtsZ. Strikingly, the effect of these compounds was much less than what we previously observed with *B. subtilis* FtsZ.

3.3.2. Polymerization assays

Whereas GTPase activity is used as a proxy for polymerization, direct detection of polymers is possible using:

- Sedimentation assays, where polymers (in a similar buffer system as used for the GTPase assay) are recovered by ultracentrifugation, and subsequently detected by SDS-PAGE (sodium dodecyl sulfate polyacrylamide gel electrophoresis) (*100*). Król *et al. (98)* showed that alkyl gallates stimulate *B. subtilis* FtsZ sedimentation and inhibit FtsZ GTPase activity.
- Transmission electron microscopy (*117, 118*). Polymers can be formed under the same conditions used for sedimentation assay, followed by negative staining with uranyl acetate and visualization (*98, 117, 118*). Electron microscopy enables the characterization of polymer shape and geometry, and the effect that regulatory proteins or antimicrobial substances might have on them, such as the bundling of polymers (*98, 119, 120*). Although many studies have been done with polymers formed in vitro, also in reconstituted vesicle systems, FtsZ polymerization in the cytoplasm cannot be observed with negative staining due to the crowded and granular nature of the cytosolic environment (*121*). However, the development of cryo-electron tomography for imaging of structures in bacteria has allowed the visualization of FtsZ polymers in the Z-ring (*122*).
- Light scattering, which is a convenient and nondestructive assay that enables the tracking of FtsZ polymerization and depolymerization in real time (*100, 117, 123*). FtsZ from *E. coli* readily polymerizes reaching a steady state phase proportional to the GTP concentration (*123*). In the presence of a GTP regeneration system like the one used for enzyme coupled GTPase assay, FtsZ polymers can remain stable for up to 85 min (*124*). Usually light scattering of FtsZ polymers is measured at a 90° angle in a fluorescence spectrophotometer with emission and excitation at 350 nm (*100, 123*).

None of these methods, however, is suitable for medium or high-throughput assays, but can render useful information on the nature of the polymers. We have tried all methods for Xac FtsZ and found that this protein has unique polymerization properties: Xac FtsZ already sediments when a divalent cation is added, independent of whether a nucleotide is used or not, and polymer detection using light scattering proved impossible (*103*). Detection of polymers by electron microscopy showed that Xac FTsZ forms short polymers that seem to bundle more in the presence of nucleotide. Our conclusion was that polymerization

methods are not useful when testing potential inhibitors of Xac FtsZ, but that GTP hydrolysis is reliable and quantitative.

3.3.3. Other FtsZ assays

There are other assays developed to study FtsZ, primarily by the Erickson lab. **Isothermal titration calorimetry** has been used (*125*) to measure affinity parameters between FtsZ and the nucleotides. FtsZ, labeled with separate pools of fluorescein and tetramethylrhodamine, has been used to measure **Förster resonance energy transfer (FRET)** during FtsZ polymerization (*126*), which confirmed previous results that showed FtsZ cannot assemble below a critical concentration. In addition, a second critical concentration was observed, at which FtsZ can assemble in the absence of GTP (*126*).

3.4. Divisome inhibitors with targets other than FtsZ

Divin is the only antimicrobial substance so far identified that inhibits cell division directly without interacting with FtsZ (*94*). Divin chelates iron and downregulates the expression of cell division genes (*127*). This results in the affected cells to become arrested at a late stage of division, and similar results were obtained using other iron chelators (*127*). Divin did not alter chromosome function, ruling out the possibility of indirect divisome inhibition, but also did not bind to or change the GTPase activity of FtsZ, but did cause dissociation of late division proteins in the divisome (*94*).

Research on cell biology and antimicrobials are complementary, and developments in one field contribute in the development of the other one. Divin is not only an antimicrobial but also a chemical probe to study cell division dynamics (*94*). It can be used to characterize new division proteins because it prevents association of late division proteins without affecting early division proteins, its reversible bacteriostatic activity can be used to synchronize *E. coli* cells, and it can be used to observe FtsZ structures with cryo-electron microscopy (*94*).

3.5. Other potential divisome targets

FtsA is an essential protein in the *E. coli (128)* and *Pseudomonas aeruginosa* (*129*), it is not essential in *B. subtilis*, but its deletion impaired growth and prevented sporulation (*130*). FtsA is also present in Xac,

but we do not know whether it is an essential protein. Moreover, FtsA is conserved among bacterial species and absent in eukaryotic cells, fulfilling an important feature of a potential target (*129*). Paradis-Bleau *et al.* (*129*) used phage display to develop peptides inhibiting FtsA activity, those peptides could inhibit 50 percent of ATPase activity, when used in concentrations from 0.7 mM. However, they showed no data about inhibition of cell growth *in vivo* (*129*). FtsA is an ATPase and this activity was detected *in vitro* using [γ-^{32}P]-ATP and monitoring ^{32}phosphate release in a similar manner used for GTPase activity of FtsZ (*131*). This technique was already applied for FtsA from *B. subtilis* (*131*) and *P. aeruginosa (129)*.

The proteins of the complex FtsQBL are also an essential and important constituent of the divisome, and have been indicated as potential target for antimicrobials (*97, 132*). Those proteins are particularly attractive as targets to block cell division because they have periplasmic domains, thus being exposed to inhibitors that does not necessarily need to penetrate through the inner membrane to be effective (*133*). In *E. coli* FtsB associates with FtsL and forms a complex that binds to FtsQ, consequently being recruited to the divisome (*132*). In *B. subtilis* the homologues of FtsQ and FtsB are named DivIB and DivIC respectively, and DivIC and FtsL are essential (*134, 135*).

FtsN is another essential divisome protein considered a potential target for antimicrobials (*97, 136*). This protein is present in *E. coli*, *Shigella* spp., and *Salmonella* spp., and an inhibitor to this protein would probably be of narrow spectrum (*97*). Moreover, since this gene is absent in *Pseudomonas* spp. (*97*) and Xac, it cannot be considered a potential target for the development of field antimicrobials.

To our knowledge, no inhibitors that directly target FtsB, FtsQ, FtsL, or FtsN have been reported so far.

3.6. Assays to detect inhibitors with targets other than the divisome

A quick and easy assay to screen for cell division inhibitors is to look at cells using phase contrast microscopy — a cell division inhibitor will result in elongated, filamentous cells (*11, 115, 137*). However, cell elongation can be induced by other antimicrobials such as the DNA synthesis inhibitors ciprofloxacin or norfloxacin (*138*), or βlactams (*139*). In this

section, assays to detect other ways of inhibiting bacterial growth will be discussed. At the end of this section a flowchart for investigations on for investigations on the mode of action of antimicrobial compounds is presented **Figure 3**.

3.6.1. Macromolecular (DNA, RNA, cell wall and protein) synthesis pathway

The majority of antibiotics affects either one of the 4 major macromolecular synthesis pathways. A classical approach to establish inhibition of macromolecular synthesis is to incubate cells in the presence of the compound whose antimicrobial activity is meant to be tested and a radioactively labeled precursor (thymidine for DNA, uridine for RNA, glucosamine for cell wall or an amino acid such as leucine for protein) of each of the four metabolic pathways (*140*). After a growth period, during which the precursor can be incorporated in a respective macromolecule, cellular material is precipitated with trichloroacetic acid and quantified for radiation. The effect on the incorporation can be compared to cells incubated without compounds or with known inhibitors of each pathway.

This is perhaps the most widely used method throughout the antimicrobial discovery community (*141*). However, this test has a few drawbacks. This test is relatively slow, and it suffers from low resolution, accuracy, and throughput. The test cannot identify different inhibitors that target different parts of the same metabolic pathway, and some compounds that rapidly inactivate cells such as nisin, bleach, and 7b-BF_4 (**Chapter 2**) affect all the metabolic pathways will thus result in a non-specific output (*141*).

3.6.2. Membrane permeability

A few antibiotics that do not (directly) target the four macromolecular pathways mentioned above have action against the bacterial membrane, such as polymixins, paenibacterin, and daptomycin, which all create membrane pores (*142–144*). The formation of pores in the cytoplasmic membrane can be tested using two fluorescent DNA stains, one of which, SYTO 9, is membrane permeable, and one of which, propidium iodide, is membrane impermeable (probe of the 'Live/dead Baclight viability kit'). In case of pore formation the membrane becomes permeable

to propidium iodide which will stain the cell in red and also quench the SYTO 9 fluorescence reducing the green intensity, whereas impermeable cells are stained only by SYTO 9 exhibiting green signal (*145*).

3.6.3. Membrane potential

Some compounds, such as CCCP, do not form large pores in the membrane but do dissipate the membrane potential by enabling the exchange of protons over the membrane. The membrane potential can be monitored using the fluorescent dye $DiSC_3$ (3,3'dipropylthiadicarbocyanine iodide). This fluorophore inserts into polarized membranes upon which fluorescence is quenched. Loss of membrane potential results in the release of the dye from membranes and thus an increase in fluorescence (*146*).

3.6.4. Intracellular ATP concentration

In 2013, Bedaquiline, a new class of antibiotic, was approved after an almost 40 years gap in the discovery of drugs with a new mode of action (the last one was rifampicin, approved for use in 1974) (*147*). Bedaquiline targets ATP synthase in mycobacteria reducing intracellular ATP concentration leading to cell death (*148*). ATP can be measured using a bioluminescence assay measuring light output of the reaction between luciferin and ATP after cell lysis.

3.6.5. Use of reporter strains and morphological observations

There are a number of reporter strains that would indicate a specific effect targeting the bacterial cell. The strong aspect of this technique is the fact that strains submitted to the right conditions will report a specific mode of action happening on the cell. However, this method requires the access to a particular strain or cloning, and they will only yield an useful result if the mode of action is the same that the one the strain is designed to report.

The *B. subtilis* strain with a fluorescent fusion of the 30S ribosomal protein S2 (RpsB) can report the effect of both RNA and protein synthesis inhibitors (*149*). Under ideal growth conditions RpsB localizes away from the nucleoids, protein synthesis inhibitors causes the nucleoids to compact, spreading the fluorescence signal from the cell pole further into the midcell, and when treated with a RNA synthesis inhibitor,

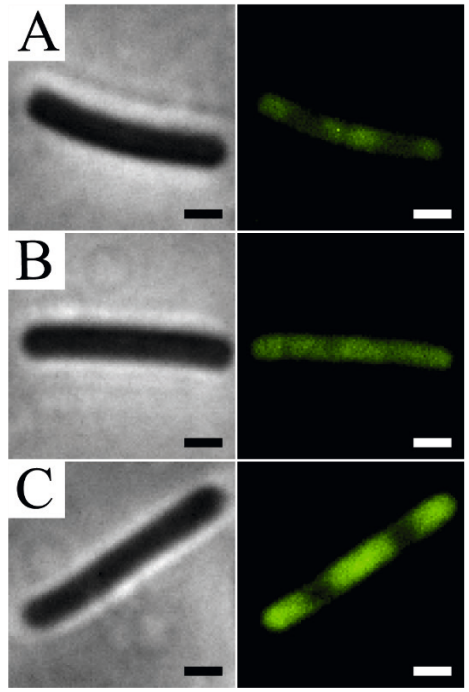

Figure 2: subcellular localization of *B. subtilis* strain 1049 (*151*) expressing with RpsB-GFP: **A** untreated, **B** treated with the RNA synthesis inhibitor 7b-BF_4, **C** treated with the protein synthesis inhibitor tetracycline**.**

intracellular localization is lost and a diffuse structure can be seen (**Figure 2**). There are a number of other fluorescent fusion proteins expressed in *B. subtilis* to report different mode of actions, such as MinD, MinC, and FtsA that can report loss in membrane potential since their localization pattern is loss when the membrane potential is dissipated (*90*). The division site regulation protein DivIVA in *B. subtilis* exhibit a solid and clear localization pattern under most conditions, including the loss of membrane potential (*90*), and is a reporter for membrane fluidity alterations (*150*).

Another series of reporter *B. subtilis* strains are based on the fusion of the *lacZ* or firefly luciferase gene with promoters known to be expressed under specific antibiotic stress conditions (*152–154*). The expression of firefly luciferase gene generates a light signal in the presence of

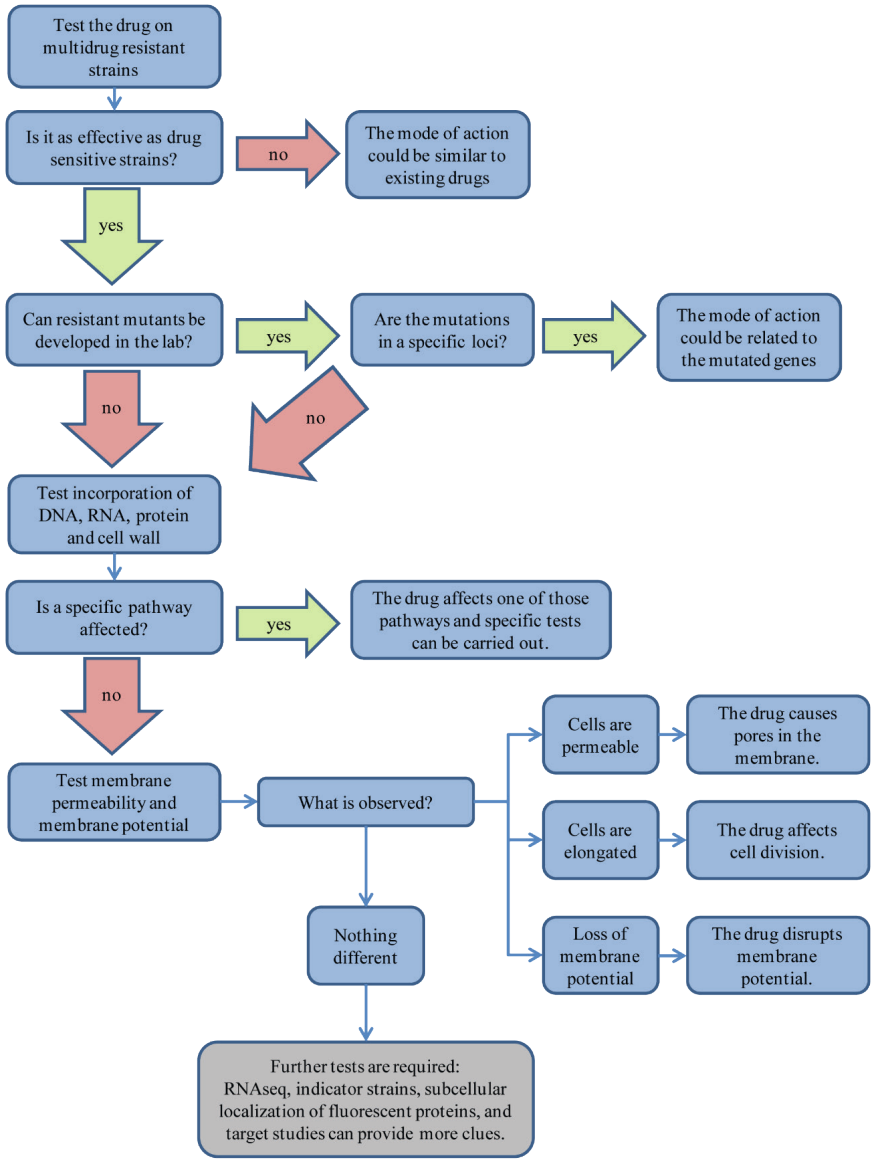

Figure 3: flowchart for investigations on MOA of antimicrobial compounds.

luciferin (*152*), and the expression of *lacZ* can be detected by measuring β-galactosidase activity (*154*) or by viewing a blue color in the presence of X-gal (*153*). The *liaI* promoter is a reporter for cell envelope stress

caused by compounds such as nisin, bacitracin, or vancomycin (*154*). The *yorB* promoter is associated with DNA synthesis, *yvgS* with RNA synthesis, *yheI* with protein synthesis, *ypuA* with cell wall synthesis and cell envelope stress, and the *fabHB* promoter is associated with fatty acid synthesis (*152*).

To tackle the necessity of constructing specific fluorescent protein fusions to make reporter strains for cytological profiling, Lamsa *et al.* (*155*) labelled cells with a combination of the membrane dye FM 4-64, the membrane permeable DNA dye DAPI, and the membrane impermeable DNA dye SYTOX Green. They observed the morphology of *B. subtilis* (*155*) and *E. coli* (*141*) cells in a fluorescence microscope in the presence of different antimicrobial compounds and it was possible to characterize specific changes in morphology depending on the mode of action of the compound. In a further study made a double blind test, with 30 known antimicrobial compounds, in which the tester was able to identify the mode of action of all the compounds by observing the morphological changes under fluorescent light microscopy, using a combination of the 3 dyes mentioned above (*141*).

4. Overview of thesis chapters

The focus of this thesis was initially intended to be a study on the mode of action and delivery of compounds developed to inhibit Xac and thus combat citrus canker. However, research in the field of mode of action of antimicrobials is often complimentary to cell biology research. New techniques developed to understand the function and behavior of microbial proteins can be used to study the mode of action of drugs, and compounds initially designed to be antimicrobials can be used to test the impact of new compounds under specific conditions. Therefore in this thesis we describe investigations on the mode of action of antimicrobial compounds as well as investigations on the cell biology of Xac, the causal agent of citrus canker.

4.1. Chapter 2 — Discovery and investigations on the antimicrobial mode of action of the Au(I) compound 7b-BF_4

This chapter describes the screening for the gold liganded, and similar compounds, for antimicrobial activity. The most active of them, 7b-BF_4,

was selected for investigations on the mode of action, using several techniques described in this introduction. This compound is active against all Gram-positive bacteria tested, including Methicillin Resistant *Staphylococcus aureus* (MRSA) and Vancomycin Resistant *Enterococcus faecium* (VRE), in concentrations varying from 0.4 µg/mL to 3.4 µg/mL. 7b-BF_4 blocks DNA and protein synthesis, but also affects RNA and cell wall synthesis to a lesser extent. 7b-BF_4 doesn't affect membrane permeability or membrane potential. However, it causes a decrease in intracellular ATP and inactivates cells within short periods of time.

4.2. Chapter 3 — Investigations on the mode of action of BC1 and T9A compounds against *Xanthomonas citri* and *Bacillus subtilis*

This chapter describes our investigations to characterize the mode of action of the antimicrobial chalcones BC1 and T9A. Since the chalcones are also effective against Xac, we adapted the techniques previously used to study 7b-BF_4 in *B. subtilis* to study Xac as well. To our knowledge this chapter is the first report of incorporation of radiolabeled precursors of DNA, RNA, protein, and peptidoglycan in Xac. Other techniques used in this chapter were membrane permeability, intracellular ATP concentration, Fourier-transform infrared (FT-IR) spectrophotometry, and observations of GFP fusions to cell division proteins. Since the chalcones caused disruption in the localization of FtsZ-GFP in *B. subtilis*, FtsZ GTPase activity assay was also performed and did not support a direct action on FtsZ. The data produced in this work do not allow us to draw a conclusion about a specific mode of action of the compounds tested and further research is required to understand the mode of action of this compounds in detail.

This chapter is followed by an appendix where our results on the mode of action of alkyl gallates against Xac are reported.

4.3. Chapter 4 — *Xanthomonas citri* MinC oscillates from pole to pole to ensure proper cell division and shape

This chapter presents our findings about the behavior of MinC in Xac cell division, chromosome segregation, and peptidoglycan incorporation. The gene *minC* was deleted using allele exchange. Xac with *minC* deleted exhibited minicells, short filamentation, and branching. The

minC gene was complemented by integrating *gfp-minC* into the *amy* locus. Xac complemented strains displayed a wild-type phenotype. In addition, GFP-MinC oscillated from pole to pole, similar to MinCD oscillations observed in *E. coli* and more recently in *Synechococcus elongatus*. Further investigation of the branching phenotype revealed that in branching cells nucleoid organization, divisome formation and peptidoglycan incorporation were disrupted.

4.4. Chapter 5 — Concluding remarks

This chapter briefly recap the main findings and conclusions of each of the thesis chapters.

5. References

1. R. N. Strange, P. R. Scott, Plant disease: a threat to global food security. *Annual review of phytopathology* **43**, (2005).
2. T. R. Gottwald, J. H. Graham, T. S. Schubert, Citrus canker: the pathogen and its impact. *Plant Health Progress* **10**, (2002).
3. J. R. Lamichhane, A. Messéan, C. E. Morris, Insights into epidemiology and control of diseases of annual plants caused by the Pseudomonas syringae species complex. *Journal of general plant pathology* **81**, 331–350 (2015).
4. S. B. Singh, K. Young, L. Miesel, Screening strategies for discovery of antibacterial natural products. *Expert review of anti-infective therapy* **9**, 589–613 (2011).
5. A. R. Coates, G. Halls, Y. Hu, Novel classes of antibiotics or more of the same? *British journal of pharmacology* **163**, 184–194 (2011).
6. M. Balasegaram *et al.*, A global biomedical R&D fund and mechanism for innovations of public health importance. *PLoS medicine* **12**, e1001831 (2015).
7. D. Nichols *et al.*, Use of ichip for high-throughput in situ cultivation of "uncultivable" microbial species. *Applied and environmental microbiology* **76**, 2445–2450 (2010).
8. L. L. Ling *et al.*, A new antibiotic kills pathogens without detectable resistance. *Nature* **517**, 455–459 (2015).
9. B. M. Hover *et al.*, Culture-independent discovery of the malacidins as calcium-dependent antibiotics with activity against multidrug-resistant Gram-positive pathogens. *Nature microbiology*, 1 (2018).
10. K. Lewis, Platforms for antibiotic discovery. *Nature reviews Drug discovery* **12**, 371 (2013).
11. I. C. Silva *et al.*, Antibacterial activity of alkyl gallates against Xanthomonas citri subsp. citri. *Journal of Bacteriology* **195**, 85–94 (2013).
12. M. F. Richter *et al.*, Predictive compound accumulation rules yield a broad-spectrum antibiotic. *Nature* **545**, 299 (2017).
13. W. H. Organization, Global priority list of antibiotic-resistant bacteria to guide research, discovery, and development of new antibiotics. *Geneva: World Health Organization*, (2017).
14. J. Mansfield *et al.*, Top 10 plant pathogenic bacteria in molecular plant pathology. *Molecular plant pathology* **13**, 614–629 (2012).
15. S. S. Hirano, C. D. Upper, Population biology and epidemiology of Pseudomonas syringae. *Annual review of phytopathology* **28**, 155–177 (1990).
16. J. Taylor, C. Dudley, Seed treatment for the control of halo-blight of beans (Pseudomonas phaseolicola). *Annals of Applied Biology* **85**, 223–232 (1977).
17. J. Taylor, K. PHELPS, C. Dudley, Epidemiology and strategy for the control of halo-blight of beans. *Annals of Applied Biology* **93**, 167–172 (1979).
18. K. S. Park, Y. T. Kim, H. S. Kim, J. S. Cha, K. H. Park, Selection of the antibacterial agents for control against Pseudomonas syringae pv. syringae causing leaf spot disease on green pumpkin (Cucurbita moschata). *The Korean Journal of Pesticide Science* **19**, 119–124 (2015).
19. B. N. Kunkel, A. F. Bent, D. Dahlbeck, R. W. Innes, B. J. Staskawicz, RPS2, an

Arabidopsis disease resistance locus specifying recognition of Pseudomonas syringae strains expressing the avirulence gene avrRpt2. *The Plant Cell* **5**, 865 (1993).
20. F. Louws *et al.*, Field control of bacterial spot and bacterial speck of tomato using a plant activator. *Plant Disease* **85**, 481–488 (2001).
21. J. W. Mansfield, From bacterial avirulence genes to effector functions via the hrp delivery system: an overview of 25 years of progress in our understanding of plant innate immunity. *Molecular plant pathology* **10**, 721–734 (2009).
22. M. Malnoy *et al.*, Fire blight: applied genomic insights of the pathogen and host. *Annual review of phytopathology* **50**, 475–494 (2012).
23. A. D. Martínez-Espinoza, M. Pearce, Fireblight: symptoms, causes, and treatment. (2009).
24. T. Van der Zwet, in *VII International Workshop on Fire Blight 411*. (1995), pp. 7–8.
25. T. H. Smits *et al.*, Complete genome sequence of the fire blight pathogen Erwinia amylovora CFBP 1430 and comparison to other Erwinia spp. *Molecular plant-microbe interactions* **23**, 384–393 (2010).
26. J. Loper *et al.*, Evaluation of streptomycin, oxytetracycline, and copper resistance of Erwinia amylovora isolated from pear orchards in Washington State. *Plant disease* **75**, 287–290 (1991).
27. P. S. McManus, V. O. Stockwell, G. W. Sundin, A. L. Jones, Antibiotic use in plant agriculture. *Annual review of phytopathology* **40**, 443–465 (2002).
28. S. M. Slack, G. W. Sundin, News on Ooze, the Fire Blight Spreader. *Fruit Quarterly* **25**, 9–12 (2017).
29. K. Johnson, V. Stockwell, Management of fire blight: a case study in microbial ecology. *Annual review of phytopathology* **36**, 227–248 (1998).
30. M. A. Draper, R. Burrows, J. Mills, Fire Blight of Apples, Pears, and Other Species. (2003).
31. S. E. Lindow, G. McGourty, R. Elkins, Interactions of antibiotics with Pseudomonas fluorescens strain A506 in the control of fire blight and frost injury to pear. *Phytopathology* **86**, 841–848 (1996).
32. C. Durel, P. Guérif, A. Belouin, M. Le Lezec, in *XI Eucarpia Symposium on Fruit Breeding and Genetics 663*. (2003), pp. 251–256.
33. M. P. Starr, in *The prokaryotes*. (Springer, 1981), pp. 742–763.
34. L. Vauterin, J. Rademaker, J. Swings, Synopsis on the taxonomy of the genus Xanthomonas. *Phytopathology* **90**, 677–682 (2000).
35. J. Jones *et al.*, Systematic analysis of xanthomonads (Xanthomonas spp.) associated with pepper and tomato lesions. *International Journal of Systematic and Evolutionary Microbiology* **50**, 1211–1219 (2000).
36. S. S. Gnanamanickam, Biological control of bacterial blight of rice. *Biological control of rice diseases*, 67–78 (2009).
37. J. C. Lozano, Cassava bacterial blight: a manageable disease. *Plant Dis* **70**, 1989–1993 (1986).
38. G. C. Wall, Bacterial Blight of Mendioka (Cassava)(Xanthomonas campestris pv. manihotis). (2000).
39. N. W. Schaad *et al.*, Emended classification of xanthomonad pathogens on citrus. *Papers in Plant Pathology*, 96 (2006).
40. N. W. Schaad *et al.*, Reclassification of Xanthomonas campestris pv. citri (ex Hasse 1915) Dye 1978 forms A, B/C/D, and E as X. smithii subsp. citri (ex Hasse) sp. nov. nom. rev. comb. nov., X. fuscans subsp. aurantifolii (ex Gabriel 1989) sp. nov. nom. rev. comb. nov., and X. alfalfae subsp. citrumelo (ex Riker and Jones) Gabriel et al., 1989 sp. nov. nom. rev. comb. nov.; X. campestris pv malvacearum (ex Smith 1901) Dye 1978 as X. smithii subsp. smithii nov. comb. nov. nom. nov.; X. campestris pv. alfalfae (ex Riker and Jones, 1935) Dye 1978 as X. alfalfae subsp. alfalfae (ex Riker et al., 1935) sp. nov. nom. rev.; and "var. fuscans" of X. campestris pv. phaseoli (ex Smith, 1987) Dye 1978 as X. fuscans subsp. fuscans sp. nov. *Systematic and Applied Microbiology* **28**, 494–518 (2005).
41. N. Gimenes-Fernandes, J. C. Barbosa, A. Ayres, C. Massari, Plantas doentes não detectadas nas inspeções dificultam a erradicação do cancro cítrico. *Summa Phytopathologica* **26**, 320–325 (2000).
42. F. Behlau, N. Barelli, J. Belasque Jr, Lessons from a case of successful eradication of citrus canker in a citrus-producing farm in São Paulo State, Brazil. *Journal of plant pathology* **96**, 561–568 (2014).
43. J. Belasque Jr, J. C. Barbosa, A. B. Filho, C. A. Massari, Probable consequences of the mitigation of citrus canker eradication methodology in São paulo state. *Prováveis consequências do abrandamento da metodologia de erradicação do cancro cítrico no Estado de São Paulo* **35**, 314–317 (2010).
44. F. Behlau, J. Belasque, Cancro cítrico: a doença e seu controle. *Fundecitrus, Araraquara, Brasil*, (2014).
45. F. Behlau, J. Belasque, J. Graham, R. Leite, Effect of frequency of copper applications on control of citrus canker and the yield of young bearing sweet orange trees. *Crop Protection* **29**, 300–305 (2010).
46. B. Canteros, A. Gochez, R. Moschini, Management of Citrus Canker in Argentina, a Success Story. *The plant pathology journal* **33**, 441 (2017).
47. F. Behlau, B. I. Canteros, G. V. Minsavage, J. B. Jones, J. H. Graham, Molecular Characterization of Copper Resistance Genes from Xanthomonas citri subsp. citri and Xanthomonas alfalfae subsp. citrumelonis. *Applied and Environmental Microbiology* **77**, 4089–4096 (2011).
48. D. Richard *et al.*, Adaptation of genetically monomorphic bacteria: evolution of copper resistance through multiple horizontal gene transfers of complex and versatile mobile genetic elements. *Molecular ecology* **26**, 2131–2149 (2017).
49. E. Jefferys, The stability of antibiotics in soils. *Microbiology* **7**, 295–312 (1952).
50. I. Nunes *et al.*, Coping with copper: legacy effect of copper on potential activity of soil bacteria following a century of exposure. *FEMS microbiology ecology* **92**, fiw175 (2016).
51. J.-W. Hyun, H.-J. Kim, P.-H. Yi, R.-Y. Hwang, E.-W. Park, Mode of action of streptomycin resistance in the citrus canker pathogen (Xanthomonas smithii subsp. citri) in Jeju Island. *The Plant Pathology Journal* **28**, 207–211 (2012).
52. D. F. Ritchie, V. Dittapongpitch, Copper-and streptomycin-resistant strains and host differentiated races of Xanthomonas campestris pv. vesicatoria in North Carolina. *Plant Dis* **75**, 733–736 (1991).
53. S.-Y. Park, H.-S. Han, Y.-S. Lee, Y.-J. Koh, J.-S. Jung, Streptomycin Resistant Genes of Pseudomonas syringae pv. syringae, the Causal Agent of Bacterial Blossom Blight of Kiwifruit. *Research in Plant Disease* **13**, 88–92 (2007).
54. P. M. Martínez-García *et al.*, Bioinformatics analysis of the complete genome sequence of the mango tree pathogen Pseudomonas syringae pv. syringae UMAF0158 reveals traits relevant to virulence and epiphytic lifestyle. *PloS one* **10**, e0136101 (2015).
55. H. R. Dillard, D. E. Legard, Bacterial Diseases of Beans. (1991).
56. D. L. Arnold, H. C. Lovell, R. W. Jackson, J. W. Mansfield, Pseudomonas syringae pv. phaseolicola: from 'has bean'to supermodel. *Molecular plant pathology* **12**, 617–627 (2011).
57. H. S. Addy, W. S. Wahyuni, Nucleic Acid and Protein Profile of Bacteriophages that Infect Pseudomonas syringae pv. glycinea, Bacterial Blight on Soybean. *Agriculture and Agricultural Science Procedia* **9**, 475–481 (2016).
58. L. Prom, J. Venette, Races of Pseudomonas syringae pv. glycinea on commercial soybean in eastern North Dakota. *Plant disease* **81**, 541–544 (1997).
59. T. V. Huynh, D. Dahlbeck, B. J. Staskawicz, Bacterial Blight of Soybean: Regulation of a Pathogen Gene Determing Host Cultivar Specificity. *Science* **245**, 1374 (1989).
60. Y. Bashan, L. E. de-Bashan, Reduction of bacterial speck (Pseudomonas syringae pv. tomato) of tomato by combined treatments of plant growth-promoting bacterium, Azospirillum brasilense, streptomycin sulfate, and chemo-thermal seed treatment. *European Journal of Plant Pathology* **108**, 821–829 (2002).
61. S. Nelson, Bacterial leaf blight of aglaonema. (2009).
62. J. Lutkenhaus, S. Pichoff, S. Du, Bacterial cytokinesis: from Z ring to divisome. *Cytoskeleton* **69**, 778–790 (2012).
63. J. Errington, R. A. Daniel, D.-J. Scheffers, Cytokinesis in bacteria. *Microbiology and Molecular Biology Reviews* **67**, 52–65 (2003).
64. A. S. Lorenzoni, G. C. Dantas, T. Bergsma, H. Ferreira, D.-J. Scheffers, Xanthomonas citri MinC Oscillates from Pole to Pole to Ensure Proper Cell Division and Shape. *Frontiers in microbiology* **8**, 1352 (2017).
65. A. P. Ucci *et al.*, Asymmetric chromosome segregation in Xanthomonas citri ssp. citri. *MicrobiologyOpen* **3**, 29–41 (2014).
66. G. C. Dantas, P. M. Martins, D. A. Martins, E. Gomes, H. Ferreira, A protein expression system for tandem affinity purification in Xanthomonas citri subsp. citri. *brazilian journal of microbiology* **47**, 518–526 (2016).
67. A. Mehta, Y. B. Rosato, A simple method for in vivo expression studies of Xanthomonas axonopodis pv. citri. *Current microbiology* **47**, 400–403 (2003).
68. A. R. da Silva *et al.*, Comparison of the genomes of two Xanthomonas pathogens with differing host specificities. *Nature* **417**, 459–463 (2002).
69. P. Buske, A. Mittal, R. V. Pappu, P. A. Levin, in *Seminars in cell & developmental biology*. (Elsevier, 2015), vol. 37, pp. 3–10.
70. P. J. Buske, P. A. Levin, The extreme C-terminus of the bacterial cytoskeletal protein FtsZ plays a fundamental role in assembly independent of modulatory proteins. *Journal of Biological Chemistry*, jbc. M111. 330324 (2012).

71. A. Martos *et al.*, FtsZ polymers tethered to the membrane by ZipA are susceptible to spatial regulation by Min waves. *Biophysical journal* **108**, 2371–2383 (2015).
72. K. Sundararajan *et al.*, The bacterial tubulin FtsZ requires its intrinsically disordered linker to direct robust cell wall construction. *Nature communications* **6**, 7281 (2015).
73. K. A. Gardner, D. A. Moore, H. P. Erickson, The C-terminal linker of Escherichia coli FtsZ functions as an intrinsically disordered peptide. *Molecular microbiology* **89**, 264–275 (2013).
74. P. A. de Boer, R. E. Crossley, L. I. Rothfield, A division inhibitor and a topological specificity factor coded for by the minicell locus determine proper placement of the division septum in E. coli. *Cell* **56**, 641–649 (1989).
75. V. W. Rowlett, W. Margolin, The bacterial Min system. *Current Biology* **23**, R553-R556 (2013).
76. L. J. Wu, J. Errington, Nucleoid occlusion and bacterial cell division. *Nature Reviews Microbiology* **10**, 8–12 (2012).
77. B. Di Ventura *et al.*, Chromosome segregation by the Escherichia coli Min system. *Molecular systems biology* **9**, 686 (2013).
78. M. Thanbichler, L. Shapiro, MipZ, a spatial regulator coordinating chromosome segregation with cell division in Caulobacter. *Cell* **126**, 147–162 (2006).
79. L. M. Galvão-Botton *et al.*, High-throughput screening of structural proteomics targets using NMR. *FEBS letters* **552**, 207–213 (2003).
80. P. M. Martins *et al.*, Subcellular localization of proteins labeled with GFP in Xanthomonas citri ssp. citri: targeting the division septum. *FEMS microbiology letters* **310**, 76–83 (2010).
81. F. J. Gueiros-Filho, R. Losick, A widely conserved bacterial cell division protein that promotes assembly of the tubulin-like protein FtsZ. *Genes & development* **16**, 2544–2556 (2002).
82. D. A. Mohl, J. W. Gober, Cell cycle–dependent polar localization of chromosome partitioning proteins in Caulobacter crescentus. *Cell* **88**, 675–684 (1997).
83. L. A. Lacerda *et al.*, Protein depletion using the arabinose promoter in Xanthomonas citri subsp. citri. *Plasmid*, (2017).
84. Y. L. Shih, M. Zheng, Spatial control of the cell division site by the Min system in E scherichia coli. *Environmental microbiology* **15**, 3229–3239 (2013).
85. E. Kuru *et al.*, In situ probing of newly synthesized peptidoglycan in live bacteria with fluorescent D-amino acids. *Angewandte Chemie International Edition* **51**, 12519–12523 (2012).
86. E. Kuru, S. Tekkam, E. Hall, Y. V. Brun, M. S. Van Nieuwenhze, Synthesis of fluorescent D-amino acids and their use for probing peptidoglycan synthesis and bacterial growth in situ. *Nature protocols* **10**, 33–52 (2015).
87. M. O. Andrade, C. S. Farah, N. Wang, The Post-transcriptional Regulator rsmA/csrA Activates T3SS by Stabilizing the 5′ UTR of hrpG, the Master Regulator of hrp/hrc Genes, in Xanthomonas. *PLoS pathogens* **10**, e1003945 (2014).
88. L.-P. Liu *et al.*, Construction of egfp-labeling system for visualizing the infection process of Xanthomonas axonopodis pv. citriinplanta. *Current microbiology* **65**, 304–312 (2012).
89. C. Van der Heijden, P. Janssen, J. Strik, Toxicology of gallates: a review and evaluation. *Food and Chemical Toxicology* **24**, 1067–1070 (1986).
90. H. Strahl, L. W. Hamoen, Membrane potential is important for bacterial cell division. *Proceedings of the National Academy of Sciences* **107**, 12281–12286 (2010).
91. G. J. Phillips, Green fluorescent protein–a bright idea for the study of bacterial protein localization. *FEMS microbiology letters* **204**, 9–18 (2001).
92. A. Savietto *et al.*, Antibacterial activity of monoacetylated alkyl gallates against Xanthomonas citri subsp. citri. *Archives of microbiology*, 1–9 (2018).
93. P. Singh, D. Panda, FtsZ inhibition: a promising approach for antistaphylococcal therapy. *Drug news & perspectives* **23**, 295–304 (2010).
94. Y.-J. Eun *et al.*, Divin: a small molecule inhibitor of bacterial divisome assembly. *Journal of the American Chemical Society* **135**, 9768–9776 (2013).
95. P. Sass, H. Brötz-Oesterhelt, Bacterial cell division as a target for new antibiotics. *Current opinion in microbiology* **16**, 522–530 (2013).
96. W. Vollmer, The prokaryotic cytoskeleton: a putative target for inhibitors and antibiotics? *Applied microbiology and biotechnology* **73**, 37–47 (2006).
97. R. L. Lock, E. J. Harry, Cell-division inhibitors: new insights for future antibiotics. *Nature Reviews Drug Discovery* **7**, 324–338 (2008).
98. E. Król *et al.*, Antibacterial activity of alkyl gallates is a combination of direct targeting of FtsZ and permeabilization of bacterial membranes. *Frontiers in Microbiology* **6**, (2015).

99. I. Kubo, K.-i. Fujita, K.-i. Nihei, Anti-Salmonella activity of alkyl gallates. *Journal of agricultural and food chemistry* **50**, 6692–6696 (2002).
100. E. Król, D.-J. Scheffers, FtsZ Polymerization Assays: Simple Protocols and Considerations. *Journal of visualized experiments: JoVE*, e50844 (2013).
101. N.-R. Ha, S.-C. Lee, J.-W. Hyun, M.-Y. Yoon, Development of inhibitory ssDNA aptamers for the FtsZ cell division protein from citrus canker phytopathogen. *Process Biochemistry* **51**, 24–33 (2016).
102. L. Dai, Y. Huang, Y. Chen, Z.-e. Long, Cloning and characterization of filamentous temperature-sensitive protein Z from Xanthomonas oryzae pv. Oryzae. *SpringerPlus* **5**, 145 (2016).
103. M. M. Kopacz, A. S. Lorenzoni, C. R. Polaquini, L. O. Regasini, D. J. J. M. Scheffers, Purification and characterization of FtsZ from the citrus canker pathogen Xanthomonas citri subsp. citri. e00706 (2018).
104. A. Mukherjee, J. Lutkenhaus, Dynamic assembly of FtsZ regulated by GTP hydrolysis. *The EMBO journal* **17**, 462–469 (1998).
105. S. Pichoff, S. Du, J. Lutkenhaus, The bypass of ZipA by overexpression of FtsN requires a previously unknown conserved FtsN motif essential for FtsA–FtsN interaction supporting a model in which FtsA monomers recruit late cell division proteins to the Z ring. *Molecular microbiology* **95**, 971–987 (2015).
106. P. De Boer, R. Crossley, L. Rothfield, The essential bacterial cell-division protein FtsZ is a GTPase. *Nature* **359**, 254 (1992).
107. A. Mukherjee, K. Dai, J. Lutkenhaus, Escherichia coli cell division protein FtsZ is a guanine nucleotide binding protein. *Proceedings of the National Academy of Sciences* **90**, 1053–1057 (1993).
108. D. N. Margalit *et al.*, Targeting cell division: small-molecule inhibitors of FtsZ GTPase perturb cytokinetic ring assembly and induce bacterial lethality. *Proceedings of the National Academy of Sciences of the United States of America* **101**, 11821–11826 (2004).
109. D. E. Anderson *et al.*, Comparison of small molecule inhibitors of the bacterial cell division protein FtsZ and identification of a reliable cross-species inhibitor. *ACS chemical biology* **7**, 1918–1928 (2012).
110. E. Ingerman, J. Nunnari, A continuous, regenerative coupled GTPase assay for dynamin-related proteins. *Methods in enzymology* **404**, 611–619 (2005).
111. B. Y. Feng, A. Shelat, T. N. Doman, R. K. Guy, B. K. Shoichet, High-throughput assays for promiscuous inhibitors. *Nature chemical biology* **1**, 146 (2005).
112. B. Y. Feng, B. K. Shoichet, A detergent-based assay for the detection of promiscuous inhibitors. *Nature protocols* **1**, 550 (2006).
113. R. Jaiswal, T. K. Beuria, R. Mohan, S. K. Mahajan, D. Panda, Totarol inhibits bacterial cytokinesis by perturbing the assembly dynamics of FtsZ. *Biochemistry* **46**, 4211–4220 (2007).
114. S. Urgaonkar *et al.*, Synthesis of antimicrobial natural products targeting FtsZ:(±)-dichamanetin and (±)-2 “‘-hydroxy-5 “-benzylisouvarinol-B. *Organic letters* **7**, 5609–5612 (2005).
115. D. J. Haydon *et al.*, An Inhibitor of FtsZ with Potent and Selective Anti-Staphylococcal Activity. *Science* **321**, 1673–1675 (2008).
116. N. L. Elsen *et al.*, Mechanism of action of the cell-division inhibitor PC190723: modulation of FtsZ assembly cooperativity. *Journal of the American Chemical Society* **134**, 12342–12345 (2012).
117. D. Bramhill, C. M. Thompson, GTP-dependent polymerization of Escherichia coli FtsZ protein to form tubules. *Proceedings of the National Academy of Sciences* **91**, 5813–5817 (1994).
118. A. Mukherjee, J. Lutkenhaus, Guanine nucleotide-dependent assembly of FtsZ into filaments. *Journal of Bacteriology* **176**, 2754–2758 (1994).
119. M. E. Gündoğdu *et al.*, Large ring polymers align FtsZ polymers for normal septum formation. *The EMBO journal* **30**, 617–626 (2011).
120. K.-H. Huang, J. Durand-Heredia, A. Janakiraman, FtsZ ring stability: of bundles, tubules, crosslinks, and curves. *Journal of bacteriology* **195**, 1859–1868 (2013).
121. S. L. Milam, M. Osawa, H. P. Erickson, Negative-stain electron microscopy of inside-out FtsZ rings reconstituted on artificial membrane tubules show ribbons of protofilaments. *Biophysical journal* **103**, 59–68 (2012).
122. Z. Li, M. J. Trimble, Y. V. Brun, G. J. Jensen, The structure of FtsZ filaments in vivo suggests a force-generating role in cell division. *The EMBO journal* **26**, 4694–4708 (2007).
123. A. Mukherjee, J. Lutkenhaus, Analysis of FtsZ assembly by light scattering and determination of the role of divalent metal cations. *Journal of Bacteriology* **181**, 823–832 (1999).
124. E. Small, S. G. Addinall, Dynamic FtsZ polymerization is sensitive to the GTP to GDP ratio and can be maintained at steady state using a GTP-regeneration system. *Microbiology* **149**, 2235–2242 (2003).

125. M. R. Caplan, H. P. Erickson, Apparent cooperative assembly of the bacterial cell division protein FtsZ demonstrated by isothermal titration calorimetry. *Journal of Biological Chemistry* **278**, 13784–13788 (2003).
126. Y. Chen, H. P. Erickson, Rapid in vitro assembly dynamics and subunit turnover of FtsZ demonstrated by fluorescence resonance energy transfer. *Journal of Biological Chemistry* **280**, 22549–22554 (2005).
127. T. M. Santos *et al.*, Small molecule chelators reveal that iron starvation inhibits late stages of bacterial cytokinesis. *ACS chemical biology*, (2017).
128. M. Sánchez, A. Valencia, M.-J. Ferrándiz, C. Sander, M. Vicente, Correlation between the structure and biochemical activities of FtsA, an essential cell division protein of the actin family. *The EMBO journal* **13**, 4919–4925 (1994).
129. C. Paradis-Bleau, F. Sanschagrin, R. C. Levesque, Peptide inhibitors of the essential cell division protein FtsA. *Protein Engineering Design and Selection* **18**, 85–91 (2005).
130. B. Beall, J. Lutkenhaus, Impaired cell division and sporulation of a Bacillus subtilis strain with the ftsA gene deleted. *Journal of bacteriology* **174**, 2398–2403 (1992).
131. A. Feucht, I. Lucet, M. D. Yudkin, J. Errington, Cytological and biochemical characterization of the FtsA cell division protein of Bacillus subtilis. *Molecular microbiology* **40**, 115–125 (2001).
132. L. M. LaPointe *et al.*, Structural organization of FtsB, a transmembrane protein of the bacterial divisome. *Biochemistry* **52**, 2574–2585 (2013).
133. M. Glas *et al.*, The soluble periplasmic domains of E. coli cell division proteins FtsQ/FtsB/FtsL form a trimeric complex with sub-micromolar affinity. *Journal of Biological Chemistry*, jbc. M115. 654756 (2015).
134. V. Katis, R. Wake, E. Harry, Septal Localization of the Membrane-Bound Division Proteins ofBacillus subtilis DivIB and DivIC Is Codependent Only at High Temperatures and Requires FtsZ. *Journal of bacteriology* **182**, 3607–3611 (2000).
135. R. Daniel, E. Harry, V. Katis, R. Wake, J. Errington, Characterization of the essential cell division gene ftsL (yllD) of Bacillus subtilis and its role in the assembly of the division apparatus. *Molecular microbiology* **29**, 593–604 (1998).
136. J. C. Yang, F. Van Den Ent, D. Neuhaus, J. Brevier, J. Löwe, Solution structure and domain architecture of the divisome protein FtsN. *Molecular microbiology* **52**, 651–660 (2004).
137. N. R. Stokes *et al.*, Novel inhibitors of bacterial cytokinesis identified by a cell-based antibiotic screening assay. *Journal of Biological Chemistry* **280**, 39709–39715 (2005).
138. T. Elliott, A. Shelton, D. Greenwood, The response of Escherichia coli to ciprofloxacin and norfloxacin. *Journal of medical microbiology* **23**, 83–88 (1987).
139. B. G. Spratt, Distinct penicillin binding proteins involved in the division, elongation, and shape of Escherichia coli K12. *Proceedings of the National Academy of Sciences* **72**, 2999–3003 (1975).
140. A. J. O'Neill, I. Chopra, Preclinical evaluation of novel antibacterial agents by microbiological and molecular techniques. *Expert opinion on investigational drugs* **13**, 1045–1063 (2004).
141. P. Nonejuie, M. Burkart, K. Pogliano, J. Pogliano, Bacterial cytological profiling rapidly identifies the cellular pathways targeted by antibacterial molecules. *Proceedings of the National Academy of Sciences* **110**, 16169–16174 (2013).
142. A. D. Berti *et al.*, Altering the proclivity towards daptomycin resistance in methicillin-resistant Staphylococcus aureus using combinations with other antibiotics. *Antimicrobial agents and chemotherapy* **56**, 5046–5053 (2012).
143. E. Huang, A. E. Yousef, The lipopeptide antibiotic paenibacterin binds to the bacterial outer membrane and exerts bactericidal activity through cytoplasmic membrane damage. *Applied and environmental microbiology* **80**, 2700–2704 (2014).
144. S. Pietschmann, K. Hoffmann, M. Voget, U. Pison, Synergistic effects of miconazole and polymyxin B on microbial pathogens. *Veterinary research communications* **33**, 489 (2009).
145. L. Boulos, M. Prevost, B. Barbeau, J. Coallier, R. Desjardins, LIVE/DEAD® BacLight™: application of a new rapid staining method for direct enumeration of viable and total bacteria in drinking water. *Journal of microbiological Methods* **37**, 77–86 (1999).
146. P. J. Sims, A. S. Waggoner, C.-H. Wang, J. F. Hoffman, Mechanism by which cyanine dyes measure membrane potential in red blood cells and phosphatidylcholine vesicles. *Biochemistry* **13**, 3315–3330 (1974).
147. S. Deoghare, Bedaquiline: a new drug approved for treatment of multidrug-resistant tuberculosis. *Indian journal of pharmacology* **45**, 536 (2013).
148. A. Koul *et al.*, Diarylquinolines target subunit c of mycobacterial ATP synthase. *Nature chemical biology* **3**, 323 (2007).

149. A. Hunt, J. P. Rawlins, H. B. Thomaides, J. Errington, Functional analysis of 11 putative essential genes in Bacillus subtilis. *Microbiology* **152**, 2895–2907 (2006).
150. A. Müller *et al.*, Daptomycin inhibits cell envelope synthesis by interfering with fluid membrane microdomains. *Proceedings of the National Academy of Sciences* **113**, E7077-E7086 (2016).
151. A. Urban *et al.*, Novel whole-cell antibiotic biosensors for compound discovery. *Applied and environmental microbiology* **73**, 6436–6443 (2007).
152. B. Kepplinger *et al.*, Mode of action and heterologous expression of the natural product antibiotic vancoresmycin. *ACS Chemical Biology*, (2017).
153. T. Mascher, S. L. Zimmer, T.-A. Smith, J. D. Helmann, Antibiotic-inducible promoter regulated by the cell envelope stress-sensing two-component system LiaRS of Bacillus subtilis. *Antimicrobial agents and chemotherapy* **48**, 2888–2896 (2004).
154. A. Lamsa, W. T. Liu, P. C. Dorrestein, K. Pogliano, The Bacillus subtilis cannibalism toxin SDP collapses the proton motive force and induces autolysis. *Molecular microbiology* **84**, 486–500 (2012).
155. P. J. Lewis, S. D. Thaker, J. Errington, Compartmentalization of transcription and translation in Bacillus subtilis. *The EMBO Journal* **19**, 710–718 (2000).

Chapter 2 — Discovery and investigations on the antimicrobial mode of action of the Au(I) compound 7b-BF_4

André S. G. Lorenzoni[1], Tessa Bergsma[1], Angela Casini[2], Dirk-Jan Scheffers[1]

[1] *Department of Molecular Microbiology, Groningen Biomolecular Sciences and Biotechnology Institute, University of Groningen, Groningen, Netherlands*

[2] *School of Chemistry, Cardiff University, Cardiff, UK*

Abstract

Decades of antibiotic use to treat and prevent bacterial infections have led to a rapid increase in bacterial pathogens that are resistant to multiple antibiotics. Simultaneously, discovery and use of novel antibiotics has almost ground to a halt. Research is needed on known chemical scaffolds that were abandoned in the past. Gold compounds have a long tradition in medicine — *eg* as an anti-tubercular agent after Robert Koch discovered that gold effectively kills *Mycobacteria*. In this work we present investigations on the mode of action of the gold compound 7b-BF_4. This compound has antimicrobial activity and a potential as an antibiotic. We have tested its minimum inhibitory and bactericidal activities (MIC and MBC). 7b-BF_4 is active against all Gram-positive bacteria tested, including Methicillin Resistant *Staphylococcus aureus* (MRSA) and Vancomycin Resistant *Enterococcus faecium* (VRE), in concentrations varying from 0.4 μg/mL to 3.4 μg/mL. To address the effect of the compound on macromolecular synthesis pathways we tested incorporation of radiolabeled precursors of DNA, RNA, protein, and cell wall in *Bacillus subtilis*. 7b-BF_4 blocks DNA and protein synthesis, but also affects RNA and cell wall synthesis to a lesser extent. Further tests showed that 7b-BF_4 doesn't affect membrane permeability or membrane potential. However, it causes a decrease in intracellular ATP and inactivates cells within short periods of time.

1. Introduction

The discovery of antibiotics, starting with penicillin in 1928, marked a revolution in biology and medicine, and ushered in the antibiotic era, in which mortality from a number of diseases drastically reduced, immediately increasing life expectancy worldwide (*1*). However, penicillin resistance dramatically increased, shortly after its mass production started (*2*), quickly becoming widespread. The introduction of β-lactams in the 1960's tackled this problem, but again, shortly after its introduction, the first cases of beta-lactam resistance were reported (*3*). This was the first of several cycles of antibiotic resistance crises which have taken place over the last century (*4, 5*). The development of new classes of antibiotics has so far outpaced the spread of antibiotic resistance (*4*). However, the continued discovery of new antibiotics is needed to avoid a widespread pandemic of antibiotic resistant bacteria (*6*).

The main strategy to discover antibiotics is to screen for microbial-derived natural products, in a similar way that lead to the discovery of penicillin (*7*). Another approach involves the screening of synthetic substances. The first synthetic substances found to have antibiotic action, in modern medicine, were the sulfonamides in the 1930s, which were synthesized even before penicillin was used in a clinical setting (*8*). Once discovered and characterized for its mode of action, antimicrobial substances can be chemically modified to improve potency, stability, and pharmacokinetics. This strategy has resulted in dozens of new antibiotics being introduced in the clinics (*8*). However, it is generally accepted that substances belonging to classes that are completely new to the clinic are more effective in tackling resistance, when compared to more commonly used strategies (*9*).

Gold and other metal compounds have a long history in medicine (*10*), and are reported to have been used from ancient times throughout the late Middle Ages and the Renaissance (*11*). Currently gold compounds are used only for the treatment of rheumatoid arthritis (*12*). The antimicrobial activity of gold cyanide was already reported for the treatment of *Mycobacterium tuberculosis (13)*. About 50 years ago platinum agents started to be used in the clinics to treat cancer (*14*). Interestingly, the inhibitory activity of platinum salts were discovered by mistake, when Rosenberg *et al.* in 1965 (*15*), were testing the effect of electric fields on *Escherichia coli* cell growth using platinum electrodes. Under those

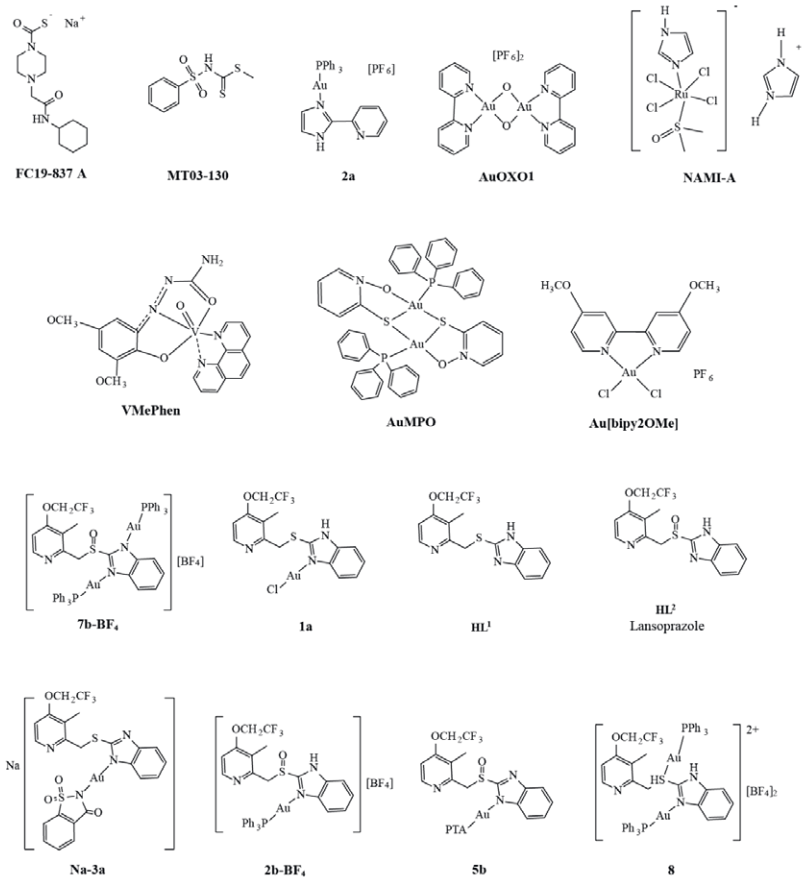

Figure 1: Structures of the compounds used in this study.

conditions platinum salts were formed, which inhibited cell division and lead to cell filamentation (*15*). Following this discovery, Rosenberg and coworkers successfully hypothesized that the inhibitory effect of platinum compounds on cell growth was also effective against tumors (*16*), leading to the development of the most widely used cancer chemotherapeutics nowadays (*14*).

Another strategy less known for the discovery of antibiotics is the repurposing of known drugs that are already used in the clinic for a different purpose. This strategy was recently used to discover the antibiotic activity of lansoprazole against *M. tuberculosis (17)*. Lansoprazole is a medicine currently used to treat peptic diseases due to its

activity as a proton pump inhibitor (PPI) (*18*). However, PPIs are also useful to induce cisplatin sensitivity in human tumor cells, because they interfere with the micro-environmental acidity of tumors, a mechanism of chemoresistance (*19*). Serratice *et al.* (*11*) synthesized gold(I) compounds featuring lansoprazole as a ligand, in order to combine the antiproliferative activity of gold with the PPI activity of lansoprazole. Those compounds were shown to have moderate activity against tumor cells (*11*).

In this work we screened the antimicrobial activity of a range of metal compounds, including the anticancer Ru(III) drug NAMI-A, the proton pump inhibitor lansoprazole, and the gold-based derivatives synthesized in the previous study (*11*) (**Figure 1**). One of these compounds showed potent antimicrobial activity against Gram-positive bacteria and we investigated its antimicrobial mode of action by monitoring DNA, RNA, protein and peptidoglycan synthesis, membrane integrity, and cellular energy levels in the presence of the compound. We also screened for the development of resistance against the compound, but failed to produce resistant mutants.

2. Methods

2.1. Minimal inhibitory and bactericidal concentration assays

The minimal inhibitory concentration (MIC) of compounds (**Figure 1**) was tested by broth microdilution. All compounds were tested against at least three strains (*E. coli; Xanthomonas citri* subsp. *citri* (Xac)*; Lactococcus lactis*, **Table 1**), in case of compound **7b-BF4**, the MIC was determined for all the strains listed in **Table 1**. Exponentially growing bacteria were diluted to OD_{600} of 0.005 in 96 well plates containing two-fold serial dilutions of the compounds, in a final volume of 200 µL of growth medium (**Table 1**). The MIC was defined as the lowest concentration of compound that prevented bacterial growth after incubating 24 hours at the indicated growth temperature (*20*).

After 24 hours incubation approximately 2 µL of culture from each well was spotted onto agar plates composed of suitable growth medium. Plates were incubated overnight (or for 40 hours for Xac) at the indicated temperatures. The minimum bactericidal concentration (MBC)

Table 1: list of strains tested with 7b-BF_4 and growth conditions.

Origin	Strains	Growth medium (temperature)
Laboratory	*Escherichia coli* MG1655	LB-Lennox (30°C)
	Bacillus subtilis 168	LB-Lennox (30°C)
	Lactococcus lactis MG1363	M17 (with 0.5% glucose) (30°C)
	Xanthomonas citri subsp. *citri* (Xac) (21, 22)	NYGB (30°C)
Clinical	*Staphylococcus aureus* UMCG #333	CAMH (35°C)
	Methicillin resistant *Staphylococcus aureus* D22 (MRSA)	CAMH (35°C)
	Enterococcus faecium VanA (VRE)	TSB (35°C)
	Enterococcus faecium	TSB (35°C)

Media composition per liter: **LB-Lennox**, 10g tryptone, 5g yeast extract, 5g NaCl. **M17**, 5.0g glucose, 5.0g pancreatic digest of casein, 5.0g soy peptone, 5.0g beef extract, 2.5g yeast extract, 0.5g ascorbic acid, 0.25g $MgSO_4$, 19.0g disodium-β-glycerophosphate. **NYGB**, 20g glycerol, 5g peptone, 3g yeast extract. **CAMH**, 20g NaCl, 17.5g casein acid hydrolysate, 3.0g beef extract, 1.5g starch, 25mg $CaCl_2$, 12.5mg $MgCl_2$. **TSB**, 17.0g casein peptone (pancreatic), 5.0g NaCl, 3.0g soya peptone (papain digest.), 2.5g glucose, 2.5g K_2HPO_4.

was defined as the lowest concentration of compound that prevented visible cell growth on compound-free agar plates.

2.2. Macromolecular synthesis

Four macromolecular synthesis pathways were evaluated by monitoring the incorporation of radioactively labelled precursors. [5^{3}H]uridine, [methyl^{3}H]thymidine, L[3,4,5^{3}H(N)]leucine and D[6^{3}H(N)]glucosamine hydrochloride (all at 0.5 μCi/mL) were used to respectively monitor RNA, DNA, protein and peptidoglycan synthesis. During this experiment *B. subtilis* cells were grown to early exponential phase in modified Davis Minimal Medium: casamino acids 2.0g/L; K_2HPO_4 7.0g/L; KH_2PO_4 3.0g/L; $MgSO_47(H_2O)$ 0.1g/L; $(NH_4)2SO_4$ 1.0g/L; tri-Sodium citrate dihydrate 0.5g/L; glucose 7.0g/L and tryptophan 10mg/L modified from (23, 24). Non-labelled precursor (1mM) was used for RNA and peptidoglycan and 10μM was used for DNA and protein.

Cells were incubated in the presence of labelled precursors for 80minutes with shaking at 30°C, in the presence of 0.43μg/mL (312nM) **7b-BF_4**, without compound (negative control) or with an antibiotic known to inhibit the synthesis pathway tested as positive control (RNA: rifampicin 0.625μg/mL, DNA: ciprofloxacin 0.625μg/mL, protein:

tetracycline 10 μg/mL, peptidoglycan: vancomycin 1.0μg/mL). At least four replicates were made per precursor tested. After incubation, samples were precipitated with ice-cold 12% trichloroacetic acid for 35minutes and then filtered through nitrocellulose membranes (pore size 0.45μm). The filters were washed with ice cold 12% trichloroacetic acid, transferred to 2mL scintillation fluid Ultima Gold MV (Perkin-Elmer) and measured in a Tri-Carb 2000CA liquid scintillation analyzer (Packard Instruments).

2.3. HADA incorporation assay

Peptidoglycan synthesis activity was further monitored using the fluorescent D-amino acid analogue HADA (Hydroxycoumarin-carboxylic acid-Amino-D-Alanine), which is incorporated at sites of active peptidoglycan synthesis (25). Cells grown to early exponential phase were either incubated simultaneously with **7b-BF_4** (at 0.43 or 1.72μg/mL) and HADA (36.5μg/mL) and grown for 35minutes, or cells were grown for 30minutes with **7b-BF_4** followed by a 5minutes pulse with HADA. HADA labelling for 5minutes in the presence of Vancomycin (2μg/mL) was used as a control.

After each treatment the cells were washed twice with Hanks' Balanced Salt Solution (KCl 0.40g/L, KH_2PO_4 60mg/L, NaCl 8.0g/L, $NaHCO_3$ 0.35g/L, Na_2HPO_4 48mg/L) and visually inspected using a Nikon Ti-E microscope (Nikon Instruments, Tokyo, Japan) equipped with a Hamamatsu Orca Flash 4.0 camera.

2.4. Killing dynamics

Freshly inoculated cultures of *B. subtilis* or *S. aureus* were grown to OD_{600} of about 0.15, equivalent to approximately 2×10^7 or 6×10^7 colony forming units (CFU), respectively. At this moment the cultures were split in 1mL test tubes with 4 times the MIC of **7b-BF_4**, together with controls without compound. Aliquots were taken after 0.75, 1.5, 3, 6, and 24 hours. The amount of CFU/mL in each sample was determined by seeding serial dilutions of aliquots on LB or CAMH agar plates which were incubated at 30°C for 20h.

To observe the effect of **7b-BF_4** in real time, a freshly grown culture of *B. subtilis* was diluted to OD_{600} of 0.005 in a 96-well plate. The plate was incubated in a microplate spectrophotometer (1000rpm; 30°C). When

OD_{600} reached 0.2, **7b-BF_4** was added at different concentrations. The OD_{600} was recorded for an additional 1.5 hours, after which the viability of the samples was determined by CFU counting as described above.

2.5. Membrane permeability assay

Membrane integrity was assessed using the commercial Live/Dead BacLight bacterial viability kit (Invitrogen) for microscopy as described by (26), with some modifications. Cells were incubated for 15 min at 30 °C in the presence of **7b-BF_4** (at 0.43 or 1.72 µg/mL), nisin (5 µg/mL, control) or without drug added. The dyes propidium iodide (14 µM) and SYTO 9 (2.4 µM) were used to stain the DNA of cells. After incubation, cells were mounted on agarose pads and analyzed using a Nikon Ti-E microscope (Nikon Instruments, Tokyo, Japan) equipped with a Hamamatsu Orca Flash 4.0 camera. Phase contrast, as well as green (FITC filter) and red (TRITC filter) fluorescence, were imaged.

2.6. Membrane potential

Membrane depolarization was measured in *B. subtilis* hyperpolarized cells with the membrane potential dye $DiSC_3$ (27) in a protocol adapted from (28, 29). Valinomycin was used to disrupt the sodium gradient and nisin was used as a control. *B. subtilis* cells were grown to OD_{600} of 0.6. Then, they were diluted 2-fold in PIPES buffer with $DiSC_3$ (6 µM) and 194 µL aliquots were dispensed in a 96 well microplate. After stabilization of the fluorescence signal (5 minutes), valinomycin (0.2 µM) was added. After the fluorescence signal had again stabilized (8 minutes), nisin (1.5 µg/mL) or different concentrations of **7b-BF_4** (varying 2 fold from 0.215 to 13.7 µg/mL) were added to the cells in the 96 well microplate (200 µL final volume). The experiment was carried out in a BioTek Synergy Mx 96-well plate reader. Fluorescence (excitation: 643 nm; emission: 666 nm; 9 nm bandwidth) was recorded every minute for 30 minutes after the addition of **7b-BF_4** or nisin.

2.7. ATP assay

ATP levels were measured in *B. subtilis* using the BacTiter-Glo™ Microbial Cell Viability Assay (Promega). CCCP (Carbonyl cyanide *m*-chlorophenyl hydrazine, 20 µg/mL) and lansoprazole (8.8 µg/mL) were used as controls, **7b-BF_4** was used in the following concentrations (in µg/mL):

0.21, 0.43, 0.86, and 1.72. The cells were incubated in a 96 well plate for 5 and 30 min (26 °C, 1000 rpm) after which 100 µL of cell culture was added to 100 µL of BacTiter-Glo™ Reagent for 5 minutes in a white 96 well plate (26 °C, 1000 rpm). Luminescence was measured in a Tecan Infinite F200 Pro luminometer. The amount of light emitted is a measure for the intracellular ATP concentration.

2.8. Subcellular localization of fluorescent proteins in *B. subtilis*

We used the strains listed in **Table 2** expressing a range of different fluorescent protein fusions that are related to specific cellular processes, to study the effect of **7b-BF_4** in those processes.

Fresh cultures were prepared by diluting overnight cultures and inducing them for about 4 hours with the respective inducer (**Table 2**) when needed. After that, cells were treated with 1.72 µg/mL **7b-BF_4**, or different controls depending on the marker observed, rifampicin (0.625 µg/mL) was used for RpoC fusion, tetracycline (10 µg/mL) was used for RpsB fusion and nisin (1.5 µg/mL) was used for all the other

Table 2: *B. subtilis* strains used for subcellular localization in this study.

Strain	Marker	Function	Inducer	Genotype	Reference
TB35	MinD	Division site regulation	0.1 % xylose	*amy::spc Pxyl-gfp-minD*	(30)
1803	DivIVA		0.5 % xylose	*divIVA::gfp-divIVA Cm*	(31)
PG62	FtsA	Cell division	0.1 mM IPTG	*aprE::spc Pspac-yfp-ftsA*	(32)
4056	FtsZ		0.1 % xylose	*amyE::spec Pxyl-gfp-pmutl-ftsZ*	(30)
1049	RpsB	DNA, RNA, Protein synthesis	0.1 % xylose	*trpC2 amyE::(spc Pxyl-rpsB-gfp)*	(33)
1048	RpoC		0.5 % xylose	*trpC2 chr::pST3 (rpoC-gfpa cat Pxyl-'rpoC)*	(33)
TNVS91	PolC		-	Δamy-E::specR-PxylR-PolC-4GS-ms-fGFP	(30)
MW10	MreB	Cytoskeleton	0.1 % xylose	*amyE::spc Pxyl-gfp-mreB*	(30)
3416 MreD			0.3 % xylose	*cat mreC::Pxyl-gfp-mreD*	(34)
3417	MreC		0.3 % xylose	*cat mreC::Pxyl-gfp-mreC*	(34)
HM160	SpooJ	Chromosome segregation	-	*kan spooJ-gfp*	(35)
JWV042	Hbs		-	*amyE::catPhbs-hbs-gfp*	(35)

strains. After 5 to 40 minutes of incubation in contact with the compounds the cells were added to agarose pads and imaged using a Nikon Ti-E microscope (Nikon Instruments, Tokyo, Japan) equipped with a Hamamatsu Orca Flash 4.0 camera.

2.9. Single step resistance

The potential incidence of single step resistance was determined using *B. subtilis*. Cells were grown to early exponential phase and approximately 2×10^9 CFU were spotted onto LB agar plates with 6.25 µM and 15.6 µM ML4. The plates were stored at 30 °C for 4 days, and were inspected every day to check for bacterial growth.

3. Results

3.1. Screening Gold-liganded compounds for antimicrobial activity

To identify potential antimicrobials we tested 16 compounds (**Figure 1**) initially synthesized for anticancer activity (*11*). The screen included two Gram-negative (Xac, *E. coli*) and one Gram-positive bacterial species (*L. lactis*). The majority of compounds showed no or only mild activity against the panel strains (**Table 3**). The compound **7b-BF4** however, showed strong antibacterial activity against the Gram-positive reference strain (**Table 3**). A MIC in the sub µg/ml range is indicative of the potential to serve as an antimicrobial. Due to this result we decided to further investigate the antibacterial activity and mode of action of this compound.

3.2. 7b-BF4 shows selective activity against Gram-positive bacteria

First, we wanted to establish whether **7b-BF4** showed potent antibacterial activity against other Gram-positive organisms, including clinical isolates of antibiotic-resistant pathogens like Methicillin Resistant *S. aureus* (MRSA) and Vancomycin Resistant *E. faecium* (VRE). Indeed, **7b-BF4** killed all Gram-positive bacteria tested, and the concentration required to kill cells (MBC) was the same required to inhibit growth (MIC, **Table 4**). This result indicates that **7b-BF4** is a bactericidal rather than a bacteriostatic agent, as the inhibition of bacterial cell growth seems to be irreversible (*36*). The MIC and MBC determined for MRSA

Table 3: Minimal inhibitory and bactericidal concentrations of the compounds tested (values displayed in µg/mL).

	Xac		*E. coli*		*L. lactis*	
Drug	**MIC**	**MBC**	**MIC**	**MBC**	**MIC**	**MBC**
FC19-837A	>98	>98	>98	>98	>98	>98
MT03-130	>79	>79	>79	>79	>79	>79
2a	30.0	30.0	240	>240	3.75	7.5
AuOXO1	10.3	20.6	10.3	41	82	82
NAMI-A	146	146	>146	>146	>146	>146
VMePhen	18.9	>151	75.4	>151	>151	>151
AuMPO	5.9	46.8	46.8	>374	46.8	374
Au[bipy2OMe]	6.29	12.6	>25.2	>25.2	6.29	12.6
7b-BF4	>55	>55	>55	>55	0.43	0.86
1a	>46.9	>46.9	46.9	46.9	>23.4	>23.4
HL[1]	>29.5	>29.5	>29.5	>29.5	>14.8	>14.8
HL[2]	>28.3	>28.3	>28.3	>28.3	>14.2	>14.2
Na-3a	>161	>161	40.2	40.2	40.2	80.4
2b-BF4	>73.2	>73.2	>73.2	>73.2	18.2	36.5
5b	28.9	28.9	28.9	28.9	28.9	28.9
8	>115	>115	>115	>115	14.4	57.6

Table 4: MIC and MBC of 7b-BF4 (values displayed in µg/mL).

Organism	**MIC** (µg/mL)	**MBC** (µg/mL)
B. subtilis	0.43	0.43
L. lactis	0.43	0.86
S. aureus	3.44	3.44
MRSA	3.41	3.44
E. faecium	0.86	0.86
VRE	0.86	0.86
Xac	>55	>55
E. coli	>55	>55

and VRE was identical to the MIC and MBC for their respective drug sensitive analogues (**Table 4**), indicating that the resistance mechanisms of these strains do not provide protection against **7b-BF4**.

3.3. 7b-BF_4 rapidly kills *B. subtilis* and *S. aureus* cells

After establishing that **7b-BF_4** is able to inhibit growth of Gram-positive organisms we decided to test how fast this inhibition and potential inactivation happens. *B. subtilis* cells are inhibited as early as 5 minutes after addition of **7b-BF_4** to a growing culture (**Figure 2**), and 99.9% of *B. subtilis* cells were killed after the treatment with 4 × MIC concentration (**Figure 2**).

To test the dynamics of the inactivation we exposed about 10^7 CFU/mL of growing cultures of *B. subtilis* or *S. aureus* to lethal concentrations (4 × MIC) of the compound for different periods of time. We observed that 99.9% of the *B. subtilis* population was killed between 90 and 180 minutes when exposed to 1.72 µg/mL of **7b-BF_4**, **Figure 3A**. The population of *S. aureus* was 99.9% inactivated after 180 minutes in the presence of 13.8 µg/mL (4 × MIC) of **7b-BF_4**, **Figure 3B**.

This rate of killing of *S. aureus* is faster than rates reported for closthioamide (37), kendomycin (38), vancomycin (39), teixobactin (39), or rifampicin (40); and similar to levofloxacin, gentamicin, and daptomycin when used at 10 times MIC concentration in *S. aureus*

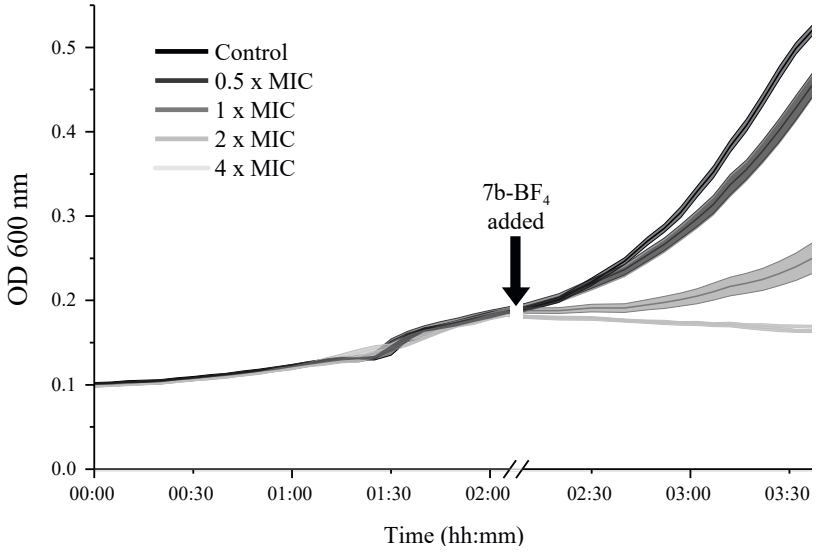

Figure 2: Short term effect of **7b-BF_4** on cell viability in *B. subtilis*. Lines are the median and shades are the standard error of 4 replicates.

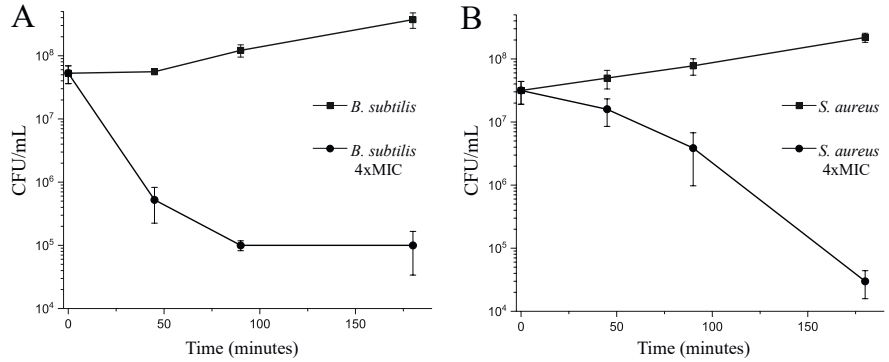

Figure 3: CFU assay in **(A)** *B. subtilis* and **(B)** *S. aureus* cells untreated or treated with 4 times the MIC of **7b-BF_4** after 45, 90, and 180 minutes.

(40). We showed inactivation curves for up to about 99.9% reduction, as this is considered the endpoint defining the complete eradication of an organism (41, 42) as a complete eradication is not readily achievable (43). However, we observed that *S. aureus* cells after 24 hours were completely inactive and we were unable to spot colonies in agar plates even when plating the equivalent of 10^5 CFU cells treated with compound.

3.4. 7b-BF_4 affects the four major macromolecular synthesis pathways

To investigate whether **7b-BF_4** targets the synthesis of specific, essential, macromolecules, cells were grown for 80 minutes, either with or without **7b-BF_4**, in the presence of radiolabeled precursors of macromolecule pathways (DNA, RNA, protein and peptidoglycan). **7b-BF_4** caused a sharp decrease in protein (leucine) and DNA (thymidine) synthesis (**Figure 4)**. However, RNA (uridine) and peptidoglycan synthesis (glucosamine) were also affected (**Figure 4)**. Although endpoint results are presented, in the case of RNA and peptidoglycan synthesis the incorporation of precursors was linear over time, and inhibition was proportional over the time curve, indicating that the inhibition is constant (not shown). These results indicate that **7b-BF_4** does not target one specific macromolecular synthesis pathway.

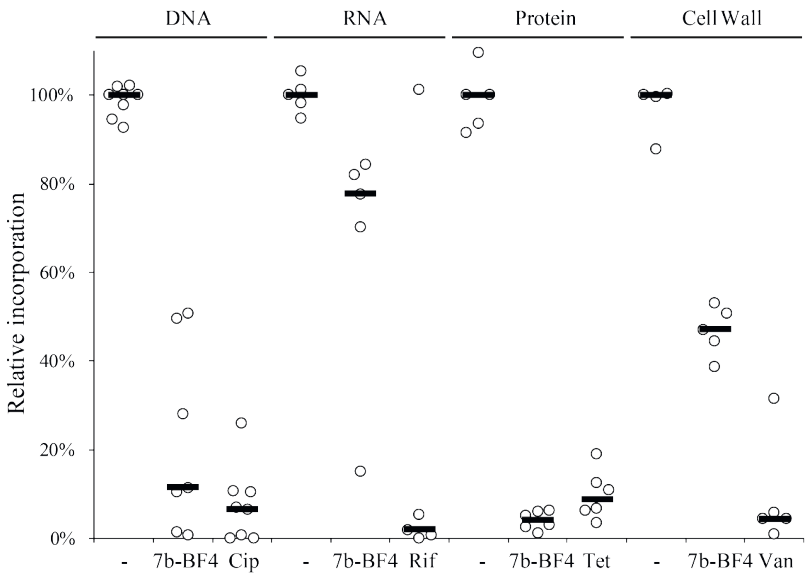

Figure 4: Effects of **7b-BF4** on the four major macromolecular synthesis pathways in comparison to negative controls (-) and antibiotics with specific activities targeting DNA, RNA, Protein, and peptidoglycan synthesis, Ciprofloxacin (Cip), Rifampicin (Rif), Tetracycline (Tet), and Vancomycin (Van) respectively. Each circle represents an experimental replicate, bars indicate the median relative incorporation at each condition tested.

3.5. 7b-BF4 affects HADA incorporation

In *B. subtilis*, the D-amino acid analogue HADA is incorporated at the 5th position of the pentapeptide of the peptidoglycan subunit, and can be used to show sites of peptidoglycan synthesis activity (25). To corroborate the results obtained with D[6^{3}H(N)]glucosamine hydrochloride, we used HADA labelling as a second test for peptidoglycan synthesis inhibition by **7b-BF4**. As expected, HADA incorporation was affected and eventually blocked in the presence of **7b-BF4** (**Table 5**). Compared to incorporation of ^{3}H-labelled glucosamine followed by scintillation counting, the observation of HADA using fluorescence microscopy is simpler and faster. Therefore, we also analyzed several different conditions, described in **Table 5**.

In a similar manner observed for glucosamine incorporation, we observed that the incorporation of HADA is visibly decreased when 0.43 µg/mL (1 × MIC) of **7b-BF4** is applied to exponentially growing

Table 5: Effect of **7b-BF4** in HADA incorporation.

Condition tested	Treatment time (min) (including labelling)	Labelling time (min)	HADA incorporation
Drug free	35	35	Yes
	35	5	Yes
	5	5	Yes
0.43 µg/mL **7b-BF4**	35	35	Yes
	5	5	Yes
	35	5	No
1.72 µg/mL **7b-BF4**	35	35	No
	5	5	No
	35	5	No
2.0 µg/mL Vancomycin	5	5	No
100 µg/mL Kanamicin	5	5	Yes

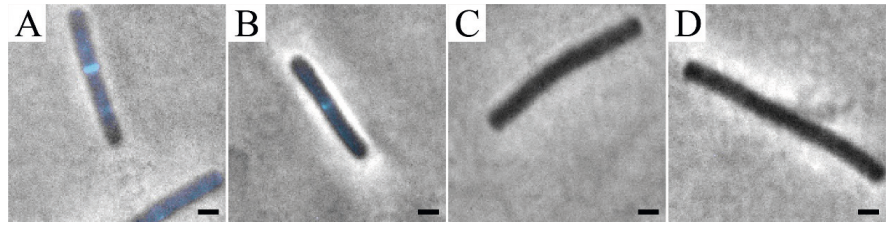

Figure 5: Overlays of phase contrast and HADA labelling (cyan) in the following conditions: **(A)** 35 min. **(B)** 35 min with 0.43 µg/mL **7b-BF4**. **(C)** 5 min with 1.72 µg/mL **7b-BF4**. **(D)** 5 min with 2 µg/mL vancomycin. Scale bar: 1 µm.

B. subtilis cells (**Figure 5A, B**). Cells that were previously treated with **7b-BF4** for 30 minutes prior to HADA labelling showed no incorporation of HADA. At an increased concentration of **7b-BF4** (1.72 µg/mL), there was no detectable HADA incorporation, even if the incubation period with **7b-BF4** was short. This was similar manner to what was observed for the peptidoglycan synthesis inhibitor vancomycin (**Figure 5C, D**).

These results indicate that HADA incorporation can be used as a fast and less laborious alternative to the classic radioactive glucosamine incorporation assay to detect inhibition of peptidoglycan synthesis.

3.6. 7b-BF_4 does not disrupt the permeability of the membrane

Most antibiotics target either DNA, RNA, protein, or peptidoglycan synthesis (*44*). However, some of them, such as polymixins, paenibacterin, and daptomycin target the cellular membrane, creating membrane pores (*45–47*). Pore formation affects all biosynthesis routes and thus could explain the effects detected in the incorporation assays. Pore formation can be detected with the bacterial viability kit Live/Dead BacLight, which is based on the use of two fluorescent DNA stains, one of which, SYTO 9, is membrane permeable, and one of which, propidium iodide, is membrane impermeable.

B. subtilis cells treated with **7b-BF_4** for 15 min were primarily green, a sign of intact membranes as this means only SYTO 9 has been able to bind DNA (**Table 6, A)**. A control experiment with the pore forming peptide nisin revealed orange cells, indicative of membrane damage which allowed propidium iodide to bind DNA and quench the SYTO 9 signal (**Table 6, B)**. Two concentrations of **7b-BF_4** were tested and no membrane damage was observed compared to the control when over 200 cells were analyzed, **Table 5**. Because the kit is meant to detect the viability of bacterial populations, one could think all green cells are viable. However, they can still maintain their membrane integrity for a short period of time while being metabolically inactive (*48*). This is likely to be the case in cells exposed to **7b-BF_4** at 4 × MIC (1.72 µg/mL) for 15 min shown in **Table 6**. For this reason we conclude that **7b-BF_4** does not affect membrane permeability.

3.7. 7b-BF_4 doesn't disrupt membrane potential

Next to pore formation, the dissipation of the membrane potential would affect membrane bound processes in the cell. The possible effect of **7b-BF_4** on the membrane potential was tested using the fluorescent dye $DiSC_3$. This fluorophore inserts into polarized membranes upon which fluorescence is quenched. Loss of membrane potential results in the release of the dye from membranes and thus an increase in fluorescence (*29*). This rapid increase in fluorescence of $DiSC_3$ was observed when *B. subtilis* cells were treated with nisin, whereas **7b-BF_4** at various concentrations gave results similar to the control (**Figure 6**). Thus, we conclude that **7b-BF_4** does not disrupt membrane potential.

Table 6: Membrane permeability of *B. subtilis* cells treated with **7b-BF_4** and nisin. **(A)** cell treated with **7b-BF_4** 1.72 µg/mL (4 × MIC). **(B)** Cell treated with nisin. Scale bar 1 µm.

Condition	Count	Green	Red/ Orange	Permeable
Control	240	228	12	5%
Nisin 5µg/mL	226	0	226	100%
7b-BF_4 0.43µg/mL	257	248	9	3.5%
7b-BF_4 1.72µg/mL	244	234	10	4.1%

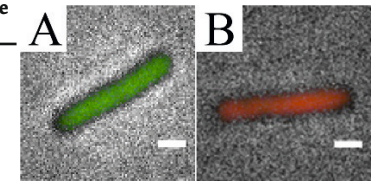

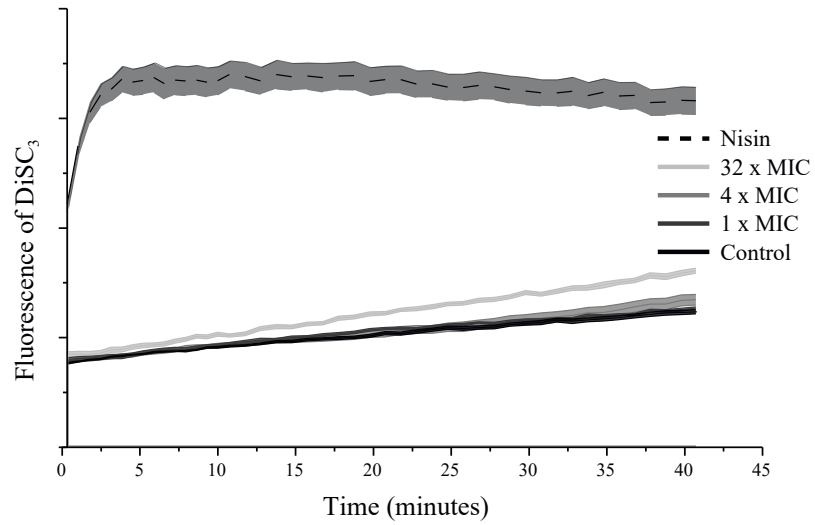

Figure 6: Fluorescence of $DiSC_3$ after treatments with 1.5 µg/mL nisin or several concentrations of **7b-BF_4**. Shaded areas represent the standard error.

3.8. 7b-BF_4 decreases intracellular ATP concentration

7b-BF_4 contains lansoprazole as a ligand for its two gold atoms. Lansoprazole is used to treat peptic diseases due to its inhibitory effect on vacuolar H-ATPases (*49*). Lansoprazole does not affect bacterial F-Type ATPases. However, it is shown that in *Mycobacterium tuberculosis* lansoprazole is converted into lansoprazole sulfide inhibiting cytochrome bc_1 and reducing intracellular ATP levels (*17*). The effect of **7b-BF_4** and lansoprazole on the ATP concentration in *B. subtilis* cells was determined using a luminescence assay. After 30 minutes in the presence of

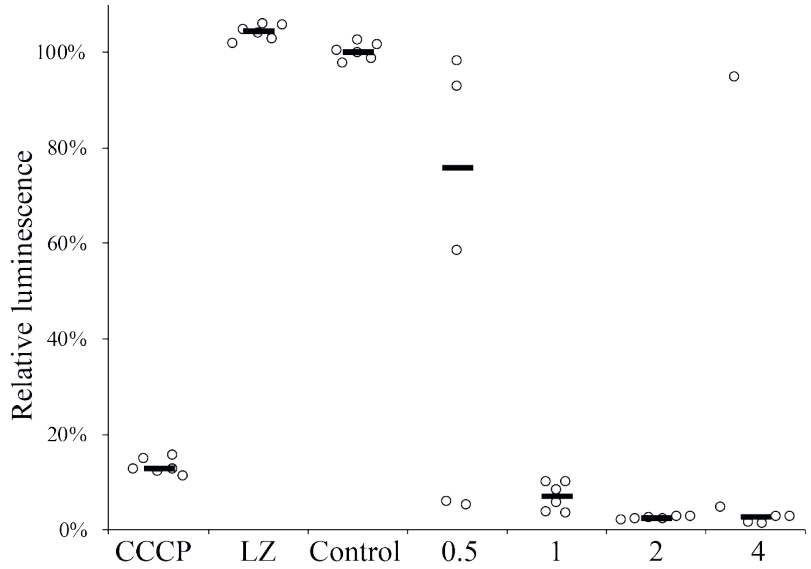

Figure 7: ATP concentration (relative light units) after 30 min treatments of *B. subtilis* cells with CCCP; Lansoprazole (LZ); or **7b-BF4** concentrations relative to the MIC concentration (0.5, 1, 2, or 4). 100% was defined as the median luminescence of the control sample (without any compound added), each circle represents a replicate, bars indicate the median of each condition tested.

8.8 µg/mL of lansoprazole the cellular ATP levels are similar to those of untreated cells, whereas **7b-BF4** caused a sharp drop in ATP, similar to the positive control CCCP (Carbonyl cyanide *m*-chlorophenyl hydrazone) (**Figure 7**). The result with lansoprazole (HL^2 in **Table 3**) is in accordance with it having no antimicrobial activity against *B. subtilis* (results not shown), Xac, *E. coli*, or *L. lactis* (**Table 3**). Therefore, the antimicrobial activity of **7b-BF4** is likely not to be caused by the lansoprazole scaffold but by the combination of the gold atoms and the triphenylphosphine moieties. The sharp decrease in ATP concentration caused by **7b-BF4** is a possible explanation for the fact that all the four macromolecular synthesis routes tested were affected by **7b-BF4**, because ATP is required for DNA, RNA, protein, and peptidoglycan synthesis.

We also determined cellular ATP concentrations after treatments of 5 minutes. Here, the decrease in ATP concentration was dependent on the concentration of **7b-BF4**, with a sharp decrease in cells treated with

4 times MIC and a lower decrease for lower concentrations. However, the variation between replicates was higher thus the accuracy of the experiment was lower (results not shown).

3.9. Effect of 7b-BF4 in subcellular localization of MinD, DivIVA, and RpsB

To further characterize the mode of action of **7b-BF4**, we tried to observe GFP-tagged proteins that can serve as markers for the mode of action of antibiotics (30). For example, GFP-MinD can be used as an indicator of intact membrane potential — normally localized at cell poles, GFP-MinD loses this location when membrane potential is disrupted (35). In agreement with the result of the membrane potential assay above (**Figure 6**), GFP-MinD localization was not affected by **7b-BF4**, whereas GFP-MinD localization was disrupted by nisin (**Figure 8A**).

We also observed that the localization of DivIVA is not disrupted even after 40 minutes in the presence of 1.72 µg/mL of **7b-BF4** (**Figure 8B**). This indicates that **7b-BF4** does not causes alterations in membrane curvatures as DivIVA binds to negatively curved membranes (50). We also observed that DivIVA localization is very stable, it is clearly seen in cells after treatments of 40 minutes with 1.5 µg/mL of nisin or 1.72 µg/mL of **7b-BF4**, that in those conditions are in their majority irreversibly inactivated.

7b-BF4 was able to block protein synthesis at 4 × MIC even more effectively than tetracycline at 10 × MIC (**Figure 4**). Therefore, we tested the localization of the ribosomal protein RpsB-GFP in the presence of either **7b-BF4** (4 × MIC) or tetracycline (10 × MIC). We observed that localization of RpsB-GFP is completely lost in the presence of **7b-BF4** (**Figure 8C**). This result is similar to the observations of RpsB-GFP in cells treated with rifampicin (RNA synthesis inhibitor) by Hunt *et al.* (51), while the treatment of *B. subtilis* with protein synthesis inhibitors such as tetracycline causes the nucleoid to compact (51), thus affecting RpsB-GFP characteristic localization, away from the nucleoid **Figure 8C**.

We could not draw conclusions from the localization pattern obtained from the other fluorescent protein fusions observed (YFP-FtsA, GFP-FtsZ, RpoC-GFP, PolC-GFP, GFP-MreB; GFP-MreD, GFP-MreC, SpooJ-GFP, and Hbs-GFP). This was due to the fact that the localization pattern was not visibly different between untreated cells and cells treated with

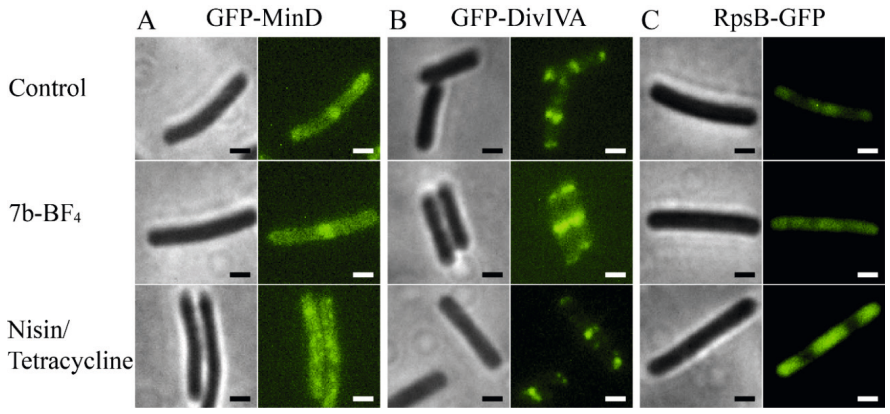

Figure 8: Subcellular localization of GFP labelled proteins in *B. subtilis* strains. **(A)** TB35 treated with **7b-BF4** or nisin for 5 minutes. **(B)** 1803 treated with **7b-BF4** or nisin for 40 minutes. **(C)** 1049 treated with **7b-BF4** or tetracycline for 5 minutes.

other compounds used as controls (nisin, rifampicin, or CCCP) which made it impossible to validate the localization assay for these fusions.

3.10. Probability of resistance is low

An assessment of the ability of an antimicrobial compound to select for resistant mutants is a crucial step in the development of an antibiotic (36). Additionally, we could get a hint about the mode of action of **7b-BF4** by characterizing resistant mutants. However, we were unable to generate mutants when seeding around 2×10^9 cells of *B. subtilis* cells in LB agar plates containing 21.5 µg/mL or 8.6 µg/mL of **7b-BF4**. In total 4 plates were made, and there were no colonies observed after 96 hours of incubation. Based on the number of cells tested, this result indicates that the chance of developing resistance through a single mutation event is lower than 10^{-8}. Resistance mutation frequencies higher than 10^{-6} could hamper the potential of **7b-BF4** as an antibiotic (36).

4. Discussion

The rapid development of antibiotic resistance warrants the search and discovery of compounds which target different aspects of bacterial growth and division (9). To this end, we screened 22 compounds for antimicrobial activity. Of these, **7b-BF4** presented the most potent

activity. **7b-BF4** killed the six Gram-positive bacteria tested, including multi drug resistant clinical isolates (MRSA and VRE). Further tests on *B. subtilis* revealed that **7b-BF4** does not target the cellular membrane nor disrupts membrane potential, but it affects DNA, RNA, protein, and peptidoglycan synthesis, and causes a sharp decrease in intracellular ATP concentration. Our results suggest that the mode of action of **7b-BF4** is to disrupt ATP synthesis, which is necessary for macromolecular synthesis.

The only antibiotic currently in use that targets ATP synthesis is bedaquiline that targets *Mycobacterium tuberculosis* (52). More recently, lansoprazole sulfate has also been reported to disrupt ATP production in *M. tuberculosis* (17). We tested the antimicrobial activity of **7b-BF4** on *B. subtilis*, which unlike *M. tuberculosis* is still able to undergo cell growth and division in the absence of an operon coding for ATP synthase using substrate level phosphorylation as a means of energy generation (53, 54). Substrate level phosphorylation is possible via glycolysis (53, 55), and in our experiments, **7b-BF4** killed *B. subtilis* in medium containing glucose (DMM) as effectively as medium without addition of glucose (LB). We also tested its activity against the anaerobic bacteria *L. lactis* in M17 medium, that contains glucose, and the MIC against this bacteria was in the same range as other Gram-positives tested. Therefore, we speculate that the decrease in ATP caused by **7b-BF4** is not (solely) from targeting F-type ATPases or other enzymes involved in ATP production via oxidative phosphorylation, like bedaquiline or lansoprazole sulfate. Additionally, drugs targeting ATPases bind at a specific region of the protein (56). This region is prone to changes via single-step mutation, which leads to resistance. Since we failed to obtain mutants resistant to **7b-BF4**, it is likely that the compound has multiple targets. Another possibility is that developing resistance to **7b-BF4** requires the modification of multiple enzymes. This is the case with vancomycin, which targets D-Ala-D-Ala amino acids in nascent peptidoglycan, for example (57). Alternatively, it could also be a target that does not mutate easily due to the mode of action, such as in the case of linezolid that targets protein synthesis by blocking the initiation complex (58). The propensity for selection of resistance for linezolid is lower than protein synthesis inhibitors that act by blocking the elongation complex (58).

While the exact mode of action of this compound is still unknown, our findings show that this gold-based compound causes intracellular ATP depletion, and this warrants further study. A possible approach is to use RNAseq, a technique that combines discovery and quantification of genes expressed in the cell (*59*). Among the four macromolecular synthesis pathways tested with radiolabels, RNA synthesis was the least affected, which is an indication that cells under stress caused by **7b-BF4** can still synthesize RNA, thus making RNAseq a promising approach in this case. Additionally, Jones *et al.* (*60*) used RNAseq analyses to show that genes are differentially expressed in *S. aureus* depending on the mode of action of the antibiotic with which the cells were treated. This approach might provide more comprehensive data about the mode of action of **7b-BF4**.

Another future perspective is to further stimulate development of resistance against **7b-BF4** in a setting in which resistance is more likely to occur, such as by using a morbidostat. This device consists of a chemostat that keeps the growth rate continuously constant by increasing antibiotic concentration over time and keeping the selective pressure constant (*61*). This device enables a higher degree of control and replication (*62*), and allowed the development of trimethoprim and chloramphenicol resistance in *E. coli* in a shorter amount of time when compared to the serial dilution method (*61*, *63*). Once obtained, resistant mutants can be sequenced and the mutations are likely to be related to the mode of action of the compound. Examples are FtsZ mutants of *S. aureus* resistant to the FtsZ inhibitor PC190723 (*64*), or cytochrome *bc1* mutants of *M. tuberculosis* resistant to the cytochrome inhibitor lansoprazole sulfate (*17*).

Another important aspect to be addressed before **7b-BF4** could be introduced to clinical use is the toxicity against human cells. **7b-BF4** is moderately toxic against rat kidney and liver tissue, with an TC_{50} of 6.9 µg/mL and 5.5 µg/mL respectively (*65*). The TC_{50} is the concentration of compound that causes a 50% decrease in ATP concentration on slices of tissue incubated 24 h with the compound. This indicates a potential nephrotoxic effect, similar to the currently used antibiotic colistin (*66*), and also a hepatotoxic effect. However, despite being moderately toxic, **7b-BF4** seems to be more toxic against Gram-positive bacteria than human cells. Additional studies characterizing the mechanism of toxicity could be helpful to understand the mode of action of this compound in bacteria, and eventually the compound could be modified to have lower toxicity and/or higher antimicrobial activity (*67*, *68*). One example is linezolid, that was developed from more toxic and less effective oxazolidinones (*69*).

In conclusion, we have shown that **7b-BF4** is a strong antimicrobial agent against Gram-positive bacteria. The mode of action of this compound is still unknown, but it seems to be different from other known antibiotics and further tests are needed to characterize its mode of action.

5. Acknowledgments

We are grateful to Danae Morales Angeles for help with lab work, Alwin Hartman and Anna Hirsch for HADA synthesis, Rieza Aprianto and Jan-Willem Veening for lending the Tecan luminometer, Tjalling Siersma and Leendert Hamoen (University of Amsterdam), for donating the *B. subtilis* strains used for subcellular localization, and Stephanie Jurburg for proof reading and structuring parts of the manuscript.

6. References

1. D. Acemoglu, S. Johnson, Disease and development: the effect of life expectancy on economic growth. *Journal of political Economy* **115**, 925–985 (2007).
2. M. Barber, M. Rozwadowska-Dowzenko, Infection by penicillin-resistant staphylococci. *The Lancet* **252**, 641–644 (1948).
3. S. Sengupta, M. K. Chattopadhyay, H.-P. Grossart, The multifaceted roles of antibiotics and antibiotic resistance in nature. *Frontiers in microbiology* **4**, (2013).
4. C. L. Ventola, The antibiotic resistance crisis: part 1: causes and threats. *Pharmacy and Therapeutics* **40**, 277 (2015).
5. H. C. Neu, The crisis in antibiotic resistance. *Science* **257**, 1064–1074 (1992).
6. G. M. Rossolini, F. Arena, P. Pecile, S. Pollini, Update on the antibiotic resistance crisis. *Current opinion in pharmacology* **18**, 56–60 (2014).
7. S. B. Singh, K. Young, L. Miesel, Screening strategies for discovery of antibacterial natural products. *Expert review of anti-infective therapy* **9**, 589–613 (2011).
8. S. B. Singh, J. F. Barrett, Empirical antibacterial drug discovery—foundation in natural products. *Biochemical pharmacology* **71**, 1006–1015 (2006).
9. S. Donadio, S. Maffioli, P. Monciardini, M. Sosio, D. Jabes, Antibiotic discovery in the twenty-first century: current trends and future perspectives. *The Journal of antibiotics* **63**, 423–430 (2010).
10. C. Orvig, M. J. Abrams, Medicinal inorganic chemistry: introduction. *Chemical Reviews* **99**, 2201–2204 (1999).
11. M. Serratice *et al.*, Gold (I) compounds with lansoprazole-type ligands: synthesis, characterization and anticancer properties in vitro. *MedChemComm* **5**, 1418–1422 (2014).
12. J. W. Sigler *et al.*, Gold salts in the treatment of rheumatoid arthritis: a double-blind study. *Annals of Internal Medicine* **80**, 21–26 (1974).
13. S. Norn, H. Permin, P. Kruse, E. Kruse, History of gold-with danish contribution to tuberculosis and rheumatoid arthritis. *Dansk Medicinhistorisk Arbog* **39**, 59–80 (2011).
14. P. M. Bruno *et al.*, A subset of platinum-containing chemotherapeutic agents kills cells by inducing ribosome biogenesis stress. *Nature Medicine*, (2017).
15. B. Rosenberg, L. Van Camp, T. Krigas, Inhibition of cell division in Escherichia coli

by electrolysis products from a platinum electrode. *Nature* **205**, 698–699 (1965).
16. B. Rosenberg, L. Vancamp, J. E. TROSKO, V. H. MANSOUR, Platinum compounds: a new class of potent antitumour agents. *Nature* **222**, 385–386 (1969).
17. J. Rybniker *et al.*, Lansoprazole is an antituberculous prodrug targeting cytochrome bc1. *Nature communications* **6**, (2015).
18. E. Lew, pharmacokinetic concerns in the selection of anti-ulcer therapy. *Alimentary pharmacology & therapeutics* **13**, 11–16 (1999).
19. C. Federici *et al.*, Exosome release and low pH belong to a framework of resistance of human melanoma cells to cisplatin. *PloS one* **9**, e88193 (2014).
20. J. M. Andrews, Determination of minimum inhibitory concentrations. *Journal of antimicrobial Chemotherapy* **48**, 5–16 (2001).
21. N. W. Schaad *et al.*, Emended classification of xanthomonad pathogens on citrus. *Papers in Plant Pathology*, 96 (2006).
22. A. R. da Silva *et al.*, Comparison of the genomes of two Xanthomonas pathogens with differing host specificities. *Nature* **417**, 459–463 (2002).
23. S. Somma, L. Gastaldo, A. Corti, Teicoplanin, a new antibiotic from Actinoplanes teichomyceticus nov. sp. *Antimicrobial agents and chemotherapy* **26**, 917–923 (1984).
24. B. D. Davis, E. S. Mingioli, Mutants of Escherichia coli requiring methionine or vitamin B12. *Journal of bacteriology* **60**, 17 (1950).
25. E. Kuru *et al.*, In situ probing of newly synthesized peptidoglycan in live bacteria with fluorescent D-amino acids. *Angewandte Chemie International Edition* **51**, 12519–12523 (2012).
26. E. Król *et al.*, Antibacterial activity of alkyl gallates is a combination of direct targeting of FtsZ and permeabilization of bacterial membranes. *Frontiers in Microbiology* **6**, (2015).
27. M. B. Tol, D. M. Angeles, D.-J. Scheffers, In vivo cluster formation of nisin and Lipid II is correlated with membrane depolarization. *Antimicrobial agents and chemotherapy* **59**, 3683–3686 (2015).
28. E. Breukink *et al.*, Use of the cell wall precursor lipid II by a pore-forming peptide antibiotic. *Science* **286**, 2361–2364 (1999).
29. P. J. Sims, A. S. Waggoner, C.-H. Wang, J. F. Hoffman, Mechanism by which cyanine dyes measure membrane potential in red blood cells and phosphatidylcholine vesicles. *Biochemistry* **13**, 3315–3330 (1974).
30. A. Müller *et al.*, Daptomycin inhibits cell envelope synthesis by interfering with fluid membrane microdomains. *Proceedings of the National Academy of Sciences* **113**, E7077-E7086 (2016).
31. H. B. Thomaides, M. Freeman, M. El Karoui, J. Errington, Division site selection protein DivIVA of Bacillus subtilis has a second distinct function in chromosome segregation during sporulation. *Genes & development* **15**, 1662–1673 (2001).
32. P. Gamba, J.-W. Veening, N. J. Saunders, L. W. Hamoen, R. A. Daniel, Two-step assembly dynamics of the Bacillus subtilis divisome. *Journal of bacteriology* **191**, 4186–4194 (2009).
33. P. J. Lewis, S. D. Thaker, J. Errington, Compartmentalization of transcription and translation in Bacillus subtilis. *The EMBO Journal* **19**, 710–718 (2000).
34. M. Leaver, J. Errington, Roles for MreC and MreD proteins in helical growth of the cylindrical cell wall in Bacillus subtilis. *Molecular microbiology* **57**, 1196–1209 (2005).
35. H. Strahl, L. W. Hamoen, Membrane potential is important for bacterial cell division. *Proceedings of the National Academy of Sciences* **107**, 12281–12286 (2010).
36. A. J. O'Neill, I. Chopra, Preclinical evaluation of novel antibacterial agents by microbiological and molecular techniques. *Expert opinion on investigational drugs* **13**, 1045–1063 (2004).
37. A. I. Chiriac *et al.*, Mode of action of closthioamide: the first member of the polythioamide class of bacterial DNA gyrase inhibitors. *Journal of Antimicrobial Chemotherapy*, dkv161 (2015).
38. Y. A. Elnakady *et al.*, Investigations to the antibacterial mechanism of action of kendomycin. *PloS one* **11**, e0146165 (2016).
39. L. L. Ling *et al.*, A new antibiotic kills pathogens without detectable resistance. *Nature* **517**, 455–459 (2015).
40. M. A. Lobritz *et al.*, Antibiotic efficacy is linked to bacterial cellular respiration. *Proceedings of the National Academy of Sciences* **112**, 8173–8180 (2015).
41. P. Taylor, F. Schoenknecht, J. Sherris, E. Linner, Determination of minimum bactericidal concentrations of oxacillin for Staphylococcus aureus: influence and significance of technical factors. *Antimicrobial Agents and Chemotherapy* **23**, 142–150 (1983).
42. R. J. Faville *et al.*, Staphylococcus aureus endocarditis: combined therapy with vancomycin and rifampin. *JAMA* **240**, 1963–1965 (1978).
43. V. Lorian, *Antibiotics in laboratory medicine*. (Lippincott Williams & Wilkins, 2005).
44. C. Walsh, *Antibiotics: actions, origins, resistance*. (American Society for Microbiology (ASM), 2003).
45. A. D. Berti *et al.*, Altering the proclivity towards daptomycin resistance in methicillin-resistant Staphylococcus aureus using combinations with other antibiotics. *Antimicrobial agents and chemotherapy* **56**, 5046–5053 (2012).
46. E. Huang, A. E. Yousef, The lipopeptide antibiotic paenibacterin binds to the bacterial outer membrane and exerts bactericidal activity through cytoplasmic membrane damage. *Applied and environmental microbiology* **80**, 2700–2704 (2014).
47. S. Pietschmann, K. Hoffmann, M. Voget, U. Pison, Synergistic effects of miconazole and polymyxin B on microbial pathogens. *Veterinary research communications* **33**, 489 (2009).
48. J. Trevors, Can dead bacterial cells be defined and are genes expressed after cell death? *Journal of microbiological methods* **90**, 25–28 (2012).
49. J. M. Shin, G. Sachs, Pharmacology of proton pump inhibitors. *Current gastroenterology reports* **10**, 528–534 (2008).
50. S. Halbedel *et al.*, Localisation of DivIVA by targeting to negatively curved membranes. *The EMBO journal* **28**, 2272–2282 (2009).
51. A. Hunt, J. P. Rawlins, H. B. Thomaides, J. Errington, Functional analysis of 11 putative essential genes in Bacillus subtilis. *Microbiology* **152**, 2895–2907 (2006).
52. K. Andries *et al.*, A diarylquinoline drug active on the ATP synthase of Mycobacterium tuberculosis. *Science* **307**, 223–227 (2005).
53. M. Santana *et al.*, Bacillus subtilis F0F1 ATPase: DNA sequence of the atp operon and characterization of atp mutants. *Journal of bacteriology* **176**, 6802–6811 (1994).
54. D. Bald, A. Koul, Respiratory ATP synthesis: the new generation of mycobacterial drug targets? *FEMS microbiology letters* **308**, 1–7 (2010).
55. P. R. Jensen, O. Michelsen, Carbon and energy metabolism of atp mutants of Escherichia coli. *Journal of bacteriology* **174**, 7635–7641 (1992).
56. S. Nesci, V. Ventrella, F. Trombetti, M. Pirini, A. Pagliarani, Thiol oxidation is crucial in the desensitization of the mitochondrial F 1 F O-ATPase to oligomycin and other macrolide antibiotics. *Biochimica et Biophysica Acta (BBA)-General Subjects* **1840**, 1882–1891 (2014).
57. T. Bugg, S. Dutka-Malen, M. Arthur, P. Courvalin, C. T. Walsh, Identification of vancomycin resistance protein VanA as a D-alanine: D-alanine ligase of altered substrate specificity. *Biochemistry* **30**, 2017–2021 (1991).
58. J. Prystowsky *et al.*, Resistance to linezolid: characterization of mutations in rRNA and comparison of their occurrences in vancomycin-resistant enterococci. *Antimicrobial agents and chemotherapy* **45**, 2154–2156 (2001).
59. A. Conesa *et al.*, A survey of best practices for RNA-seq data analysis. *Genome biology* **17**, 13 (2016).
60. M. B. Jones *et al.*, Reducing the bottleneck in discovery of novel antibiotics. *Microbial ecology* **73**, 658–667 (2017).
61. E. Toprak *et al.*, Evolutionary paths to antibiotic resistance under dynamically sustained drug selection. *Nature genetics* **44**, 101–105 (2012).
62. B. Regenbogen *et al.*, Rapid and consistent evolution of colistin resistance in XDR Pseudomonas aeruginosa during morbidostat culture. *Antimicrobial Agents and Chemotherapy*, AAC. 00043–00017 (2017).
63. T. Oz *et al.*, Strength of Selection Pressure Is an Important Parameter Contributing to the Complexity of Antibiotic Resistance Evolution. *Molecular Biology and Evolution* **31**, 2387–2401 (2014).
64. D. J. Haydon *et al.*, An Inhibitor of FtsZ with Potent and Selective Anti-Staphylococcal Activity. *Science* **321**, 1673–1675 (2008).
65. N. Estrada Ortiz, *Development of novel anticancer agents for protein targets*. (University of Groningen, Groningen, 2017), pp. 248.
66. A. Michalopoulos, S. Tsiodras, K. Rellos, S. Mentzelopoulos, M. Falagas, Colistin treatment in patients with ICU-acquired infections caused by multiresistant Gram-negative bacteria: the renaissance of an old antibiotic. *Clinical microbiology and infection* **11**, 115–121 (2005).
67. F. Li, J. G. Collins, F. R. Keene, Ruthenium complexes as antimicrobial agents. *Chemical Society Reviews* **44**, 2529–2542 (2015).
68. A. C. Komor, J. K. Barton, The path for metal complexes to a DNA target. *Chemical Communications* **49**, 3617–3630 (2013).
69. C. Ford, G. Zurenko, M. Barbachyn, The discovery of linezolid, the first oxazolidinone antibacterial agent. *Current Drug Targets-Infectious Disorders* **1**, 181–199 (2001).

Chapter 3 — Investigations on the mode of action of the antimicrobial compounds BC1 and T9A

André S. G. Lorenzoni[1], Luana G. Morão[2], Lúcia B. Cavalca[1,2], Guilherme Dilarri[2], Henrique Ferreira[2], Dirk-Jan Scheffers[1]

[1]Department of Molecular Microbiology, Groningen Biomolecular Sciences and Biotechnology Institute, University of Groningen, Groningen, Netherlands
[2]Department of Biochemistry and Microbiology, Institute of Biosciences, São Paulo State University, Rio Claro, SP, Brazil

Abstract

Xanthomonas citri subsp. *citri* (Xac) is the causal agent of citrus canker, a severe disease that affects citrus crops, decreases fruit production and is a major threat to the orange industry. The most effective way to control the disease is to eradicate infected trees. New antimicrobials are needed to combat citrus canker. To this end we explored the antimicrobial activity of chalcones. Chalcones are plant derived compounds, which belong to the class of flavonoids, which consist of two aromatic rings linked by an α,β-unsaturated ketone (enone bridge). In this chapter we present investigations on the mode of action of the methoxychalcone BC1 and the hydroxychalcone T9A against Xac and the model organism *Bacillus subtilis*. We have tested the minimum inhibitory activity (MIC) and, under the conditions tested, BC1 and T9A prevented growth of Xac and *B. subtilis* in concentrations varying from 20μg/mL to 40μg/mL. BC1 and T9A decreased incorporation of radiolabeled precursors of DNA, RNA, protein, and peptidoglycan in Xac and *B. subtilis*. The effect of the compounds on intracellular ATP concentration was small — intracellular ATP was not decreased in *B. subtilis* and slightly decreased in Xac. Finally, the effect of chalcones on cell division was tested using GFP fusions to cell division proteins, they were not disrupted in Xac but we did observe a disruption in the localization of FtsZ-GFP in *B. subtilis*. However, a subsequent FtsZ GTPase activity assay did not support a direct action on FtsZ. The data produced in this work do not allow us to draw a conclusion about a specific mode of action of the compounds tested and further research is required to understand the mode of action of this compounds in detail.

1. Introduction

Xanthomonas citri subsp. *citri* (Xac) is a bacterial phytopathogen that can infect nearly all the commercially important plants of sweet orange and is a major threat to their industry (*1*). This organism causes citrus canker, and the most effective way to control the disease is to eradicate infected trees. However, the pathogen can infect the trees before being detected (*2*). Sprays of copper-containing bactericides in the field are another measure of control, which have resulted in resistant strains (*3*). In addition copper is stable and accumulates in the soil which has a negative impact on bacterial richness (*4*).

New antimicrobials are needed to tackle the problem of phytopathogens infecting citrus plants. In this study, we focus on the antimicrobial activity of chalcones. Chalcones are plant derived compounds, which belong to the class of flavonoids, they are constituted by two aromatic rings linked by α,β-unsaturated ketone (enone bridge). There have been several studies reporting biological activities from the chalcones, including their potential use as antibiotics. Chalcones are secondary metabolites from plants. They are precursors of flavonoids and isoflavonoids that belong to the plant defense mechanisms, which prevent damage by microorganisms, insects and animals and counteract reactive oxygen species preventing molecular damage (*5*). Chalcones have antioxidant, anti-inflammatory, antitumor, antimitotic, cytotoxic, and anti-infection activities, as reviewed in (*6, 7*). Due to their relatively low redox potential, they have a great probability of undergoing electron transfer reactions.

Many chalcones have been studied for their antimicrobial activity (*5, 8*). Licochalcone A, naturally produced by the roots of *Glycyrrhiza inflata* has activity against *Bacillus subtilis* and *Staphylococcus aureus*, and is able to prevent their growth at 3 μg/mL. However, this compound shows no activity against Gram-negative bacteria (*9, 10*). Licochalcone A was shown to inhibit oxidation of NADH and oxygen consumption in *Micrococcus luteus* (*10*) and induce membrane permeability in *S. aureus* (*11*). Despite being inactive against Gram-negative bacteria, Licochalcone A is able to inhibit NADH oxydases in membranes isolated from *Escherichia coli* and *Pseudomonas aeruginosa* suggesting that the compound cannot penetrate the outer membrane (*10*). Accordingly, some chemically modified chalcones are effective against Gram-negative bacteria (*5, 11*)

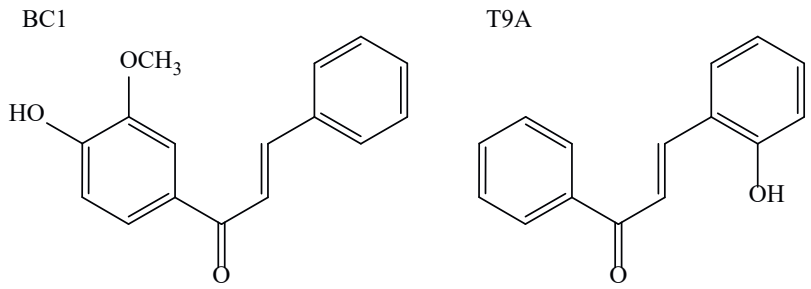

Figure 1: Structures of the compounds used in this study.

including *Mycobacterium tuberculosis* (*12*). The anti-tubercular activity is associated with inhibition of the protein tyrosine phosphatase B (*12*). Phloretin, a chalcone present in apple and kumquat, is effective only against Gram-positive bacteria (*13*). This compound inhibits acetate dehydrogenase, isocitrate dehydrogenase, and catalase from *S. aureus* (*13*). DNA gyrase was reported to be a target for synthetic chalcones active against both Gram-positive and Gram-negative bacteria (*14*).

In a recent study our collaborators identified and synthesized chalcones substituted by hydroxyl groups (hydroxychalcones) and tested their antibacterial activity against *S. aureus* and *Pseudomonas aeruginosa* (Ayusso *et al.*, in preparation). The most active compound against *S. aureus*, **T9A** (**Figure 1**, hydroxychalcone 5, **Table 1**), inhibited growth of both bacteria albeit with a 16 fold higher minimal inhibitory concentration (MIC) for the Gram-negative bacteria. As the minimal bactericidal concentration (MBC) for this compound could not be determined, it appears that T9A stops growth but does not kill the bacterial cells. **BC1**, a methoxychalcone, was synthesized by our collaborators inspired by a simplified curcumin compound with antibacterial activity (*15*) (**Figure 1**). As BC1 and T9A both display antimicrobial activity against Xac (see below), we decided to further characterize their mode of action. Here, we tested the influence of T9A and BC1 on macromolecular synthesis (DNA, RNA, protein, and peptidoglycan), ATP concentration, and membrane permeability using Xac and the Gram-positive model organism *B. subtilis*.

Table 1: Structures and minimum inhibitory concentration of hydroxychalcones synthesized and tested by (Ayusso *et al.*, in preparation). MIC50 is the concentration necessary to cause 50% decrease in resazurin reduction by *S. aureus* (Sa) or *P. aeruginosa* (Pa) cells after 24 hours in the presence of the compound, values displayed are in µg/mL.

Compound	MIC_{50} Sa	MIC_{50} Pa	R	R'
3	12.5	50.0	3'-hydroxyphenyl	phenyl
4	50.0	100	4'-hydroxyphenyl	phenyl
5 (T9A)	6.2	100	phenyl	2-hydroxyphenyl
6	25.0	50.0	phenyl	3-hydroxyphenyl
vancomycin	2.0	-	-	-
gentamicin	-	4.0	-	-

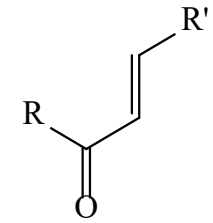

2. Methods

2.1. Minimal inhibitory concentration assays

The minimal inhibitory concentration (MIC) of compounds (**Figure 1**) was tested by broth microdilution. BC1 and T9A were tested against Xac and *B. subtilis*.

Exponentially growing bacteria were diluted to OD_{600} of 0.005 in 96 well plates containing two-fold serial dilutions of the compounds, in a final volume of 200µL of growth medium. Davis Minimal Medium (DMM): casamino acids 2.0g/L; K_2HPO_4 7.0g/L; KH_2PO_4 3.0g/L; $MgSO_4 \cdot 7(H_2O)$ 0.1g/L; $(NH_4)2SO_4$ 1.0g/L; $Na_3C_6H_5O_7 \cdot 2(H_2O)$ 0.5g/L; glucose 7.0g/L and tryptophan 10mg/L; modified from (*16*, *17*), was used for *B. subtilis*. Xam1 medium: glycerol 2.46g/L; $MgSO_4 \cdot 7H_2O$ 0.247g/L; $(NH_4)_2SO_4$ 1.0g/L; K_2HPO_4 10.5g/L; KH_2PO_4 4.5g/L; $Na_3C_6H_5O_7 \cdot 2H_2O$ 0.5g/L; casamino acids 0.3g/L; BSA 1g/L; (pH 5.4 adjusted with HCl) was used for Xac. The MIC was defined as the lowest concentration of compound that prevented bacterial growth after incubating 24 hours at 30°C (*18*).

2.2. Membrane permeability assay

Membrane permeability was tested using the commercial assay Live/Dead BacLight bacterial viability kit (Thermo-Scientific). An overnight culture of *B. subtilis* grown in LB, or Xac grown in NYGB (**Chapter 2**), at 29°C, was diluted to 10^6 cells per mL. *B. subtilis* cells were incubated

in the presence of BC1 (50µg/mL), T9A (40µg/mL), DMSO (1%) as a negative control, and nisin (5.0 µg/mL) as a positive control; Xac cells were incubated in the presence of BC1 (90µg/mL), T9A (50µg/mL), DMSO (1%) as a negative control, and 20min at 60°C as a positive control; for 15min and 30min at 23°C. Propidium iodide (5.0mM) and SYTO 9 (835µM) were added to each test. After incubation, cells were mounted on agarose pads for microscopy analysis and the green and red fluorescence were imaged using an Olympus BX61 microscope with an OrcaFlash-2.8 camera using DAPI/FITC and Texas Red fluorescence filter cubes. Propidium iodide (shown in Texas Red fluorescence filter) is membrane impermeable and thus only stains cells with disrupted membrane, whereas SYTO 9 (shown in DAPI/FITC fluorescence filter) is membrane permeable and stain all the cells. The Olympus cellSens platform was used for image analysis.

2.3. Macromolecular synthesis

Four macromolecular synthesis pathways were evaluated by monitoring the incorporation of radioactively labelled precursors. [5^{3}H] uridine, [methyl^{3}H]thymidine, L[3,4,5^{3}H(N)]leucine and D[6^{3}H(N)] glucosamine hydrochloride (all at 0.5µCi/mL) were used to respectively monitor RNA, DNA, protein and peptidoglycan synthesis. During this experiment *B. subtilis* cells were grown to early exponential phase in DMM and Xac cells were grown to early exponential phase in Xam1. 1mM of non-labelled precursor was used for RNA and peptidoglycan and 10µM was used for DNA and protein. For DNA incorporation, *B. subtilis* cells were grown in LB medium instead of DMM.

Cells were incubated in the presence of labelled precursors for up to 80minutes with shaking at 30°C. *B. subtilis* was tested in the presence of 40µg/mL of BC1 or T9A, without compound (negative control), or with an antibiotic known to inhibit the synthesis pathway tested as a positive control (RNA: rifampicin 0.625µg/mL, DNA: ciprofloxacin 0.625µg/mL, protein: tetracycline 10µg/mL, peptidoglycan: vancomycin 1.0µg/mL). Xac was tested in the presence of 30µg/mL of BC1, 20µg/mL of T9A, without compound (negative control), or with an antibiotic supposed to inhibit the synthesis pathway tested as positive control (RNA: rifampicin 0.625µg/mL, DNA: ciprofloxacin 10.0µg/mL, protein: tetracycline 10µg/mL, peptidoglycan: penicillin G 800µg/mL).

For every precursor tested, at least 8 technical replicates were taken, from 4 biological replicates. During incubation, aliquots were taken and precipitated with ice-cold 12% trichloroacetic acid for 35min and then filtered through nitrocellulose membranes (pore size 0.45 µm). The filters were washed with ice cold 12% trichloroacetic acid, transferred to 2mL scintillation fluid Ultima Gold MV (PerkinElmer), and measured in a Tri-Carb 2000CA liquid scintillation analyzer (Packard Instruments).

2.4. Resazurin assay

The Resazurin assay (REMA) was performed in order to evaluate the impact of the compounds on the respiratory activity after a short period of time. Cells of *B. subtilis* or Xac were incubated in contact with resazurin in the same medium used for MIC evaluations (DMM and Xam1 respectively) in 96-well plates. The compound BC1 was used at a final concentration of 40µg/mL for *B. subtilis* and 30µg/mL for Xac; T9A was used at 40µg/mL for *B. subtilis* and 20µg/mL for Xac. Rifampicin 0.625µg/mL, ciprofloxacin 0.625µg/mL, tetracycline 10 µg/mL, and vancomycin 1.0µg/mL were used as controls for *B. subtilis* and rifampicin 0.625µg/mL, ciprofloxacin 10.0µg/mL, tetracycline 10µg/mL, and penicillin G 800 µg/mL were used as controls for Xac, along with samples without added compound. Resazurin was added to a final concentration of 0.1mg/mL. Fluorescence (excitation 530nm, emission 560nm, bandwidth 9nm) was recorded every 20min up to 120min in a BioTek Synergy Mx 96-well plate reader.

2.5. Intracellular ATP concentration assay

ATP levels were measured in *B. subtilis* and Xac using the BacTiter-Glo™ Microbial Cell Viability Assay (Promega). CCCP (Carbonyl cyanide *m*-chlorophenyl hydrazine, 40µg/mL) was used as a positive control for ATP depletion in Xac, and 7b-BF_4 (**Chapter 2**) was used as control for ATP depletion in *B. subtilis* (1.72µg/mL). The cells were incubated in a 96 well plate (30°C, 1000rpm), 30min for *B. subtilis* (in DMM) and 80min for Xac (in Xam1) after which 100µL of cell culture was added to 100µL of BacTiter-Glo™ Reagent for 5minutes in a white 96 well plate (26°C, 1000rpm). Luminescence was measured in a Tecan Infinite F200 Pro luminometer. The amount of light emitted is a measure for the intracellular ATP concentration.

2.6. FT-IR spectrophotometry

Fourier-transform infrared (FT-IR) spectrophotometry was done on *B. subtilis* cells in a FT-IR spectrophotometer (Shimadzu, model 8300), as described by Morão *et al.* (15). Cells were cultivated in LB medium (29 °C) up to the concentration of 10^5 cells/mL, then treated with BC1 (50 µg/mL), T9A (40 µg/mL), nisin (5 µg/mL), or a negative control without addition of extra compounds for 30 min. Aliquots of 1.5 mL of cells were then centrifuged at 10 000 g for 2 min, washed with water and centrifuged two more times to remove traces of medium. After that, the samples were mixed with 150 mg of KBr, dried at 50 °C for 24 h, homogenized and compressed at 40 kN for 5 min. Absorbance was measured from 400 cm^{-1} to 4000 cm^{-1}, with 32 scans at a resolution of 4 cm^{-1}. Data treatment and analyses were performed using the software Origin 8.00.

2.7. Cell division investigations

The effect of chalcones on cell division was investigated using GFP fusions to cell division proteins, and by evaluating the GTPase activity of FtsZ from *B. subtilis*.

Xac labeled with GFP-ZapA (Xac *amy::gfp-zapA*, **Chapter 4, Table 1**) was grown in NYGB and induced with Xylose (0.5%) for 90 min. Cells were treated with BC1 (90 µg/mL), T9A (50 µg/mL), DMSO (1%, as a negative control) or hexyl gallate (60 µg/mL, as a positive control) for 30 min and samples were prepared and visualized in the microscope as described in section 2.2. GFP fluorescence was visualized in GFP filter cubes.

B. subtilis labeled with FtsZ-GFP (15) was cultivated in presence of 0.02 mM IPTG (isopropyl-β-D-1-thiogalactopyranoside) to induce the expression of the protein fusion from *pspac* promoter. Cells were treated with BC1 (50 µg/mL), T9A (40 µg/mL), DMSO (1%) as a negative control, and hexyl gallate (60 µg/mL) as a negative control for 15 and 30 minutes. Samples were prepared and visualized in the microscope as described in section 2.2. GFP fluorescence was visualized in GFP filter cubes.

FtsZ from *B. subtilis* was expressed and purified using the ammonium sulfate precipitation method as described by Mukherjee & Lutkenhaus (19) and Król & Scheffers (20). The FtsZ GTP hydrolysis rate was determined using the malachite green phosphate assay as described by Król *et al.* (21), with a few modifications. Stocks of BC1 (50 µg/mL), T9A (40 µg/mL), and DMSO (1%) as a negative control, with FtsZ (24 µM), $MgCl_2$ (20 mM) and Triton X-100 (0.02%) prepared in polymerization buffer (Hepes 50 mM, KCl 300 mM, pH 7.5) were stabilized at 30 °C for 5 min. Then, GTP dissolved in the same buffer was added (1 mM final concentration) at different time points (0, 2.5, 5, 10, 15, 20, and 30 min). The reactions were kept at 30 °C and developed in accordance with Malachite Green Phosphate Assay Kit (MAK307, SigmaAldrich).

2.8. Stimulation of resistance

For resistance development by sequential passaging, 2 parallel populations of Xac were diluted in NYGB medium containing 2 fold serial dilutions of BC1 or T9A (starting with 10–160 µg/mL), during the exponential phase, similar to the method described by Oz *et al.* (22). Each day, those cells that grew at the highest concentration of drugs were diluted to fresh medium containing serial dilutions of antimicrobial. Dilutions were done after about 24 h of growth at 29 °C over a period of 23 days.

3. Results

3.1. Minimal inhibitory concentration

First, we needed to decide the minimum inhibitory concentration of BC1 and T9A for our chosen model organisms, Xac and *B. subtilis*, which was done by a standard broth microdilution assay (**Table 2**). Xac is slightly more sensitive to the compounds when compared to *B. subtilis*. Compared to the earlier results from our collaborators, we note that *B. subtilis* is less sensitive to BC1 as the Gram-positive model *S. aureus*, whereas Xac is more sensitive compared to the Gram-negative *P. aeruginosa*. However, as our collaborators assayed MIC by determining metabolic

Table 2: Minimal inhibitory concentrations of the compounds tested.

	Xac	*B. subtilis*
Drug	**MIC**	**MIC**
BC1	30 µg/mL	40 µg/mL
T9A	20 µg/mL	40 µg/mL

Table 3: Permeabilization of Xac and *B. subtilis* cells by chalcones and controls.

Condition	**Xac cells** (mean ± SD)	***B. subtilis* cells** (mean ± SD)
Negative control	2.38 ± 0.08%	2.86 ± 1.78%
DMSO 1%	2.95 ± 0.53%	4.02 ± 3.16%
BC1 (90/50µg/mL; 15min)	2.22 ± 1.34%	66.23 ± 0.62%
BC1 (90/50µg/mL; 30min)	6.98 ± 1.67%	75.32 ± 0.28%
T9A (50/40µg/mL; 15min)	2.91 ± 0.89%	3.67 ± 0.63%
T9A (50/40µg/mL; 30min)	3.86 ± 0.22%	4.81 ± 3.29%
Heat shock (60°C; 20min)	97.16 ± 0.76%	not done
Nisin (5.0g/mL; 15min)	not done	97.22 ± 2.72%

Results from two independent replicates with 200 cells each.

activity after incubation for 24h with the drug using resazurin, the results cannot be directly compared (short incubations already strongly affect the metabolic activity of the cells, see below). We used the MIC values to guide our assays to determine the drugs' mode of action.

3.2. Membrane permeability

Then, we tested whether these compounds are capable of disrupting the membrane, which is a mode of killing that we observed earlier with gallic acid derivatives, compounds with aromatic rings (*23*, *24*). T9A had no effect on the membrane of both *B. subtilis* and Xac, whereas BC1 did not affect Xac but did affect *B. subtilis* membranes (**Table 3**). The last observation in combination with the fact that BC1 has a slightly lower MIC for Xac than for *B. subtilis*, suggests that its mode of action may be different between the two organisms.

Images of Xac and *B. subtilis* cells stained with propidium iodide and SYTO 9 can be seen in **Figure S1**.

3.3. Macromolecular synthesis

Subsequently, we tested whether BC1 or T9A inhibit the synthesis of the macromolecules DNA, RNA, proteins and peptidoglycan using radiolabeled precursors of each macromolecule and following their incorporation. Although these assays are common practice in antibiotics research we needed to establish conditions for Xac as this bacterium

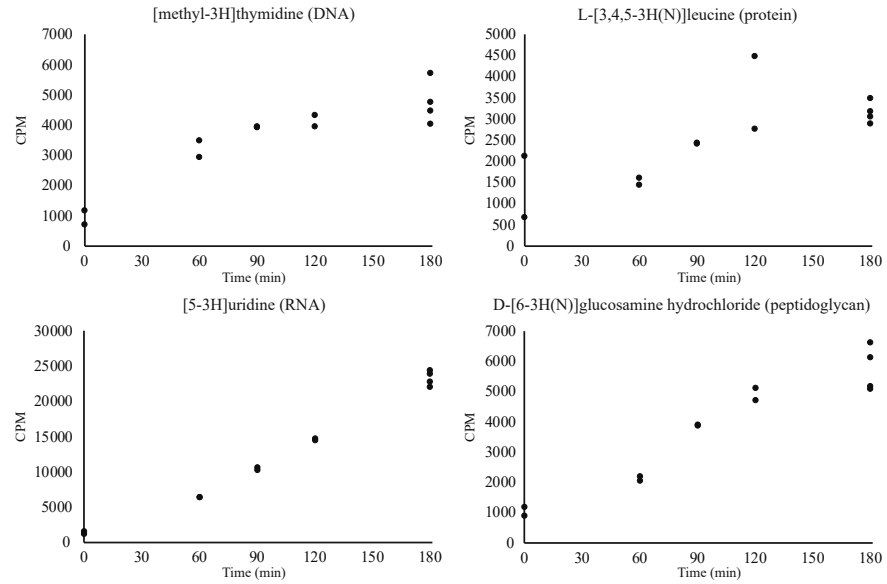

Figure 2: Incorporation of radiolabels in Xac over time. Cells were grown in Xam1 at 30°C without antimicrobial compounds. Each circle is a replicate.

grows slower than organisms such as *B. subtilis* and *E. coli*, which are routinely used for these assays. It turned out that a period of 80min was sufficient to measure label incorporation, and that incorporation over this time period was linear (**Figure 2**) indicating that the bacteria continued growing under the experimental conditions used. As control for each macromolecular synthesis pathway, an antibiotic was included that targets the specific pathway. Because BC1 and T9A were tested at MIC, the MICs for the control antibiotics were determined — and penicillin instead of vancomycin was used to inhibit peptidoglycan synthesis in Xac.

Results of each of the macromolecular synthesis pathways tested can be seen in **Figure 3**. As is evident, both compounds inhibit all pathways to some extent in both Xac and *B. subtilis,* with the sole exception of T9A that does not affect DNA synthesis in *B. subtilis*. Also, in all cases BC1 is more effective at blocking macromolecular synthesis than T9A. Finally, whereas all control antibiotics are very effective in blocking their respective pathways in *B. subtilis*, the block is not so strong in

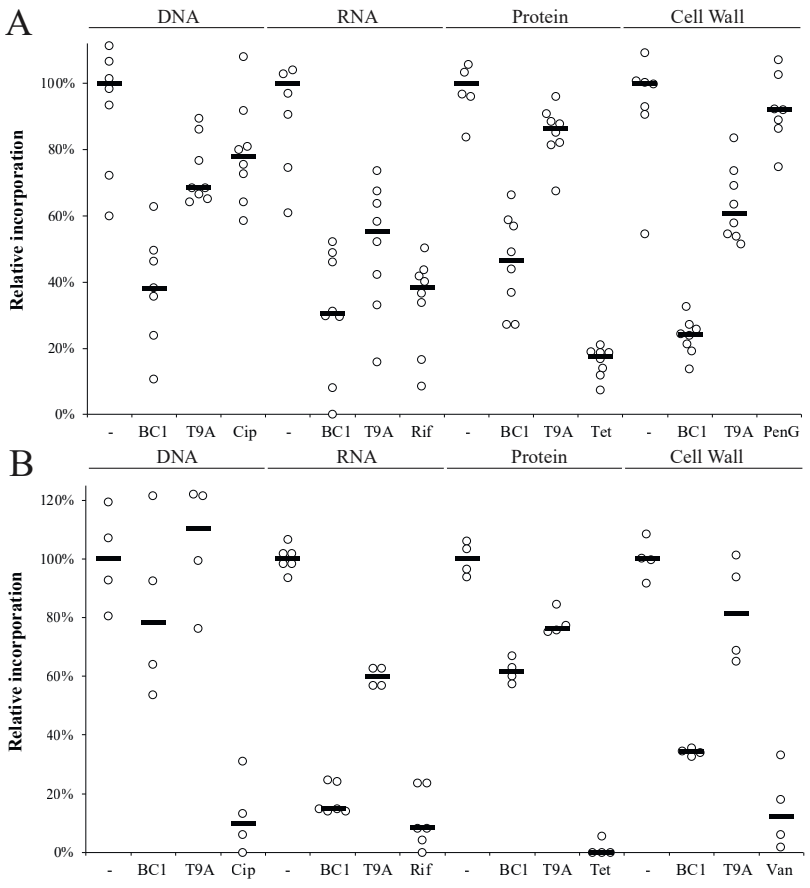

Figure 3: Effects of BC1 and T9A on the four major macromolecular synthesis pathways of: **A** Xac, **B** *B. subtilis*, in comparison to negative controls (-) and antibiotics with specific activities targeting DNA, RNA, Protein, and Peptidoglycan synthesis, Ciprofloxacin (Cip), Rifampicin (Rif), Tetracycline (Tet), and: **A** Benzyl penicillin (PenG), **B** Vancomycin (Van), respectively. Each circle represents an experimental replicate; bars indicate the median relative incorporation at each condition tested.

Xac with only tetracyclin blocking protein synthesis almost completely (see discussion).

3.4. Resazurin assay

To determine whether the inhibition of macromolecular synthesis was specific or caused by cells dying, the metabolic activity of the

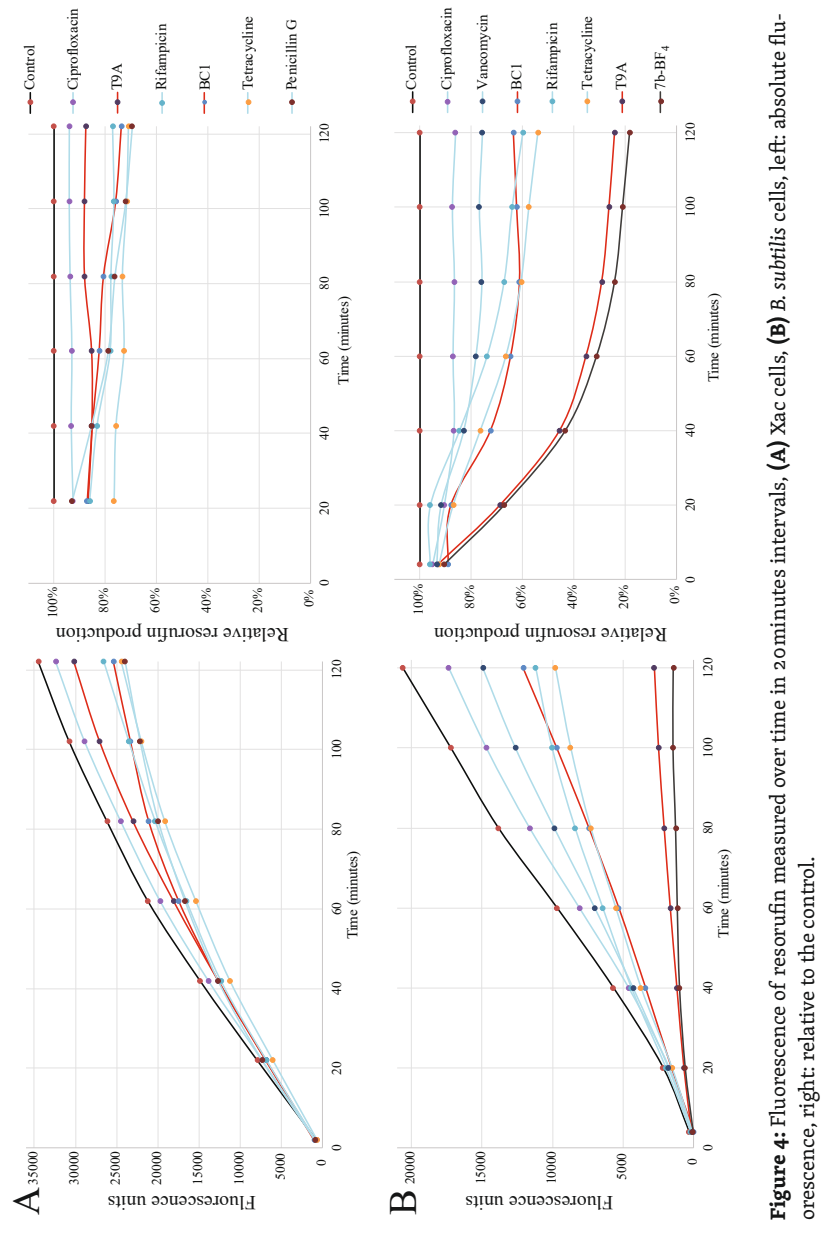

Figure 4: Fluorescence of resorufin measured over time in 20 minutes intervals, **(A)** Xac cells, **(B)** *B. subtilis* cells, left: absolute fluorescence, right: relative to the control.

cells in the presence of BC1, T9A and pathway specific antibiotics was measured using the REMA assay. This assay is based on the reduction of resazurin to resorufin as a result of bacterial respiration (25). Cells (Xac or *B. subtilis*) were mixed with the compounds/antibiotics and their metabolic activity was measured in 20 minutes intervals for up to 120 minutes (**Figure 4**). For Xac, this showed that even though there was some inhibition of metabolic activity, this did not go below 75% of uninhibited activity, nor displayed a large decline over the 2 h that activity was followed. Thus, inhibition of synthesis pathways to levels below 70% in **Figure 3** is not caused by overall cell death. For *B. subtilis* the results were different, and rather puzzling. T9A almost completely blocked metabolic activity, similar to control compound 7b-BF_4, which is striking as the effect of T9A on macromolecular synthesis in *B. subtilis* was not very pronounced. BC1 reduced the respiration to about 60%.

3.5. Intracellular ATP concentration

The relative intracellular ATP levels were determined in Xac and *B. subtilis* after 80 or 30 min of compound treatments, respectively (Shown in **Figure 5**). At 1×MIC, T9A and BC1 cause a decrease in Xac ATP levels compared to control to a similar extent as their effect on overall respiratory activity. BC1, at two times MIC led to a complete loss of ATP, when compared to the control CCCP (**Figure 5A**). Strikingly, in *B. subtilis* the ATP levels increased, which is especially surprising given the loss of metabolic activity caused by T9A (**Figure 5B**). This suggests that in the presence of these compounds cells may switch to anaerobic metabolism, together with an inhibition of ATP-consuming pathways.

3.6. FT-IR spectrophotometry

FT-IR of *B. subtilis* cells treated with BC1 and T9A was measured, together with a negative control and a positive control with nisin (shown in **Figure 6**). FT-IR is a technique that can provide a 'fingerprint' of different components of the bacterial cell, and thus can also report on the disruption of cellular structures (15). The peaks shown in the spectrum represent perturbations of diverse chemical structures from compounds present in *B. subtilis* (26). The peaks at 1083 cm^{-1} are due to stretching of C-O bonds present in glycogen and PO_2^- symmetric stretching present in nucleic acids and phospholipids. The peaks at

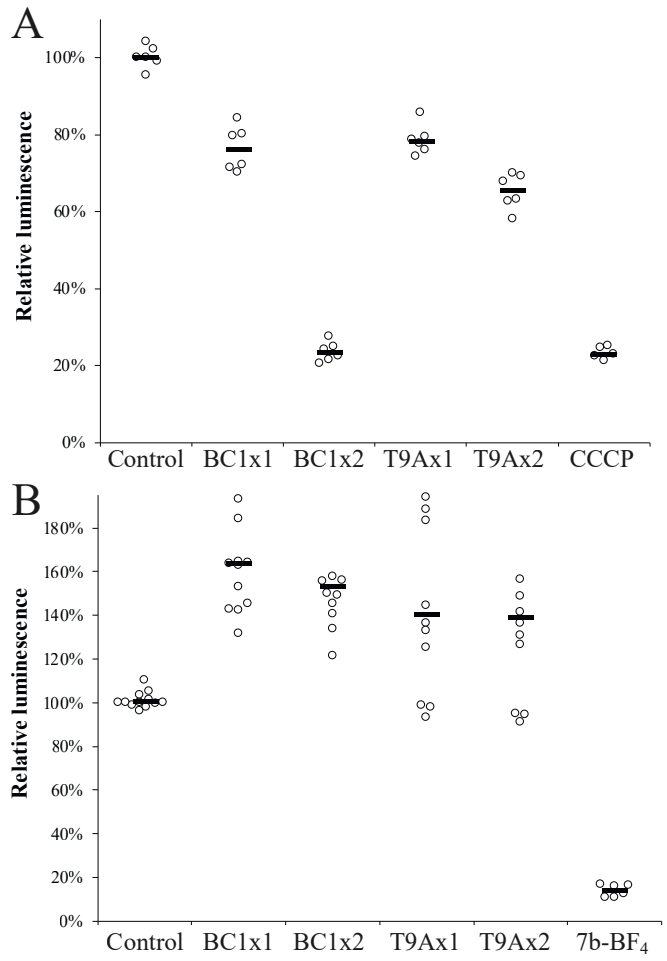

Figure 5: ATP concentration (relative light units): **A** (after 80 minutes treatments of Xac cells), **B** (after 30 min treatments of *B. subtilis* cells), with 1x and 2x the MIC of BC1 or T9A or 40 µg/mL of CCCP. 100% was defined as the median luminescence of the control sample (without any compound added), each circle represents a replicate, bars indicate the median of each condition tested.

1231 cm^{-1} are due to PO_2^- asymmetric stretching, mainly from nucleic acids with little contribution from phospholipids. The peaks at 1404 cm^{-1} corresponds to COO^- symmetric stretching from aminoacid side chains and fatty acids. The peaks at 1450 cm^{-1} are due to CH_2 bending from lipids. The peaks at 1540 cm^{-1} are from N-H bending and C-N

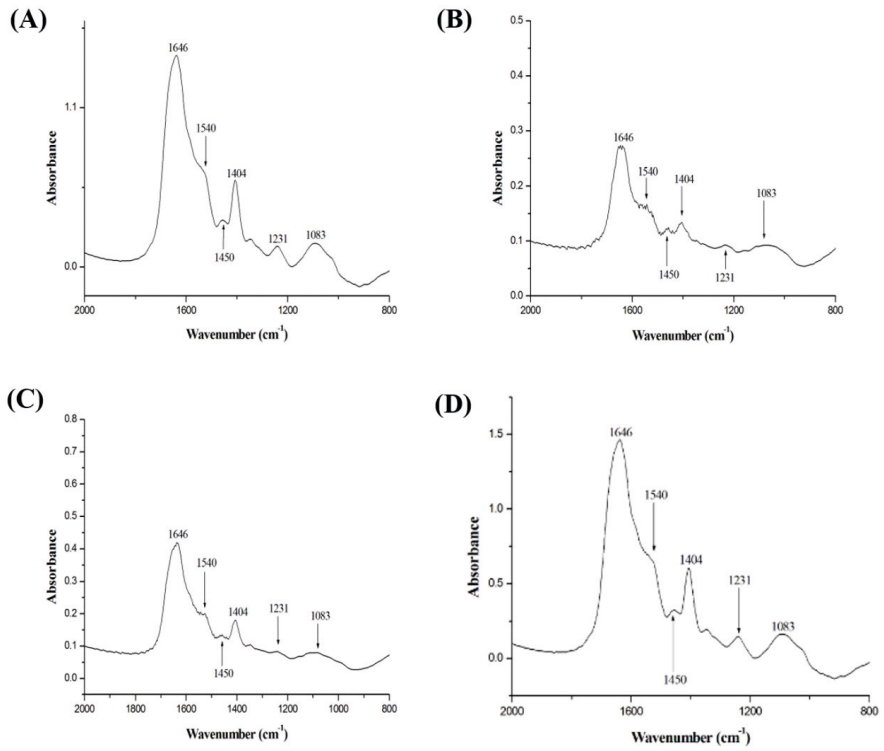

Figure 6: FT-IR spectra of *B. subtilis* cells after 30 minutes treatments with **(A)** no compounds added; **(B)** nisin (5 µg/mL); **(C)** BC1 (50 µg/mL); and **(D)** T9A (40 µg/mL).

stretching from amide II present in α helixes of proteins. Finally, the peaks at 1646 cm^{-1} are from C=O stretching from amide I α helixes (26). The intensity of the spectrum of the negative control (**Figure 6A**) was similar to the spectrum of the cells treated with T9A (**Figure 6D**), and the intensity of the spectrum of cells treated with nisin (**Figure 6B**) was similar to the spectrum of the cells treated with BC1 (**Figure 6D**).

We could not identify any obvious differences between the spectra regarding a particular peak. However, the similar intensities between the spectrum of the negative control and T9A and between BC1 and nisin, corroborates with the results of our membrane permeability assay (**Table 3**). In there we can see that T9A does not cause membrane disruption in *B. subtilis* whereas BC1 is able to disrupt the cellular membrane similar to nisin.

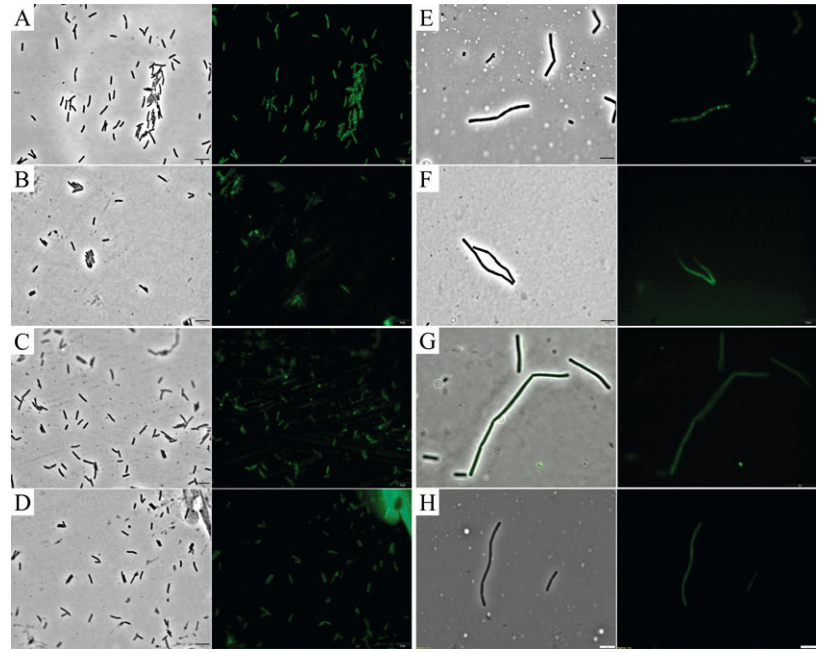

Figure 7: Phase contrast (left) and GFP (right) images of: Xac labeled with GFP-ZapA treated for 30 min with **(A)** 1% DMSO, **(B)** BC1 (90 µg/mL), **(C)** T9A (50 µg/mL), **(D)** hexyl gallate (60 µg/mL), and *B. subtilis* labeled with FtsZ-GFP treated for 30 min with **(E)** 1% DMSO, **(F)** BC1 (50 µg/mL), **(G)** T9A (40 µg/mL), **(H)** hexyl gallate (60 µg/mL). Scale bar: 5 µm.

We attempted to FT-IR on Xac cells as well. However, Xac produces xanthan gum and biofilms (27) generating noise on the spectra, thus preventing other compounds to be detected.

3.7. Cell division investigations

Our last attempt to find a specific cellular process targeted by the chalcones was focused on cell division. **Figure 7B-C** shows that the localization of GFP-ZapA, our marker for cell division, in Xac was not affected by BC1 or T9A.

Figure 7F-G shows that the localization of FtsZ-GFP, our marker for cell division, in *B. subtilis* was affected by both BC1 and T9A. Since BC1 is able to disrupt membrane permeability in *B. subtilis* (disrupting membrane potential as well), it is possible that FtsZ-GFP localization is disrupted due to membrane potential disruption (28). However, T9A

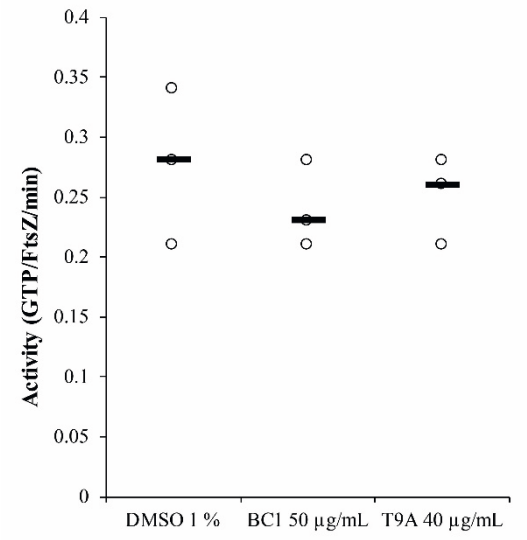

Figure 8: GTPase activity of FtsZ in the presence of DMSO, BC1, or T9A.

does not disrupt membrane permeability in *B. subtilis*, suggesting that the mode of action of T9A is linked to cell division. To investigate this in more detail we tested the effect of BC1 and T9A on the GTPase activity of FtsZ.

Figure 8 shows that the GTPase activity of FtsZ was not affected by BC1 or T9A, indicating that FtsZ is not a direct target of the chalcones tested.

3.8. Resistance studies

Xac grown in sublethal concentrations of BC1 or T9A was able to develop resistance and grow in higher concentrations of compound **Figure 8**. Resistance increased 2 fold every 3 days reaching a maximum of 4 fold (360µg/mL) for BC1 and 8 fold (400µg/mL) for T9A.

4. Discussion

Xac causes citrus canker leading to an economic impact on citriculture (1). In this chapter we investigated the antibacterial mode of action of the methoxychalcone BC1 and the hydroxychalcone T9A on Xac using techniques previously used to investigate the mode of action of drugs in *B. subtilis* and other organisms such as *E. coli* and *S. aureus* (29–32).

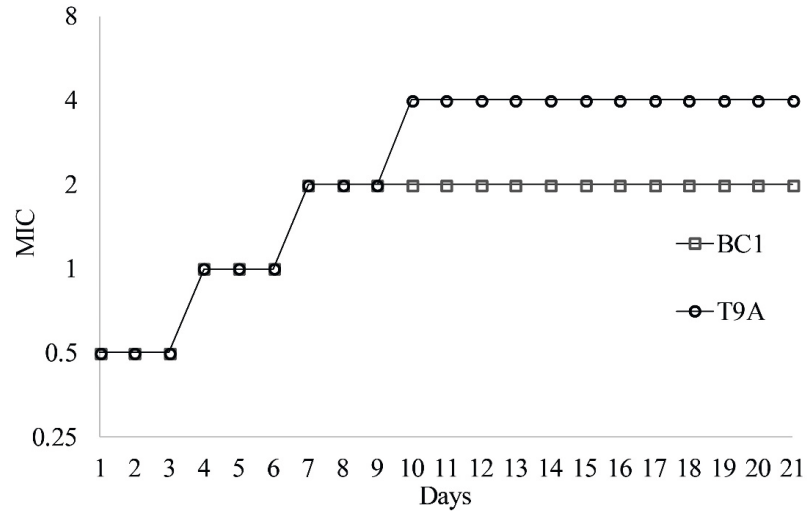

Figure 9: minimum inhibitory concentration of BC1 and T9A against an exposed population of Xac growing in NYGB medium at 29 °C recorded on a daily basis.

We also tested the mode of action of these compounds in *B. subtilis* due to the ease of working and our experience with this organism in the lab.

Vancomycin does not affect Gram-negative bacteria (33), and Xac is resistant to ampicillin (34). Therefore we decided to use benzyl penicillin as a control for cell wall incorporation, since this antibiotic was previously reported to be effective against Xac (35). We tested the minimum inhibitory concentration of benzyl penicillin in our lab and 200µg/mL was able to prevent Xac growth for 24 hours. Therefore, we used 4 times this concentration as a control for glucosamine incorporation (800µg/mL). However, to our surprise Xac cells exposed to penicillin were able to incorporate 92 % of glucosamine when compared to the control. This could possibly be due to benzyl penicillin having more affinity for penicillin binding proteins (PBPs) responsible for hydrolysis and less affinity for PBPs responsible for synthesis of peptidoglycan, thus cells could still build peptidoglycan and elongate without being able to undergo cell division, ultimately leading to cell death (36).

The DNA synthesis inhibitor ciprofloxacin caused only 22 % reduction in thymidine incorporation when compared to the control. Incorporation of radiolabels in Xac might be less affected by known specific

controls in 80 minutes due to possible delays in the compounds to penetrate the outer membrane. Xac divides once every 5.1 hours in Xam1 medium at 30°C, therefore the time used for incorporation corresponds to only 26% of a doubling time. Probably the metabolic processes in Xac are slower than in *B. subtilis* and the antibiotics take a longer time to kick-in. The concentration of ciprofloxacin used in this experiment was 10.0 μg/mL, which is 4 times the concentration necessary to inhibit Xac growth for 24 hours.

There is also very limited published data to compare our controls with. Most publications about incorporation of radiolabeled precursors do not report the use of antibiotics as positive controls (*10*, *30*, *31*, *37–40*). Three studies described macromolecular synthesis assay with antibiotics as a positive controls, but they were on the Gram-positive bacteria *B. subtilis (29)*, *S. aureus (41)*, and *Staphylococcus simulans* (*32*), and all of them used vancomycin as a control for blocking peptidoglycan incorporation. To our knowledge this is the first report on the incorporation of macromolecular precursors in Xac.

Despite not being able to detect a block of all the pathways with positive controls, our experiment showed that all the metabolic pathways are affected by the compounds within the 80 minutes monitored which is a strong indication of an aspecific mechanism. Similarly, for *B. subtilis* all the metabolic pathways are affected within the 60 minutes tested. This result is similar to what was obtained by Haraguchi *et al.* (*10*) when testing the mode of action of licochalcone A. This chalcone inhibited incorporation of DNA, RNA, and protein (peptidoglycan was not tested) in *Micrococcus luteus* (*10*). In this case it is because licochalcone A inhibits oxygen consumption and interferes with energy metabolism (*10*). Intriguingly, in our experiments we showed that both compounds (BC1 and T9A) caused an increase in ATP concentration in *B. subtilis* (**Figure 5B**). It could be that these compounds cause a switch of *B. subtilis* to anaerobic growth which causes ATP levels to be maintained (*42*), but the increase in ATP could also be due to processes such as cell wall and RNA synthesis being inhibited or blocked, causing a difference between ATP production and consumption. The latter effect was previously observed for the protein inhibitors chloramphenicol and streptomycin (*43*). From these results we can conclude that those compounds do not directly affect ATP synthesis in *B.* subtilis. In Xac,

a small decrease was observed (**Figure 5A**), which is an indication of indirect effect, but not as conclusive as in *B. subtilis*.

Cell division process was investigated by observing the localization of GFP fusions with cell division proteins. In Xac neither BC1 or T9A caused delocalization of our cell division marker (GFP-ZapA) which rules out the possibility of those compounds to cause a direct effect in Xac cell division.

In *B. subtilis* both compounds caused delocalization of our cell division marker (FtsZ-GFP). BC1 is able to permeabilize *B. subtilis* membranes, therefore this result could be due to membrane potential disruption, similar to what was observed by Strahl, *et al.* (*28*). However, T9A is not able to permeabilize *B. subtilis* membranes. Therefore, we tested GTPase activity and since neither chalcone caused an effect in GTPase activity we rule out the possibility of cell division being directly affected by T9A or BC1.

The data produced in this work do not allow us to draw a conclusion about a specific mode of action of the compounds tested. However, we were able to generate Xac strains with resistance to T9A and BC1, which opens the possibility to sequence and carry out genomic analyses to understand the mode of action of this compounds.

5. Author contributions

AL performed the MIC, macromolecular synthesis, resazurin, and ATP concentration experiments. LM performed MIC, membrane permeability, microscopy, and resistance experiments and assembled the microscopy pictures. LC performed GTPase experiments and assembled the respective graph. GD performed FT-IR experiments and assembled the respective figure. AL, LG, HF, and DS analyzed the data. AL and DS wrote the manuscript.

6. Acknowledgements

We would like to thank Rieza Aprianto and his colleagues from the Molecular Genetics group of the University of Groningen, for help in using the Tecan Infinite F200 Pro luminometer, and Luiz O. Regasini (UNESP, São José do Rio Preto) for synthesizing and providing us with the compounds BC1 and T9A used in this study.

7. References

1. T. R. Gottwald, J. H. Graham, T. S. Schubert, Citrus canker: the pathogen and its impact. *Plant Health Progress* **10**, (2002).
2. N. Gimenes-Fernandes, J. C. Barbosa, A. Ayres, C. Massari, Plantas doentes não detectadas nas inspeções dificultam a erradicação do cancro cítrico. *Summa Phytopathologica* **26**, 320–325 (2000).
3. F. Behlau, B. I. Canteros, G. V. Minsavage, J. B. Jones, J. H. Graham, Molecular Characterization of Copper Resistance Genes from Xanthomonas citri subsp. citri and Xanthomonas alfalfae subsp. citrumelonis. *Applied and Environmental Microbiology* **77**, 4089–4096 (2011).
4. I. Nunes *et al.*, Coping with copper: legacy effect of copper on potential activity of soil bacteria following a century of exposure. *FEMS microbiology ecology* **92**, fiw175 (2016).
5. A.-M. Katsori, D. J. E. o. o. t. p. Hadjipavlou-Litina, Recent progress in therapeutic applications of chalcones. **21**, 1575–1596 (2011).
6. A.-M. Katsori, D. Hadjipavlou-Litina, Recent progress in therapeutic applications of chalcones. *Expert opinion on therapeutic patents* **21**, 1575–1596 (2011).
7. A. Valavanidis, T. Vlachogianni, in *Studies in Natural Products Chemistry*. (Elsevier, 2013), vol. 39, pp. 269–295.
8. S. F. Nielsen, M. Larsen, T. Boesen, K. Schønning, H. Kromann, Cationic chalcone antibiotics. Design, synthesis, and mechanism of action. *Journal of medicinal chemistry* **48**, 2667–2677 (2005).
9. R.-I. Tsukiyama, H. Katsura, N. Tokuriki, M. J. A. a. a. c. Kobayashi, Antibacterial activity of licochalcone A against spore-forming bacteria. **46**, 1226–1230 (2002).
10. H. Haraguchi, K. Tanimoto, Y. Tamura, K. Mizutani, T. J. P. Kinoshita, Mode of antibacterial action of retrochalcones from Glycyrrhiza inflata. **48**, 125–129 (1998).
11. S. F. Nielsen, M. Larsen, T. Boesen, K. Schønning, H. J. J. o. m. c. Kromann, Cationic chalcone antibiotics. Design, synthesis, and mechanism of action. **48**, 2667–2677 (2005).
12. B. Zhou *et al.*, Targeting mycobacterium protein tyrosine phosphatase B for antituberculosis agents. **107**, 4573–4578 (2010).
13. D. Barreca, E. Bellocco, G. Laganà, G. Ginestra, C. J. F. c. Bisignano, Biochemical and antimicrobial activity of phloretin and its glycosilated derivatives present in apple and kumquat. **160**, 292–297 (2014).
14. M. I. Abdullah, A. Mahmood, M. Madni, S. Masood, M. J. B. c. Kashif, Synthesis, characterization, theoretical, anti-bacterial and molecular docking studies of quinoline based chalcones as a DNA gyrase inhibitor. **54**, 31–37 (2014).
15. L. G. Morão *et al.*, A simplified curcumin targets the membrane of Bacillus subtilis. *MicrobiologyOpen*, e00683 (2018).
16. S. Somma, L. Gastaldo, A. Corti, Teicoplanin, a new antibiotic from Actinoplanes teichomyceticus nov. sp. *Antimicrobial agents and chemotherapy* **26**, 917–923 (1984).
17. B. D. Davis, E. S. Mingioli, Mutants of Escherichia coli requiring methionine or vitamin B12. *Journal of bacteriology* **60**, 17 (1950).
18. J. M. Andrews, Determination of minimum inhibitory concentrations. *Journal of antimicrobial Chemotherapy* **48**, 5–16 (2001).
19. A. Mukherjee, J. Lutkenhaus, Dynamic assembly of FtsZ regulated by GTP hydrolysis. *The EMBO journal* **17**, 462–469 (1998).
20. E. Król, D.-J. Scheffers, FtsZ Polymerization Assays: Simple Protocols and Considerations. *Journal of visualized experiments: JoVE*, e50844 (2013).
21. E. Król *et al.*, Antibacterial activity of alkyl gallates is a combination of direct targeting of FtsZ and permeabilization of bacterial membranes. *Frontiers in Microbiology* **6**, (2015).
22. T. Oz *et al.*, Strength of Selection Pressure Is an Important Parameter Contributing to the Complexity of Antibiotic Resistance Evolution. *Molecular Biology and Evolution* **31**, 2387–2401 (2014).
23. A. Savietto *et al.*, Antibacterial activity of monoacetylated alkyl gallates against Xanthomonas citri subsp. citri. *Archives of microbiology*, 1–9 (2018).
24. M. M. Kopacz, A. S. Lorenzoni, C. R. Polaquini, L. O. Regasini, D. J. J. M. Scheffers, Purification and characterization of FtsZ from the citrus canker pathogen Xanthomonas citri subsp. citri. e00706 (2018).
25. C. Mann, J. Markham, A new method for determining the minimum inhibitory concentration of essential oils. *Journal of applied microbiology* **84**, 538–544 (1998).
26. S. Garip, A. C. Gozen, F. Severcan, Use of Fourier transform infrared spectroscopy for rapid comparative analysis of Bacillus and Micrococcus isolates. *Food Chemistry* **113**, 1301–1307 (2009).
27. L. A. Rigano *et al.*, Biofilm formation, epiphytic fitness, and canker development in Xanthomonas axonopodis pv. citri. *Molecular Plant-Microbe Interactions* **20**, 1222–1230 (2007).
28. H. Strahl, L. W. Hamoen, Membrane potential is important for bacterial cell division. *Proceedings of the National Academy of Sciences* **107**, 12281–12286 (2010).
29. A. Müller *et al.*, Daptomycin inhibits cell envelope synthesis by interfering with fluid membrane microdomains. *Proceedings of the National Academy of Sciences* **113**, E7077-E7086 (2016).
30. C. A. Cherrington, M. Hinton, I. Chopra, Effect of short-chain organic acids on macromolecular synthesis in Escherichia coli. *Journal of Applied Bacteriology* **68**, 69–74 (1990).
31. Y. A. Elnakady *et al.*, Investigations to the antibacterial mechanism of action of kendomycin. *PloS one* **11**, e0146165 (2016).
32. A. I. Chiriac *et al.*, Mode of action of closthioamide: the first member of the polythioamide class of bacterial DNA gyrase inhibitors. *Journal of Antimicrobial Chemotherapy*, dkv161 (2015).
33. P. E. Reynolds, Structure, biochemistry and mechanism of action of glycopeptide antibiotics. *European Journal of Clinical Microbiology and Infectious Diseases* **8**, 943–950 (1989).
34. S.-F. Weng, C.-Y. Chen, Y.-S. Lee, J.-W. Lin, Y.-H. Tseng, Identification of a Novel β-Lactamase Produced byXanthomonas campestris, a Phytopathogenic Bacterium. *Antimicrobial agents and chemotherapy* **43**, 1792–1797 (1999).
35. M. Mubeen *et al.*, In-vitro efficacy of antibiotics against Xanthomonas axonopodis pv. citri through inhabitation zone techniques (2015).
36. A. Typas, M. Banzhaf, C. A. Gross, W. Vollmer, From the regulation of peptidoglycan synthesis to bacterial growth and morphology. *Nature Reviews Microbiology* **10**, 123 (2012).
37. H. Haraguchi, T. Abo, K. Hashimoto, A. J. B. Yagi, biotechnology, and biochemistry, Action-mode of antimicrobial altersolanol A in Pseudomonas aeruginosa. **56**, 1221–1224 (1992).
38. H. Ulvatne, Ø. Samuelsen, H. H. Haukland, M. Krämer, L. H. Vorland, Lactoferricin B inhibits bacterial macromolecular synthesis in Escherichia coli and Bacillus subtilis. *FEMS microbiology letters* **237**, 377–384 (2004).
39. R. Smith, J. Midgley, The effect of trimethoprim on macromolecular synthesis in Escherichia coli. General effects on ribonucleic acid and protein synthesis. *Biochemical Journal* **136**, 225–234 (1973).
40. A. Patrzykat, C. L. Friedrich, L. Zhang, V. Mendoza, R. E. Hancock, Sublethal concentrations of pleurocidin-derived antimicrobial peptides inhibit macromolecular synthesis in Escherichia coli. *Antimicrobial agents and chemotherapy* **46**, 605–614 (2002).
41. L. L. Ling *et al.*, A new antibiotic kills pathogens without detectable resistance. *Nature* **517**, 455–459 (2015).
42. M. M. Nakano, P. Zuber, Anaerobic growth of a "strict aerobe"(Bacillus subtilis). *Annual Reviews in Microbiology* **52**, 165–190 (1998).
43. T. Ohwada, S. Sagisaka, An immediate and steep increase in ATP concentration in response to reduced turgor pressure in Escherichia coli B. *Archives of biochemistry and biophysics* **259**, 157–163 (1987).

8. Supporting information

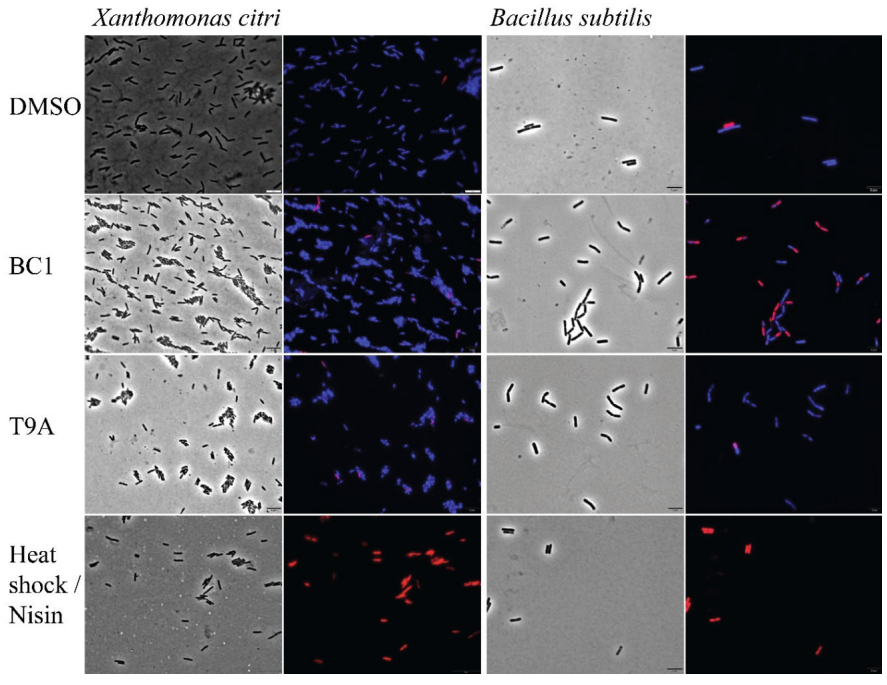

Figure S1: Xac and *B. subtilis* cells, phase contrast (left) and overlay of Texas Red and DAPI/FITC (right). Treatments of 15 min; Scale bars are 5 μm.

Appendix 1 — Investigations on the mode of action of alkyl gallates against *Xanthomonas citri*

André S. G. Lorenzoni and Dirk-Jan Scheffers

Department of Molecular Microbiology, Groningen Biomolecular Sciences and Biotechnology Institute, University of Groningen, Groningen, Netherlands

Adapted from: Malgorzata M. Kopacz, André S. G. Lorenzoni, Carlos R. Polaquini, Luis O. Regasini, Dirk-Jan Scheffers. Purification and characterization of FtsZ from the citrus canker pathogen Xanthomonas citri subsp. citri. MicrobiologyOpen (2018): e00706.

1. Background

Due to the negative impact caused by Xac described in the previous chapters, we investigated the potential of alkyl gallates as an alternative to combat or prevent citrus canker. Alkyl gallates have been used as food additives (1), but also showed antimicrobial activity with potential inhibitory effect on cell division (2). Silva *et al. (2)* showed that pentyl, hexyl, heptyl, and octyl gallates disrupt the septum of Xac, raising the hypothesis that those compounds target cell division process. At the time, purification or characterization of Xac cell division proteins had not been established. Therefore, Król *et al.* (3) tested those alkyl gallates *in vitro* using *Bacillus subtilis* FtsZ. They tested GTPase and sedimentation activity of FtsZ in the presence of gallates, and binding of alkyl gallates to FtsZ, showing that FtsZ is a direct target for alkyl gallates in *B. subtilis* (3). In this short report we will discuss additional tests to further characterize the activity of alkyl gallates against Xac.

2. Methods

2.1. Minimal inhibitory concentration assays

The minimum inhibitory concentration (MIC) of pentyl, hexyl, heptyl, and octyl gallates was tested by broth microdilution. Exponentially growing Xac cells were diluted to OD_{600} of 0.005 in 96 well plates containing two-fold serial dilutions of the compounds, in a final volume of 200µL of NYGB medium (glycerol 20g/L, peptone 5.0g/L, and yeast extract 3.0g/L). The MIC was defined as the lowest concentration of compound that prevented bacterial growth after incubating 24 hours at the indicated growth temperature (4).

2.2. Resistance development assay

For resistance development by sequential passaging, 2 parallel populations of Xac were diluted in NYGB medium containing 2 fold serial dilutions of heptyl gallate (starting with 5–80µg/mL) or kanamycin (starting with 0.78–25µg/mL), during the exponential phase, similar to the method described by Oz *et al.* (5). Each day, those cells that grew at the highest concentration of drugs were diluted to fresh medium containing serial dilutions of antimicrobial. Dilutions were done after 21h of growth at 30°C over a period of 23 days.

2.3. Membrane permeability assay

Membrane integrity was assessed using the commercial Live/Dead BacLight bacterial viability kit (Invitrogen) for microscopy, as previously tested in our lab by Król *et al.* (3), with some modifications for Xac. 100µL aliquots of exponentially growing cells (OD600 ≈ 0.5, 30°C, NYGB) were incubated for 45 min with either alkyl gallates at 32 µg/mL or Nisin (10µg/ml) and EDTA (30 mM) as a control for permeabilization, or without treatment as a negative control. After 45 min, 0.3µL of dye mixture (propidium iodide (5.0 mM) and SYTO 9 (835µM), used as described by manufacturer) was added to the cells to stain the DNA — incubation was continued for 15 min and the cells were immediately imaged on agarose pads using bright-field, FITC (50 ms exposure), and TRITC (100 ms exposure) fluorescence filter cubes. Images were analyzed using the Fiji (https://fiji.sc/) software package, the function "Find Maxima" was used to automatically detect green and red fluorescent cells with thresholds of 11000 and 3000 respectively.

3. Results

The minimum inhibitory concentration measured in our lab was 32 µg/mL for each of the alkyl gallates tested, which is identical to what was found by Silva *et al.* (2) (31.2 µg/mL), despite the differences in the way of measuring. Silva *et al.* (2) used LB medium and measured growth inhibition using a REMA assay, which measures the reductive capability of cells as a measure for cell viability, whereas we used NYGB medium and measured growth inhibition after 24 h in liquid. Since the minimum inhibitory concentration is measured by 2 fold dilutions (e.g. 16, 32, and 64) the values of 32 µg/mL and 31.2 µg/mL can be considered identical. The minimum inhibitory concentration we measured for kanamycin for wild type Xac was 6.25 µg/mL.

For resistance development two populations of Xac cells were grown in duplicate in different concentrations of antimicrobials and each day the culture growing at the highest concentration was diluted to fresh medium with different concentrations of antimicrobial, allowing the gradual development of increased resistance. We chose heptyl gallate for this experiment as it was the most active inhibitor of *B. subtilis* FtsZ (3), and kanamycin as a control. After 23 days this resulted in one population that was able to grow in 20µg/mL of heptyl gallate, and

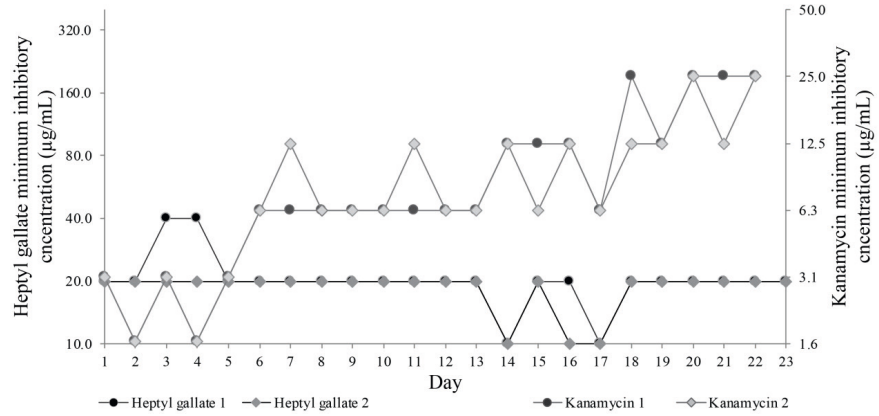

Figure 1: minimum inhibitory concentration of heptyl gallates and kanamycin for exposed parallel populations recorded on a daily basis.

one population that grew at 25.0µg/mL of kanamycin. The evolution of each population can be seen in **Figure 1**. The populations exposed to kanamycin had increased resistance and grew at a kanamycin concentration that was 8 times the initial MIC. However, the populations exposed to heptyl gallate remained as sensitive as wild type strains even after 23 days of growth in the presence of the compound.

In *B. subtilis*, the antibacterial activity of alkyl gallates is a combination of direct targeting of FtsZ and permeabilization of bacterial membranes (3). In our lab, we recently managed to purify Xac FtsZ and showed that the effects of alkyl gallates on Xac FtsZ are only mild [MBO3–2018–03–0093.R3]. Thus, it was necessary to test the effect of alkyl gallates on Xac membranes, especially since acetylated alkyl gallates were recently shown to permeabilize Xac membranes (6). We tested membrane permeability by incubating cells with alkyl gallates and followed by fluorescent labelling with two DNA dyes, one membrane permeable, the other membrane impermeable. This assay showed that at MIC (32µg/mL), pentyl gallate permeabilized 42% of Xac cells, and the other alkyl gallates permeabilized 94% or more Xac cells (**Table 1**), which is more than our positive control with nisin in combination with EDTA. Thus the alkyl gallates permeabilize Xac membranes.

Table 1: Permeabilization of Xac cells by alkyl gallates.

Condition (n/n)	**Permeabilized cells** (mean ± SD)
Control (10536/10010)	0.8 ± 0.2%
pentyl gallate (308/268)	42.2 ± 0.3%
hexyl gallate (457/858)	94.5 ± 4.2%
heptyl gallate (1931/5701)	99.9 ± 0.1%
octyl gallate (1523/3508)	99.8 ± 0.1%
Nisin EDTA (452/5437)	94.0 ± 5.9%

Results from two independent replicates, n represents the number of cells counted in each experiment.

4. Concluding remarks

In this report we tried to develop resistant strains of Xac that are resistant to heptyl gallate. This experiment provide initial information about the possibility of resistance development when alkyl gallates would be used in agriculture. Also, if we had found a resistant strain it could be helpful to characterize the mode of action of the compound as sequencing the strain would give indications about possible targets of the alkyl gallates. Alkyl gallates are FtsZ inhibitors in *B. subtilis* (3) and caused septum mislocalization in Xac (2) suggesting that FtsZ is also a target in this bacteria. In case of a single target the probability of resistance occurring would be from 10^6 to 10^9, which would be possible to generate in the lab, and the mutations would be probably related to the target (7). However, Xac could not develop resistance against heptyl gallate. This is an indication that the compound could have multiple targets, or a target that is not a protein. This fits our observation that the antibacterial activity of alkyl gallates against Xac is primarily caused by its effect on the membranes.

5. References

1. C. Van der Heijden, P. Janssen, J. Strik, Toxicology of gallates: a review and evaluation. *Food and Chemical Toxicology* **24**, 1067–1070 (1986).
2. I. C. Silva *et al.*, Antibacterial activity of alkyl gallates against Xanthomonas citri subsp. citri. *Journal of Bacteriology* **195**, 85–94 (2013).
3. E. Król *et al.*, Antibacterial activity of alkyl gallates is a combination of direct targeting of FtsZ and permeabilization of bacterial membranes. *Frontiers in Microbiology* **6**, (2015).
4. J. M. Andrews, Determination of minimum inhibitory concentrations. *Journal of antimicrobial Chemotherapy* **48**, 5–16 (2001).
5. T. Oz *et al.*, Strength of Selection Pressure Is an Important Parameter Contributing to the Complexity of Antibiotic Resistance Evolution. *Molecular Biology and Evolution* **31**, 2387–2401 (2014).
6. A. Savietto *et al.*, Antibacterial activity of monoacetylated alkyl gallates against Xanthomonas citri subsp. citri. *Archives of microbiology*, 1–9 (2018).
7. A. J. O'Neill, I. Chopra, Preclinical evaluation of novel antibacterial agents by microbiological and molecular techniques. *Expert opinion on investigational drugs* **13**, 1045–1063 (2004).

Chapter 4 — *Xanthomonas citri* MinC oscillates from pole to pole to ensure proper cell division and shape

André Soibelmann Glock Lorenzoni[1], Giordanni Cabral Dantas[2], Tessa Bergsma[1], Henrique Ferreira[2], Dirk-Jan Scheffers[1]

[1]Department of Molecular Microbiology, Groningen Biomolecular Sciences and Biotechnology Institute, University of Groningen, Groningen, Netherlands
[2]Department of Biochemistry and Microbiology, Institute of Biosciences, São Paulo State University, Rio Claro, SP, Brazil

Frontiers in Microbiology *8:1352. doi: 10.3389/fmicb.2017.01352*

Abstract

Xanthomonas citri (Xac) is the causal agent of citrus canker, a disease that affects citrus crops and causes economic impact worldwide. To further characterize cell division in this plant pathogen, we investigated the role of the protein MinC in cell division, chromosome segregation, and peptidoglycan incorporation by deleting the gene *minC* using allele exchange. Xac with *minC* deleted exhibited the classic Δ*min* phenotype observed in other bacteria deleted for *min* components: minicells and short filamentation. In addition we noticed the formation of branches, which is similar to what was previously described for *Escherichia coli* deleted for either *min* or for several low molecular weight penicillin-binding proteins (PBPs). The branching phenotype was medium dependent and probably linked to gluconeogenic growth. We complemented the *minC* gene by integrating *gfp-minC* into the *amy* locus. Xac complemented strains displayed a wild-type phenotype. In addition, GFP-MinC oscillated from pole to pole, similar to MinCD oscillations observed in *E. coli* and more recently in *Synechococcus elongatus*. Further investigation of the branching phenotype revealed that in branching cells nucleoid organization, divisome formation and peptidoglycan incorporation were disrupted.

1. Introduction

Xanthomonas citri subsp. *citri* (Xac) is the causal agent of citrus canker: a disease that affects citrus crops, decreases fruit production and causes economic losses (*1*). This disease is currently present in South and North America, Asia, Africa, and Oceania (*2–5*). The current strategy to combat citrus canker in the state of São Paulo, Brazil, the largest producer of concentrate orange juice in the world, comprises the eradication of symptomatic trees along with spraying copper-containing bactericides in a radius of 30 m having the symptomatic tree as the center point (*1, 6*). However, this strategy is costly and has limited effectiveness (*3, 7*).

The genome of Xac was fully sequenced 14 years ago, opening up several possibilities for molecular and genetic characterization of this plant pathogen (*8*). Since then, some studies have expanded upon the knowledge we have about biological processes in Xac, mostly concerning pathogenicity mechanisms (*9–13*). Recently, new tools for gene expression in Xac have been developed (*14, 15*), enabling studies on chromosome segregation and cell division. These cellular systems represent potential targets for antimicrobials, as the proteins involved in such processes share little homology with eukaryotic equivalents (*16–19*). Anti-Xac compounds that disrupt the localization of the cell division proteins ZapA and FtsZ *in vivo*, and that act on FtsZ *in vitro*, also affect localization of ParB (*20, 21*). Xac cells expressing truncated forms of ParB exhibit a filamentation phenotype (*22*). Inhibition of cell division in other bacteria like *E. coli* and *B. subtilis* leads to filamentation without chromosome segregation defects (*23*), suggesting a difference in the relation between cell division and chromosome segregation in Xac.

FtsZ is the central protein of the cell division machinery (*23*). At the start of cell division, FtsZ assembles a ring like structure at midcell called the Z ring. Z ring formation is followed by mid-cell constriction that generates two daughter cells. FtsZ is conserved among prokaryotic cells, yet different mechanisms have evolved in different bacteria that ensure that the Z ring assembles at midcell, at a specific time during the cell cycle, and does not constrict over the nucleoids. In the most studied gammaproteobacterium, *Escherichia coli*, Z ring localization is mediated by the Min system that consists of the proteins MinC, MinD, and MinE (*24*). MinC forms a complex with MinD to inhibit FtsZ function at the cell poles (*25*). The localization of MinC is mediated by MinD, which forms a

membrane-associated complex at one of the cell poles. MinE assembles at midcell in a ring like structure, and then cycles back and forth toward the cell poles stimulating the dissociation of the MinC/MinD complex. As soon as MinC/D dissociate from one of the poles, they are re-oriented to the opposite cellular pole in such a way that MinC, the FtsZ inhibitor, resides closer to the cellular poles far longer than it is in transit between them. This behavior creates a concentration gradient through the cell with MinCD lowest at midcell, which enables Z ring formation at this site (*26*). For a long time, MinCD oscillation had only been identified in *E. coli*, but recently it has also been observed in *Synechococcus elongatus* (*27*). Although inhibition of polar Z ring formation by MinCD is conserved in many bacteria, oscillation of MinCD seems restricted to bacteria that also contain MinE. In bacteria that do not have MinE, MinCD is anchored to the poles via other proteins such as DivIVA/MinJ (*28*).

Another mode of control of Z ring formation is the partially redundant nucleoid occlusion system, in *E. coli* mediated by SlmA (*29*). SlmA binds to specific DNA sites and depolymerizes FtsZ, and this way the Z ring cannot assemble over a nucleoid (*30*). In several alphaproteobacteria including the model organism *Caulobacter crescentus*, the DNA-binding protein ParB colocalizes with the edges of the nucleoids to drive chromosome segregation (*22*, *31*). Then ParB forms a complex with MipZ, a FtsZ inhibitor that tracks along the ParB-chromosomal origin region (the bacterial centromere) in such a way that the inhibitory effect of MipZ will be concentrated at the cell poles and distal from the mid-cell where the divisional septum will be assembled (*32*).

Although Xac is a member of the gammaproteobacteria, in terms of chromosome segregation, it seems, at least mechanistically, related to *C. crescentus* and *V. cholerae*, as in these bacteria chromosome segregation is asymmetric. However, Xac does not have an obvious MipZ homolog. In terms of FtsZ regulation, Xac is closer to *E. coli* and *V. cholerae*, due to the presence of the Min system composed of the MinCDE proteins (*33*), although Xac doesn't have an obvious SlmA homolog that could mediate nucleoid occlusion (*22*).

In this study, we have made a Xac mutant deleted for *minC* and observed that this mutant not only forms minicells but also exhibits branching. This phenotype has also been described in *E. coli* deleted for *min* (*34*, *35*). In *E. coli*, branching is dependent on the medium

composition, and seems associated (or more prominent) with minimal media and the presence of casamino acids, and a disturbed localization of the nucleoids (*35*). Branching increased in cells grown in the presence of low concentrations of beta-lactam antibiotics, indicating that interfering with PBP function increases this phenotype (*34*). This was confirmed in a series of papers from the Young laboratory, who observed a similar branching phenotype in *E. coli* deleted for several low-molecular-weight penicillin-binding proteins (LMW PBPs), most notably PBP5, the major DD-carboxypeptidase (*36*, *37*). Branching most likely results from aberrant positioning of FtsZ and concomitant synthesis of so-called "inert peptidoglycan" (iPG), which is not associated with cell division. iPG is consistently observed at the tips of branches and at branch sites (*38*–*41*).

2. Methods

2.1. Bacterial Strains and Growth Conditions

Bacterial strains and plasmids are listed in **Table 1**. Xac was cultivated at 30°C in various media: nutrient yeast glycerol broth (NYGB, peptone 5g/L; yeast extract 3g/L; glycerol 20g/L) or on plates containing agar (15g/L, NYGA) supplemented with D-glucose (1% w/v) or L-arabinose (0.05% w/v) when required; nutrient yeast citrate broth (NYCB, peptone 5g/L; yeast extract 3g/L; glycerol 2.46g/L; $Na_3C_6H_5O_7$ 0.44g/L); Xam1 medium (glycerol 2.46g/L; $MgSO_4{\cdot}7H_2O$ 0.247g/L; $(NH_4)_2SO_4$ 1.0g/L; KH_2PO_4 4.5g/L; K_2HPO_4 10.5g/L; $Na_3C_6H_5O_7{\cdot}2H_2O$ 0.5g/L; casamino acids 0.3g/L; BSA 1g/L; pH 5.4 adjusted with HCl); or Xamg1 medium which is identical to Xam1 except for glycerol which is at 20g/L. LB 0% is Lysogeny Broth without NaCl (tryptone 10g/L; yeast extract 5g/L), whereas LB 0.5% contains NaCl 5g/L.

For the cloning steps, we used *E. coli* DH10B (Invitrogen) cultivated in LB 0.5%-agar/LB 0.5% at 37°C (*42*). The antibiotics kanamycin, gentamicin, and ampicillin were used at the concentration of 20µg/mL.

2.2. Construction of the replicative plasmid expressing Xac MinC

The *minC* gene was amplified by PCR using Xac genomic DNA as a template and the primers minC_pLAL1F/minC_pLAL1R (all oligonucleotides

Table 1: list of strains and plasmids.

Strains	Relevant characteristics	Reference
X. citri subsp. *citri* (Xac)	Wild type strain 306 (Xac); Ap^R	IBSBF-1594* (*8, 43, 44*)
E. coli DH10B	Cloning strain	Invitrogen
Xac Δ*minC*	Xac Δ*minC*; Ap^R	This work
Xac *amy::gfp*	Xac with pGCD21 integrated in *amy*; Ap^R Km^R	This work
Xac Δ*minC amy::gfp*	Xac Δ*minC* with pGCD21 integrated in *amy*; Ap^R Km^R	This work
Xac Δ*minC amy::gfp-minC*	Xac Δ*minC* with pGCD2c integrated in *amy*; Ap^R Km^R	This work
Xac *amy::gfp-zapA*	Xac with pPM2a-ZapA integrated in *amy*; Ap^R Km^R (former name: pPM2a-XAC3408)	(*14*)
Xac Δ*minC amy::gfp-zapA*	Xac Δ*minC* with pPM2a-ZapA integrated in *amy*; Ap^R Km^R	This work
Xac *parB::parB-gfp*	Xac with pPM7g-parB integrated in *parB*; Ap^R Km^R (former name: *parB*::pAPU3)	(*22*)
Xac Δ*minC parB::parB-gfp*	Xac Δ*minC* with pPM7g-parB integrated in *parB*; Ap^R Km^R	This work
Plasmids		
pPM2a and pPM7g	GFP expression vectors; *xylR pxyl gfpmut1 bla neo*	(*14*)
pAPU3	pPM7g-parB: xylR pxyl parB-gfpmut1 bla neo	(*22*)
pHF5Ca	TAP-tag expression vector; *xylR pxyl tap1479 bla neo*	(*22*)
pEB304	pBAD derivative and source of the *araC-para-acp-tap1479* cassette; Ap^R	(*45*)
pNPTS138	*Bacillus subtilis sacB* gene; Km^R; suicide vector in Xac	Prof. L. Shapiro (Stanford University, USA)
pGCD21	Derivative of pHF5Ca (*22*); *araC-para-gfp-mut1*; *amy106–912*; Ap^R Km^R; integrative vector in Xac	This work GenBank KU678206
pLAL1	*araC-para-acp-tap1479*; Gm^R; replicative vector in Xac	(*46*) GenBank KP696472
pGCD1C	Derivative of pLAL1; *araC-para-minC*; Gm^R; replicative vector in Xac	This work
pGCD19	GFP expression vector; *xylR pxyl gfpmut1* Ap^R Km^R	This work
pGCD2C	Derivative of pGCD21; *araC-para-gfp-mut1-minC; amy106–912;* Ap^R Km^R	This work

Ap^R = ampicillin resistance, Gm^R = gentamicin resistance, Km^R = kanamycin resistance, *bla* = *betalactamase*, *neo* = *neomycin*, *Instituto Biológico, Seção de Bacteriologia Fitopatológica, Campinas, SP, Brazil

are listed **Table S1**). The resultant DNA fragment was digested with *Eco*RI/*Hind*III and ligated into the Xac expression vector pLAL1 (GenBank KP696472; (*46*)) digested with the same enzymes, which resulted in pGCD1C.

2.3. Vector for Xac *minC* deletion

Two DNA fragments flanking the genomic sequence of *minC*, minCup (870 bp), and minCdown (929 bp) were obtained by PCR using the primer pairs minCupF/minCupR and minCdownF/minCdownR, respectively. The PCR products minCup and minCdown were digested with the restriction enzymes *Bam*HI/*Xba*I and *Xba*I/*Hind*III, respectively, and ligated to pNPTS138 (kindly donated by Lucy Shapiro, Stanford University, USA) digested with *Bam*HI/*Hind*III, which generated pNPTSΔ*minC*.

2.4. Vector for GFP-fusions and *gfp-minC* vector

GFP-MinC was expressed using the integrative vector pGCD21, a derivative of pHF5Ca (*22*), , which enables the expression of GFP (gfp-mut1, GenBank ADF80258.1) fusion proteins in Xac under the control of the arabinose promoter. To construct pGCD21, *gfp* was removed from pPM7g (*47*) using the restriction enzyme *Bam*HI/*Xba*I; the isolated *gfp* cassette was ligated to the backbone of pHF5Ca digested with the same enzymes, giving rise to pGCD19 (GenBank KJ619486). Next, the arabinose repressor and promoter (*araC-para*) were amplified by PCR using pEB304 (*45*) as a template and the primer pair pARAF/pARAR. The PCR product was digested with *Eco*RI/*Bgl*II and ligated to the backbone of pGCD19/*Eco*RI/*Bgl*II, generating pGCD21 (GenBank KU678206). In order to clone Xac *minC* in pGCD21, the gene was isolated by PCR using genomic DNA and the primers minCF/201402minCR. The PCR product was digested with *Not*I/*Xba*I prior to ligation into pGCD21/*Not*I/*Xba*I, which resulted in pGCD2C.

All the constructs were checked by DNA sequencing.

2.5. Xac *minC* gene deletion

All plasmids were transformed in Xac by electrotransformation (*48*). First, Xac was transformed with the replicative vector pGDC1C, which provides an additional copy of *minC*. Afterwards, Xac/pGCD1C was transformed with pNPTSΔ*minC*, which mediates removal of chromosomal

minC by allele exchange. Mutant strains carrying one of the first crossover events (integration of pNPTSΔ*minC* into minCup or minCdown) were selected on NYGA/kanamycin. To obtain the second crossover, deletion of *minC*, individual colonies were cultivated for 16 h in NYGB supplemented with 0.01 % arabinose and gentamycin only, which is the marker of pGCD1C. The final selection of Xac/pGCD1C Δ*minC* was carried out in NYGA supplemented with 3 % sucrose. Deletion of *minC* was verified by diagnostic PCR and Southern Blot experiments using *minCD* as a probe. To cure pGCD1C, Xac/pGCD1C Δ*minC* was cultivated for ~20 generations without gentamycin (Xac Δ*minC*).

Xac Δ*minC* was complemented with GFP-MinC by transformation with pGCD2C. The vector was stably integrated into the *amy* locus (Xac Δ*minC amy::gfp-minC*). For a GFP only control strain, Xac Δ*minC* was transformed with pGCD21. The vector was stably integrated into the *amy* locus (Xac Δ*minC amy::gfp*). To test whether GFP-MinC was expressed as full-length protein and not proteolytically cleaved inside the cell, cell extracts of cells expressing GFP only or GFP-MinC were analyzed by SDS-PAGE/Western Blot using antibodies against GFP (**Figure S1**).

2.6. Microscopy and data analysis.

Xac cells were grown to exponential phase in either NYGB or Xam1 medium and directly imaged or labeled with a fluorescent dye prior to imaging.

DAPI (4',6-diamidino-2-phenylindole) was used to image DNA. Exponential phase cells were harvested, resuspended in 10 µM DAPI in Phosphate Buffered Saline (PBS) buffer, pH 7, for 30 min, washed twice in PBS and imaged.

HADA (Hydroxycoumarin-carboxylic acid-Amino-D-Alanine) labeling, to detect sites of peptidoglycan synthesis, was done as previously described by Kuru *et al.* (49). HADA was added to 125 µM in exponential phase Xac cells, labeling time was 24 min in Xam1 or 10 min in NYGB (8 % of doubling time under these growth conditions). Cells were either imaged directly when simultaneous detection of GFP was required, or fixed with ice-cold ethanol for 10 min, and washed before imaging.

Cells were imaged using a Nikon Ti-E microscope (Nikon Instruments, Tokyo, Japan) equipped with a Hamamatsu Orca Flash 4.0

camera. Image analysis was performed using the software ImageJ (http://rsb.info.nih.gov/ij/).

Xac *amy::gfp* (wild type control) and Xac Δ*minC amy::gfp* were analyzed to observe MinC deletion effects. Xac Δ*minC amy::gfp-minC* was analyzed to see if GFP-MinC could complement the Δ*minC* phenotype. GFP producing strains were used as the cytosolic GFP allowed for an easier determination of whether a cell had divided or not. First, images were manually inspected for short filamentation, minicells and branching. Two biological replicates were analyzed with at least 200 cells each. Subsequently, cell lengths of rod-shaped cells (not minicells or branched cells) were measured using the public domain program ColiInspector, which runs under ImageJ in combination with the plugin ObjectJ, written by Norbert Vischer (http://simon.bio.uva.nl/objectj/). After the automatic selection process, a manual check was done to make sure only single cells were selected. Cells with a length equal to or longer than 3.15 µm were defined as short filaments. Two biological replicates of each strain were analyzed with at least 500 cells per replicate.

The nucleoid length in cells of Xac *parB::parB-gfp* and Xac Δ*minC parB::parB-gfp* stained with DAPI was manually measured using ObjectJ.

Xac *amy::gfp-zapA* and Xac Δ*minC amy::gfp-zapA* were were analyzed to observe co-localization of HADA (peptidoglycan incorporation) with GFP-ZapA (division sites), and possible MinC deletion effects. After the pictures were taken, the fluorescence channels CFP (HADA) and FITC (GFP-ZapA) were merged. Linescans were made of the cells displayed using the plot profile function of ImageJ. The maximum fluorescence intensity of each cell was defined as 100 %, the minimum at 0 %, and plots were made relative to those levels (**Figure S5**). Linescans confirmed that colocalization could be scored manually from image overlays, which was done for a total of more than 100 cells per strain.

3. Results

3.1. Xac deleted for *minC* displays a branching phenotype

To study the role of the Min system in Xac we deleted *minC* in a strain that expresses *gfp*. This resulted in a strain that exhibited the classical Δ*min* phenotype: next to rod-shaped cells of normal length, minicells and longer cells, both the result of polar divisions, could be observed

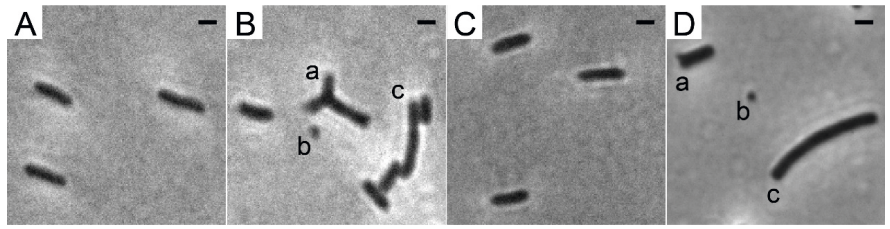

Figure 1: Phase contrast images showing the morphology of Xac strains grown to exponential phase in Xam1 medium. **(A)** Xac *amy::gfp*. **(B)** Xac Δ*minC amy::gfp* with (a) branching, (b) minicells, and (c) short filamentation. **(C)** Xac Δ*minC amy::gfp-minC*. **(D)** Xac Δ*minC* with (a) branching, (b) minicells, and (c) short filamentation. Scale bar: 1 μm.

Table 2: Phenotype observations in different strains.

Strain	Minicells	Branching	Short Filaments[1]	Normal	Total
Xac *amy::gfp*	ND[2]	ND[2]	1.4 ± 0.6%	98.6 ± 0.6%	1599
Xac Δ*minC amy::gfp*	7.3 ± 2.5%	12.9 ± 2.7%	16.0 ± 2.9%	63.8 ± 3.0%	424
Xac Δ*minC amy::gfp-minC*	ND[2]	ND[2]	1.9 ± 1.6%	98.1 ± 1.6%	1624

[1]Cells with length ≥ 3.15 μm; [2]Not detected.

(**Figure 1B**; b, c). However, in addition to these phenotypes, branched cells were also observed in the *minC* mutants (**Figure 1B**; a). Similar results were obtained in a strain that did not carry a copy of the *gfp* gene (**Figure 1D**). To show that the phenotype was due to the deletion of *minC*, and not caused by any polar effects, we complemented the strain with *gfp-minC* at the ectopic *amy* locus. This complementation restored the wild type phenotype (**Figure 1C**, **Table 2**).

Branches and minicells were not observed in the wild type strain nor in the strain complemented with *gfp-minC*. Branches and minicells could not be detected automatically, thus the frequency of their occurrence in the *minC* deletion strain was scored by visual inspection, which revealed that around 20% of the cells were either minicells or branched cells (**Table 2**, see Section Branching in the *minC* Deletion Strain is Dependent on Growth Medium for more details on branching). Subsequently, the length of the rod-shaped cells was determined by automatic

length analysis using Coli-inspector (methods). This showed that the length distribution of the *minC* deletion strain was a lot broader than that of the wild type and *gfp-minC* complemented strain (**Figure S2**). This is most likely because the longer cells in the *minC* deletion population are the result of the outgrowth from an asymmetric division. It is impossible to precisely determine which cells are derived from an asymmetric division. Therefore, we defined "short filaments", which are likely to represent such cells, as cells with a length of over 3.15 μm (this is 1.5 times the median length of cells in the wild type strain). These short filaments comprised around 16% of the cells observed in the *minC* deletion strain, whereas the wild type strain, and the strain complemented with *gfp-minC* had less than 3% of these cells. As the *gfp-minC* complemented strain is so similar to the wild type, while the *minC* deletion is strikingly different, and as GFP-MinC does not show signs of degradation even when overexpressed (**Figure S1**), we conclude that GFP-MinC is fully functional.

3.2. MinC is localized at the poles and oscillates from pole to pole

The strain Xac Δ*minC amy::gfp-minC*, in which *gfp-minC* is the only copy of *minC*, was studied using fluorescence microscopy. As expected, GFP-MinC was localized in a gradient throughout the cell with the maximum at one of the poles (**Figure 2**). To see whether MinC oscillates from pole to pole, as previously described for *E. coli* and recently for *S. elongatus* (27), we imaged the cells with 10s intervals. These short time lapses clearly show that GFP-MinC localization is dynamic, and that the

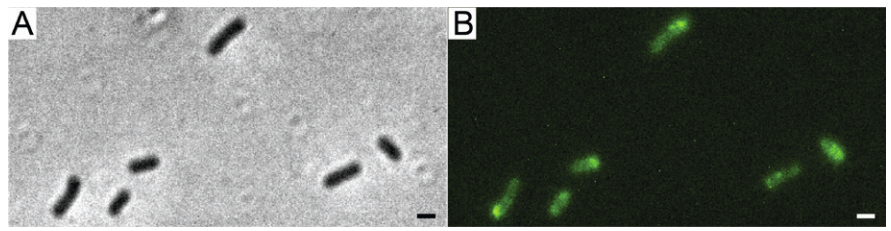

Figure 2: Xac Δ*minC amy::gfp-minC* grown to exponential phase in Xam1 medium. **(A)** phase contrast showing phenotype similar to wild-type. **(B)** FITC showing GFP-MinC located mostly at cell poles. Scale bar 1 μm.

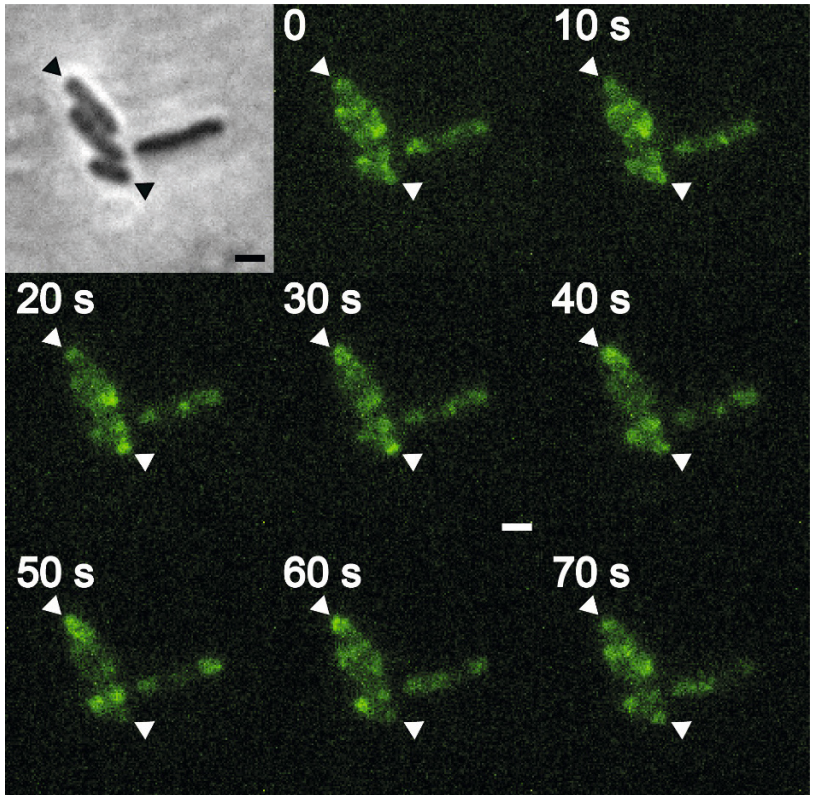

Figure 3: Xac Δ*minC amy::gfp-minC*, contrast (inset), and FITC time lapse. Triangles indicate cell poles showing MinC oscillation pattern. Scale bar 1 μm.

protein oscillates from pole to pole (**Figure 3**, **Video 1** (50)). Following several oscillations in various cells over time revealed that GFP-MinC oscillates with a periodicity of roughly 65 s, which is comparable to the oscillations described in *E.coli* (51).

3.3. Branching in the *minC* deletion strain is dependent on growth medium

The branching phenotype of *E. coli min* mutants has been described in two studies from the 1990's (34, 35), but the phenotype, to paraphrase a paper from the Young lab, has received much less attention than other questions related to bacterial morphology (41). Branching of *min* mutants was shown to be dependent on the composition of the growth

Table 3: Xac Δ*minC amy::gfp* phenotypes in different media.

Medium	Minicells	Branching	Short Filaments	Normal	Total
Xam1	7.3 ± 2.5%	12.9 ± 2.7%	16.9 ± 2.9%	63.8 ± 3.0%	424
Xamg1	16.3 ± 4.0%	18.0 ± 5.6%	13.4 ± 4.4%	52.4 ± 6.1%	401
LB 0%	11.6 ± 1.6%	6.9 ± 0.4%	18.8 ± 0.6%	62.8 ± 4.2%	262
LB 0.5%	11.6 ± 1.3%	8.7 ± 3.4%	17.2 ± 1.7%	68.4 ± 9.5%	387
NYCB	12.4 ± 2.2%	0.78 ± 0.03%	17.4 ± 2.2%	69.5 ± 2.3%	387
NYGB	11.7 ± 3.4%	1.4 ± 1.9%	15.3 ± 3.5%	71.6 ± 1.2%	488

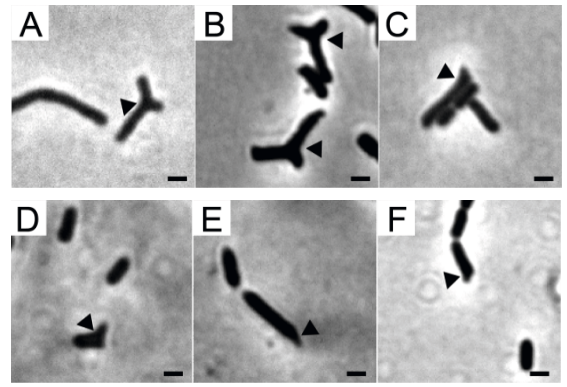

Figure 4: Phase contrast images showing branching of Xac Δ*minC amy::gfp* grown to exponential phase in different media. **(A)** Xam1. **(B)** Xamg1. **(C)** LB 0%. **(D)** LB 0.5%. **(E)** NYCB. **(F)** NYGB. Scale bar 1 μm.

medium. Some branching was observed on rich (LB) medium, whereas growth on minimal salt (M9) media supplemented with casaminoacids and either succinate or acetate, but not glucose, resulted in branching in 5% to 20% of the cells depending on the *E. coli* strain studied (34, 35). We tested the medium dependency of the branching phenotype of the Xac *minC* deletion strain and observed similar results: hardly any branches on the rich NYG/CB media and roughly 12% of branches on the minimal salt Xam1 medium. An intermediate phenotype was observed on LB where cells showed bulges and abnormal extensions at the poles. These cells were scored as branching cells (**Table 3**; **Figure 4**). We would like to remark that it is formally possible that minicells do not only originate

from polar divisions but also from budding of branches. However, as the frequency of mini cell formation under non-branching conditions is almost the same as on branching conditions we deem this unlikely.

3.4. Nucleoid organization in the Xac *minC* deletion strain

Disruption of the *min* system in *E. coli* (52, 53) results in aberrant nucleoids, and in the case of branching cells large masses of DNA are often located at branching points (35). To study nucleoid distribution and organization we made use of strains carrying a functional GFP fusion to ParB (22). In a wild type background, GFP-ParB localizes to the origin-proximal *parS* site on the chromosome. Upon *parS* duplication during chromosome replication and segregation, ParB bound to the second *parS* copy moves from one pole to the other during the cell cycle (22) (**Figure 5**). We introduced the *parB-gfp* allele into the Δ*minC* background to construct the strain Xac Δ*minC parB::parB-gfp*, and studied nucleoid distribution with DAPI and nucleoid organization using ParB-GFP. In branching cells, we observed longer nucleoid length and the occasional accumulation of DNA at branch points (**Figure 5B**; **Figure 6**), although the accumulation at branch points was not a typical feature of branching cells (9 out of 36 branching cells on Xam1 had DNA at the branch point). The ParB-GFP pattern appeared less clearly defined on Xam1 medium (**Figure 5A, B**) with more faint fluorescent spots visible in the cells compared to the one or two spots per cell seen with NYGB medium (**Figure 5C, D**).

3.5. Branching cells have deficiencies in positioning cell division and peptidoglycan synthesis

In *E. coli*, branch formation is the result of defects in positioning the cell division machinery, notably FtsZ (41). In *min* mutants the FtsZ ring can form at the poles, but there is also an increased zone for FtsZ polymerization at midcell, which also occurs in cells with defective PBP5 (41). In *E. coli* some peptidoglycan (PG) is synthesized in an FtsZ-dependent manner at a site that will form the new pole, and strikingly this PG is not subject to turnover of material, which is why it is called inert PG (iPG) (54). iPG is always found at the poles and at the tips of branches, which originate from places on the side wall that contained iPG. We studied the

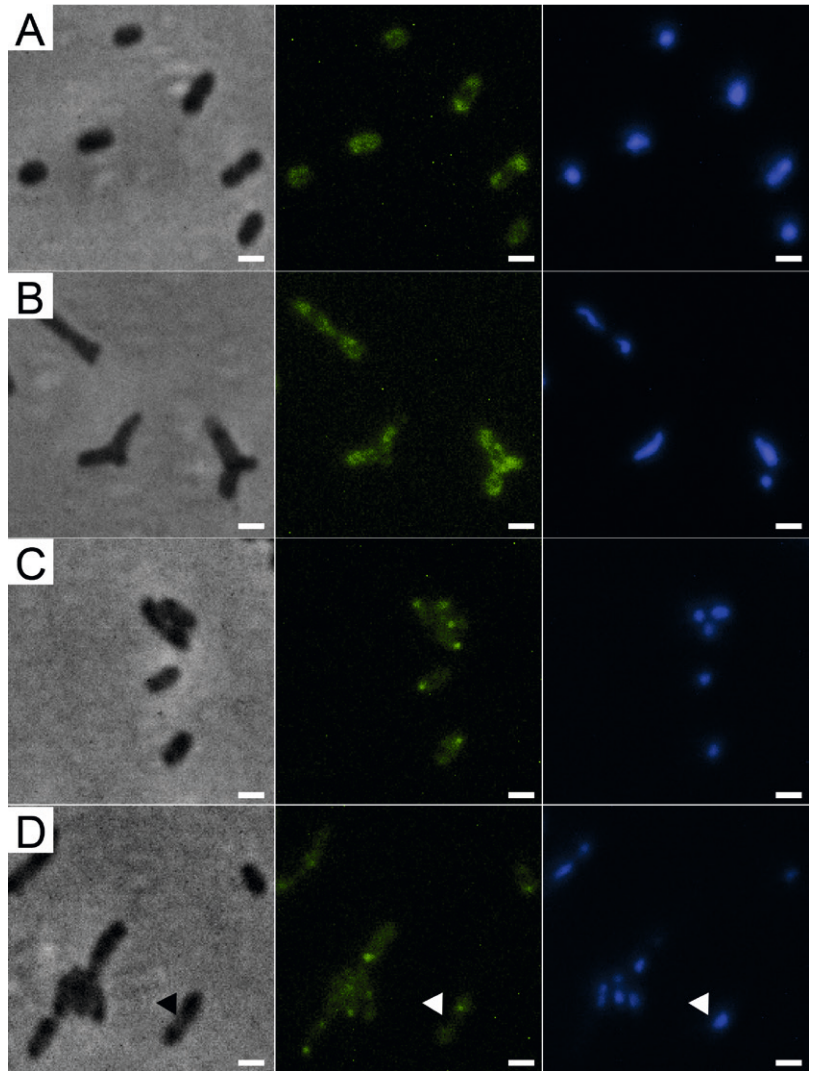

Figure 5: (A) Xac *parB::parB-gfp* grown in Xam1. **(B)** Xac Δ*minC parB::parB-gfp* grown in Xam1. **(C)** Xac *parB::parB-gfp* grown in NYGB. **(D)** Xac Δ*minC parB::parB-gfp* grown in NYGB, triangles indicate divisions initiated over non-segregated nucleoids. All cells in the figure were labeled with DAPI. Phase contrast (left), DAPI (center) exhibiting nucleoids, and FITC (right) exhibiting ParB-GFP. Scale bar: 1 μm.

relation between cell division site placement and peptidoglycan synthesis by using GFP-ZapA (14) as a proxy for division site localization and

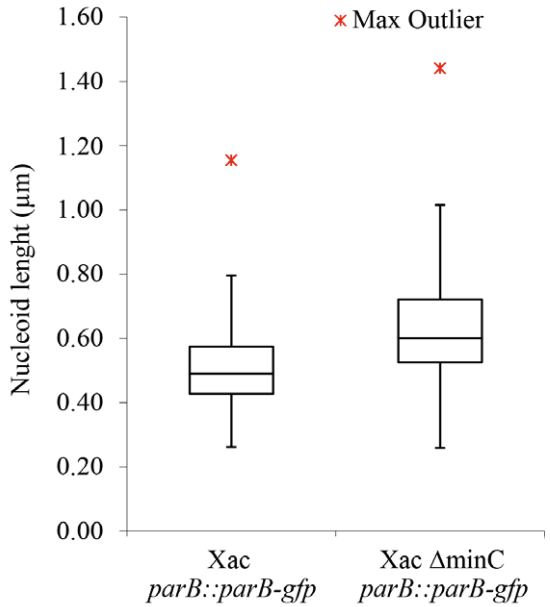

Figure 6: Nucleoid length of Xac cells, with and without MinC, grown to exponential phase in Xam1 medium, measured manually with ObjectJ. Whiskers at the top represent the 1.5 interquartile range and whiskers at the bottom extend to the minimum value. $p < 0.001$ (Mann-Whitney *U*-Test).

the fluorescent D-amino acid analog HADA (55) to label sites of active, ongoing PG synthesis. Cells were grown for 24 min (8% of the doubling time) in the presence of HADA and analyzed. In wild type cells, most PG synthesis occurred at division sites at midcell, which could also be identified by fluorescent bands of GFP-ZapA (**Figure 7A, C**). This pattern is similar to HADA labeling in other rod-shaped bacteria such as *E. coli* and *B. subtilis* (55). Sometimes, spots of HADA were seen at some poles, which could be due to the fact that the HADA was incorporated in the septum just before cell division. In non-dividing cells, GFP-ZapA localized throughout the cytosol as described (14). Sometimes, spots of HADA were seen at some poles, which could be due to the fact that the HADA was incorporated in the septum just before cell division. In non-dividing cells, GFP-ZapA localized throughout the cytosol as described (**Table 4**). In the *minC* deletion mutant, this colocalization of GFP-ZapA and HADA incorporation at division sites was lost (**Figure 7B**, **D**, **Table 4**). The

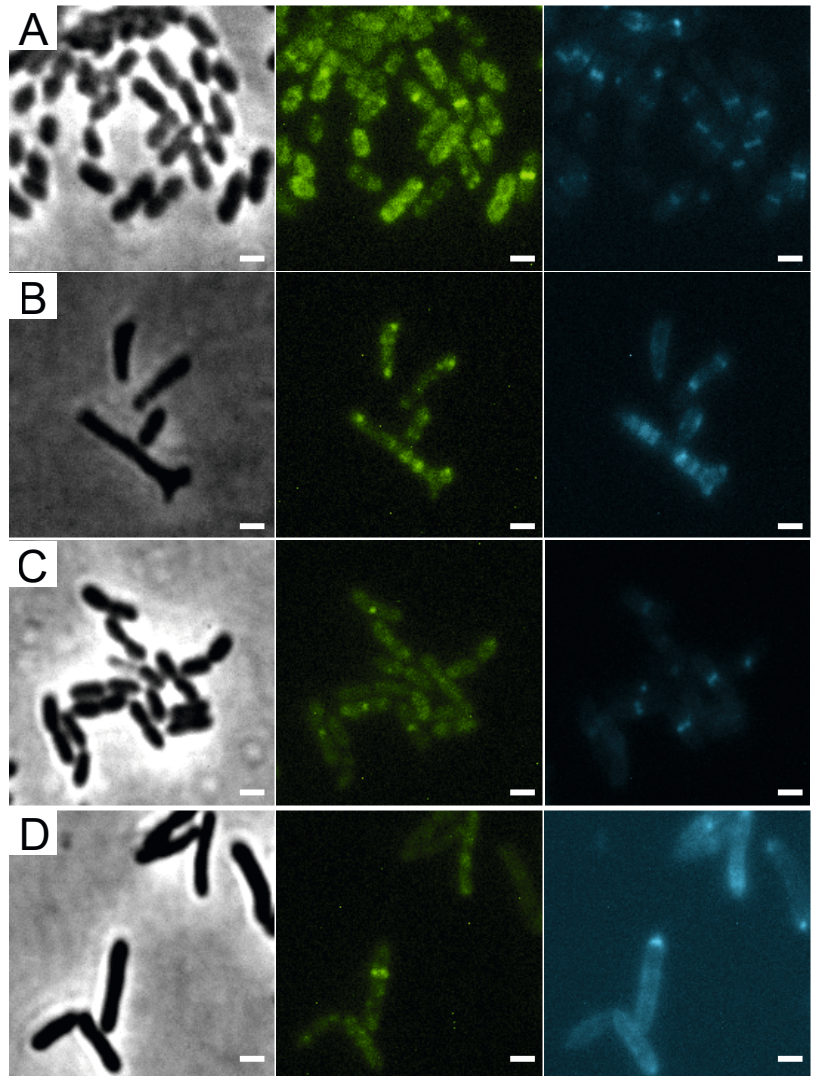

Figure 7: (A) Xac *amy::gfp-zapA* grown to exponential phase in Xam1, labeled with 125 µM of HADA for 24 min. **(B)** Xac Δ*minC amy::gfp-zapA* grown to exponential phase in Xam1, labeled with 125 µM of HADA for 24 min. **(C)** Xac *amy::gfp-zapA* grown to exponential phase in NYGB, labeled with 125 µM of HADA for 10 min. **(D)** Xac Δ*minC amy::gfp-zapA* grown to exponential phase in NYGB, labeled with 125 µM of HADA for 10 min. Phase contrast (left). FITC (center) exhibiting GFP-ZapA at the septum. CFP (right) exhibiting HADA (peptidoglycan incorporation sites) mostly at the septum. Scale bar 1 µm.

Table 4: Overlapping events in pictures of cells with HADA and GFP-ZapA signals.

Strain	Medium	Overlap	No overlap	Total
Xac *amy::gfp-zapA*	Xam1	97% (101)	3% (3)	100% (104)
Xac *ΔminC amy::gfp-zapA*	Xam1	18% (25)	82% (114)	100% (139)
Xac *amy::gfp-zapA*	NYGB	73% (76)	27% (28)	100% (104)
Xac *ΔminC amy::gfp-zapA*	NYGB	16% (19)	84% (102)	100% (121)

minC deletion strain when grown in conditions that promote branching, shows less complete GFP-ZapA rings, which also do not appear to be fully perpendicular to the cell axis, and strong GFP-ZapA signals are not overlapping with bands of HADA that can be observed at sites that show constrictions that would be indicative of ongoing divisions. When these cells are grown under non-branching conditions, this defect in colocalization of GFP-ZapA and HADA was not rescued (**Table 4**). Recent work has pointed at a role for metabolism in the control of cell division, with pyruvate levels in *B. subtilis* stimulating efficient Z ring formation under nutrient rich conditions through pyruvate dehydrogenase E1α (*56, 57*). We tested whether the addition of pyruvate to the medium in which branching occurs can rescue Z ring positioning and branching, but this was not the case (**Figure S3**).

4. Discussion

In this work, we have shown that MinC oscillates from pole to pole to ensure proper cell division and cell shape in Xac. Although the oscillation of MinCD was described nearly 20 years ago (*51, 58*), it was only last year that the second and third cases of oscillating Min proteins in the homologous host were described in *S. elongates* (*27*), and *V. cholera* (*33*). Our observation of GFP-MinC oscillations in Xac now provides the fourth example. Oscillations of Min system proteins have also been reported in heterologous systems. For example, MinDE from *Neisseria gonorrhoeae* have been shown to oscillate when expressed in *E. coli* (*59*), and MinDE from *Clostridium difficile* have been shown to oscillate when expressed in *B. subtilis* (*60*). Combined, these reports support the idea that an oscillating Min system is a common feature as long as the Min system protein MinE is present.

The Min system is responsible for ensuring that the cell division machinery assembles at the right place; this goal is achieved by negative regulation of FtsZ by MinC (*61*). The absence of MinC creates more space for Z rings to assemble, both at the poles of cells and at midcell, resulting in the formation of minicells, the characteristic phenotype of *min* mutants. The presence of other regulatory systems, such as nucleoid occlusion and the composition of the cell wall, generally confine Z rings at midcell sufficiently to ensure "normal" divisions, perpendicular to the length of the cell, but under certain conditions branches can start to form. Branching is thought to arise from a disruption in the organization of Z rings in such a way that Z rings are allowed to form in more places and at unnatural angles. This is in line with the observation that branching in *E. coli* is exacerbated upon overexpression of *ftsZ* (*41*), as higher levels of FtsZ result in the formation of abnormal rings in multiple bacteria. Branching of *min* mutants of *E. coli* does not always occur — but seems to be dependent on growth conditions and correlated with the general physiology of the cell rather than specific media components (*34*). We have observed a similar, growth condition dependent, branching phenotype in Xac.

Several papers in the past decade have pointed to a role for metabolism in the control of cell division and shape (*56*). For example, Z ring formation is directly controlled in *E. coli* and *B. subtilis* by two different metabolic enzymes that moonlight as FtsZ inhibitors (*62*). *In vitro* evidence points to UDP-glucose as the molecule responsible for the metabolic control but an (additional) role for increased levels of peptidoglycan precursors in triggering enhanced division is possible (*56*). In addition, pyruvate dehydrogenase E1α (PDH E1α) has been identified as a positive regulator of FtsZ ring formation in *B. subtilis*, which links the presence of high levels of pyruvate to increased division at midcell (*57*). High levels of pyruvate are linked to a high glycolytic flux and a switch to gluconeogenic conditions has implications for the availability of cell wall precursors and FtsZ positioning (*57*). In this respect it is interesting to note that the general physiology in which branching occurs most in the *min* mutants in both *E. coli* (*34*) and Xac is gluconeogenic growth.

A branching phenotype is a common feature among asymmetric polar growing bacteria (*63*), such as in Actinomycetes, Rhizobiales and Caulobacterales (*64*). Here, branching is caused by dedicated proteins,

not aberrantly positioned Z rings (65). In *E. coli*, positioning of FtsZ not exactly at midcell can result in the synthesis of inert PG that will form the future tip of a branch. We studied the relation between cell division and PG synthesis in the branching *min* mutants of Xac. We used the fluorescent D-amino acid analog HADA, which can be used to track PG synthesis in many different bacteria (55), to establish that wild type Xac grows similar to other rod-shaped bacteria, with PG incorporated both at the lateral wall and at division sites. In wild type cells, PG synthesis at division sites and visible GFP-ZapA rings clearly overlapped. In the branching *minC* mutant, these patterns were lost. Cell division was clearly impaired as shown by the scattered localization of ZapA patches that often did not form perpendicular rings that would support division, and scattered HADA incorporation. Interestingly, the ZapA and HADA localization patterns hardly overlapped in the *minC* mutant, something one would expect if the aberrant placement of division sites would recruit PG synthesis enzymes.

Potluri *et al.* (41) observed similar branching formation in *E. coli* cells deleted for PBP5 and other low molecular weight penicillin-binding proteins (PBPs). They proposed a link between branching formation and aberrant cell division. In the absence of PBPs, and PBP5 in particular, the organization of Z rings is disturbed in such a way that they are allowed to form in more places and at unnatural angles. This leads to malformation of daughter cells, which leads to branching phenotypes. Our observations of GFP-ZapA and HADA incorporation demonstrate that the *minC* deletion in Xac leads to disruption of both cell division and peptidoglycan incorporation, but the effects on Z-ring placement seem more drastic compared to the *E. coli* phenotype. However, it is likely that the disruption of division site placement and peptidoglycan incorporation result in similar branching of daughter cells as previously reported for *E. coli* (41).

Finally, we observed that similar to *E. coli min* mutant branching cells, Xac *min* mutants that branch, show disorganization of the nucleoids. Whether this is a result of the deformation of the cells only, or whether the Min system influences asymmetric chromosome segregation in Xac we cannot say. We noticed that ParB-GFP localized in clear spots in cells grown on NYGB medium, whereas the localization pattern was more faint in Xam1 medium. We don't know the cause of this difference — but it is probably not caused by the effect of the media on GFP as GFP-ZapA did not show such a difference.

In conclusion, we have shown that Xac *min* mutants display a metabolism-dependent branching phenotype which is the result of delocalized cell division and peptidoglycan synthesis. Also, we have shown that MinC oscillation occurs in a third organism next to *E. coli* and *S. elongatus*.

5. Author contributors

HF and DS conceived the study. AL, GD, HF, and DS designed the research. GD constructed the plasmids and strains. AL and TB performed the microscopy experiments. AL quantified the morphological data and assembled the pictures and graphs. AL, GD, HF, and DS analyzed the data. AL, HF, and DS wrote the manuscript. All authors have read and approved the final manuscript.

6. Funding

This work was funded by the bilateral research program "Biobased Economy" from the Netherlands Organisation for Scientific research (NWO) and the São Paulo Research Foundation (FAPESP, 2013/50367-8, Brazil, to DS and HF), a FAPESP (2013/14013-7) grant to HF, a NWO Vidi grant to DS, and a Science without Borders grant to AL (CNPq, Brazil).

7. Acknowledgments

We are grateful to Anabela de Sousa Borges and Danae Morales Angeles for help with lab work, to Alwin Hartman and Anna Hirsch for HADA synthesis, and to Riccardo Iacovelli for help with graphics.

8. References

1. T. R. Gottwald, J. H. Graham, T. S. Schubert, Citrus canker: the pathogen and its impact. *Plant Health Progress* **10**, (2002).
2. R. Davis *et al.*, First record of citrus canker, caused by Xanthomonas citri subsp. citri in Solomon Islands. *Australasian Plant Disease Notes* **10**, 1–4 (2015).
3. F. Behlau, A. Fonseca, J. Belasque, A comprehensive analysis of the Asiatic citrus canker eradication program in São Paulo State, Brazil, from 1999 to 2009. *Plant Pathology*, (2016).
4. E. Stover *et al.*, Incidence and severity of asiatic citrus canker on diverse citrus and citrus-related germplasm in a Florida field planting. *HortScience* **49**, 4–9 (2014).
5. A. Leduc *et al.*, Bridgehead invasion of a monomorphic plant pathogenic bacterium: Xanthomonas citri pv. citri, an emerging citrus pathogen in Mali and Burkina Faso. *Environmental microbiology* **17**, 4429–4442 (2015).
6. F. Behlau, B. I. Canteros, G. V. Minsavage, J. B. Jones, J. H. Graham, Molecular Characterization of Copper Resistance Genes from Xanthomonas citri subsp. citri and Xanthomonas alfalfae subsp. citrumelonis. *Applied and Environmental Microbiology* **77**, 4089–4096 (2011).
7. F. Behlau, B. I. Canteros, J. B. Jones, J. H. Graham, Copper resistance genes from different xanthomonads and citrus epiphytic bacteria confer resistance to Xanthomonas citri subsp. citri. *European journal of plant pathology* **133**, 949–963 (2012).
8. A. R. da Silva *et al.*, Comparison of the genomes of two Xanthomonas pathogens with differing host specificities. *Nature* **417**, 459–463 (2002).
9. J. Li, N. Wang, The gpsX gene encoding a glycosyltransferase is important for polysaccharide production and required for full virulence in Xanthomonas citri subsp. citri. *BMC microbiology* **12**, 1 (2012).
10. A. Casabuono, S. Petrocelli, J. Ottado, E. G. Orellano, A. S. Couto, Structural analysis and involvement in plant innate immunity of Xanthomonas axonopodis pv. citri lipopolysaccharide. *Journal of Biological Chemistry* **286**, 25628–25643 (2011).
11. A. V. Alexandrino, L. S. Goto, M. T. M. Novo-Mansur, treA Codifies for a Trehalase with Involvement in Xanthomonas citri subsp. citri Pathogenicity. *PloS one* **11**, e0162886 (2016).
12. M. C. Alegria *et al.*, New protein-protein interactions identified for the regulatory and structural components and substrates of the type III Secretion system of the phytopathogen Xanthomonas axonopodis Pathovar citri. *Journal of bacteriology* **186**, 6186–6197 (2004).
13. T.-P. Huang, K.-M. Lu, Y.-H. Chen, A novel two-component response regulator links rpf with biofilm formation and virulence of Xanthomonas axonopodis pv. citri. *PloS one* **8**, e62824 (2013).
14. P. M. Martins *et al.*, Subcellular localization of proteins labeled with GFP in Xanthomonas citri ssp. citri: targeting the division septum. *FEMS microbiology letters* **310**, 76–83 (2010).
15. G. C. Dantas, P. M. Martins, D. A. Martins, E. Gomes, H. Ferreira, A protein expression system for tandem affinity purification in Xanthomonas citri subsp. citri. *brazilian journal of microbiology* **47**, 518–526 (2016).
16. C. E. Broughton, H. A. Van Den Berg, A. M. Wemyss, D. I. Roper, A. Rodger, Beyond the Discovery Void: New targets for antibacterial compounds. *Science Progress* **99**, 153–182 (2016).
17. P. Sass, H. Brötz-Oesterhelt, Bacterial cell division as a target for new antibiotics. *Current opinion in microbiology* **16**, 522–530 (2013).
18. P.-S. Pan *et al.*, Novel antibiotics: C-2 symmetrical macrocycles inhibiting Holliday junction DNA binding by E. coli RuvC. *Bioorganic & medicinal chemistry* **14**, 4731–4739 (2006).
19. W. Vollmer, The prokaryotic cytoskeleton: a putative target for inhibitors and antibiotics? *Applied microbiology and biotechnology* **73**, 37–47 (2006).
20. I. C. Silva *et al.*, Antibacterial activity of alkyl gallates against Xanthomonas citri subsp. citri. *Journal of Bacteriology* **195**, 85–94 (2013).
21. E. Król *et al.*, Antibacterial activity of alkyl gallates is a combination of direct targeting of FtsZ and permeabilization of bacterial membranes. *Frontiers in Microbiology* **6**, (2015).
22. A. P. Ucci *et al.*, Asymmetric chromosome segregation in Xanthomonas citri ssp. citri. *MicrobiologyOpen* **3**, 29–41 (2014).
23. W. Margolin, FtsZ and the division of prokaryotic cells and organelles. *Nature Reviews Molecular Cell Biology* **6**, 862–871 (2005).
24. Y. L. Shih, M. Zheng, Spatial control of the cell division site by the Min system in E scherichia coli. *Environmental microbiology* **15**, 3229–3239 (2013).
25. D. Ghosal, D. Trambaiolo, L. A. Amos, J. Löwe, MinCD cell division proteins form alternating copolymeric cytomotive filaments. *Nature communications* **5**, (2014).
26. V. W. Rowlett, W. Margolin, The bacterial Min system. *Current Biology* **23**, R553-R556 (2013).
27. J. S. MacCready, J. Schossau, K. W. Osteryoung, D. C. Ducat, Robust Min-System Oscillation in the Presence of Internal Photosynthetic Membranes in Cyanobacteria. *Molecular Microbiology*, (2016).
28. M. Bramkamp, S. van Baarle, Division site selection in rod-shaped bacteria. *Current opinion in microbiology* **12**, 683–688 (2009).
29. T. G. Bernhardt, P. A. De Boer, SlmA, a nucleoid-associated, FtsZ binding protein required for blocking septal ring assembly over chromosomes in E. coli. *Molecular cell* **18**, 555–564 (2005).
30. E. J. Cabré *et al.*, The nucleoid occlusion SlmA protein accelerates the disassembly of the FtsZ protein polymers without affecting their GTPase activity. *PloS one* **10**, e0126434 (2015).
31. D. A. Mohl, J. W. Gober, Cell cycle–dependent polar localization of chromosome partitioning proteins in Caulobacter crescentus. *Cell* **88**, 675–684 (1997).
32. M. Thanbichler, L. Shapiro, MipZ, a spatial regulator coordinating chromosome segregation with cell division in Caulobacter. *Cell* **126**, 147–162 (2006).
33. E. Galli *et al.*, Cell division licensing in the multi-chromosomal Vibrio cholerae bacterium. *Nature microbiology* **1**, 16094–16094 (2016).
34. B. Gullbrand, T. Åkerlund, K. Nordström, On the Origin of Branches inEscherichia coli. *Journal of bacteriology* **181**, 6607–6614 (1999).
35. T. Åkerlund, K. Nordström, R. Bernander, Branched Escherichia coli cells. *Molecular microbiology* **10**, 849–858 (1993).
36. D. E. Nelson, K. D. Young, Penicillin binding protein 5 affects cell diameter, contour, and morphology of Escherichia coli. *Journal of bacteriology* **182**, 1714–1721 (2000).
37. D. E. Nelson, K. D. Young, Contributions of PBP 5 anddd-Carboxypeptidase Penicillin Binding Proteins to Maintenance of Cell Shape in Escherichia coli. *Journal of bacteriology* **183**, 3055–3064 (2001).
38. A. Varma, K. D. Young, FtsZ collaborates with penicillin binding proteins to generate bacterial cell shape in Escherichia coli. *Journal of bacteriology* **186**, 6768–6774 (2004).
39. A. Varma, M. A. de Pedro, K. D. Young, FtsZ directs a second mode of peptidoglycan synthesis in Escherichia coli. *Journal of bacteriology* **189**, 5692–5704 (2007).
40. A. Varma, K. D. Young, In Escherichia coli, MreB and FtsZ direct the synthesis of lateral cell wall via independent pathways that require PBP 2. *Journal of bacteriology* **191**, 3526–3533 (2009).
41. L. P. Potluri, M. A. de Pedro, K. D. Young, Escherichia coli low-molecular-weight penicillin-binding proteins help orient septal FtsZ, and their absence leads to asymmetric cell division and branching. *Molecular microbiology* **84**, 203–224 (2012).
42. J. Sambrook, E. F. Fritsch, T. Maniatis, *Molecular Cloning: A laboratory manual*. (Cold Spring Harbor Laboratory Press, Cold Spring Harbor, NY, ed. 2nd Edition, 1989).
43. N. W. Schaad *et al.*, Emended classification of xanthomonad pathogens on citrus. *Papers in Plant Pathology*, 96 (2006).
44. N. W. Schaad *et al.*, Reclassification of Xanthomonas campestris pv. citri (ex Hasse 1915) Dye 1978 forms A, B/C/D, and E as X. smithii subsp. citri (ex Hasse) sp. nov. nom. rev. comb. nov., X. fuscans subsp. aurantifolii (ex Gabriel 1989) sp. nov. nom. rev. comb. nov., and X. alfalfae subsp. citrumelo (ex Riker and Jones) Gabriel et al., 1989 sp. nov. nom. rev. comb. nov.; X. campestris pv malvacearum (ex Smith 1901) Dye 1978 as X. smithii subsp. smithii nov. comb. nov. nom. nov.; X. campestris pv. alfalfae (ex Riker and Jones, 1935) Dye 1978 as X. alfalfae subsp. alfalfae (ex Riker et al., 1935) sp. nov. nom. rev.; and "var. fuscans" of X. campestris pv. phaseoli (ex Smith, 1987) Dye 1978 as X. fuscans subsp. fuscans sp. nov. *Systematic and Applied Microbiology* **28**, 494–518 (2005).
45. D. Gully, D. Moinier, L. Loiseau, E. Bouveret, New partners of acyl carrier protein detected in Escherichia coli by tandem affinity purification. *FEBS Lett* **548**, 90–96 (2003).
46. L. A. Lacerda *et al.*, Protein depletion using the arabinose promoter in Xanthomonas citri subsp. citri. *Plasmid*, (2017).
47. P. M. Martins *et al.*, Subcellular localization of proteins labeled with GFP in Xanthomonas citri ssp. citri: targeting the division septum. *FEMS microbiology letters* **310**, 76–83 (2010).
48. H. Ferreira, F. J. A. Barrientos, R. L. Baldini, Y. B. Rosato, Electrotransformation in three pathovars of Xanthomonas campestris. *Appl. Microbiol. Biotechnol.* **43**, 651–655 (1995).

4

49. E. Kuru, S. Tekkam, E. Hall, Y. V. Brun, M. S. Van Nieuwenhze, Synthesis of fluorescent D-amino acids and their use for probing peptidoglycan synthesis and bacterial growth in situ. *Nature protocols* **10**, 33–52 (2015).
50. A. S. Lorenzoni, G. C. Dantas, T. Bergsma, H. Ferreira, D.-J. Scheffers, Xanthomonas citri MinC Oscillates from Pole to Pole to Ensure Proper Cell Division and Shape. *Frontiers in microbiology* **8**, 1352 (2017).
51. D. M. Raskin, P. A. de Boer, MinDE-dependent pole-to-pole oscillation of division inhibitor MinC in Escherichia coli. *Journal of bacteriology* **181**, 6419–6424 (1999).
52. A. Jaffe, R. D'Ari, S. Hiraga, Minicell-forming mutants of Escherichia coli: production of minicells and anucleate rods. *Journal of bacteriology* **170**, 3094–3101 (1988).
53. E. Mulder, M. El'Bouhali, E. Pas, C. L. Woldringh, The Escherichia cohi minB mutation resembles gyrB in defective nucleoid segregation and decreased negative supercoiling of plasmids. *Molecular and General Genetics MGG* **221**, 87–93 (1990).
54. M. De Pedro, J. C. Quintela, J. Höltje, H. Schwarz, Murein segregation in Escherichia coli. *Journal of bacteriology* **179**, 2823–2834 (1997).
55. E. Kuru *et al.*, In situ probing of newly synthesized peptidoglycan in live bacteria with fluorescent D-amino acids. *Angewandte Chemie International Edition* **51**, 12519–12523 (2012).
56. A. M. Sperber, J. K. Herman, Metabolism shapes the cell. *Journal of Bacteriology*, JB. 00039–00017 (2017).
57. L. G. Monahan, I. V. Hajduk, S. P. Blaber, I. G. Charles, E. J. Harry, Coordinating bacterial cell division with nutrient availability: a role for glycolysis. *MBio* **5**, e00935–00914 (2014).
58. D. M. Raskin, P. A. de Boer, Rapid pole-to-pole oscillation of a protein required for directing division to the middle of Escherichia coli. *Proceedings of the National Academy of Sciences* **96**, 4971–4976 (1999).
59. S. Ramirez-Arcos, J. Szeto, J. A. R. Dillon, W. Margolin, Conservation of dynamic localization among MinD and MinE orthologues: oscillation of Neisseria gonorrhoeae proteins in Escherichia coli. *Molecular microbiology* **46**, 493–504 (2002).
60. J. Makroczyová, J. Jamroškovič, E. Krascsenitsová, N. Labajová, I. Barák, Oscillating behavior of Clostridium difficile Min proteins in Bacillus subtilis. *MicrobiologyOpen*, (2016).
61. V. W. Rowlett, W. Margolin, The Min system and other nucleoid-independent regulators of Z ring positioning. *Frontiers in microbiology* **6**, (2015).
62. N. S. Hill, P. J. Buske, Y. Shi, P. A. Levin, A moonlighting enzyme links Escherichia coli cell size with central metabolism. *PLoS Genet* **9**, e1003663 (2013).
63. V. L. Wells, W. Margolin, A new slant to the Z ring and bacterial cell branch formation. *Molecular microbiology* **84**, 199–202 (2012).
64. P. J. Brown *et al.*, Polar growth in the Alphaproteobacterial order Rhizobiales. *Proceedings of the National Academy of Sciences* **109**, 1697–1701 (2012).
65. M. Howell, P. J. Brown, Building the bacterial cell wall at the pole. *Current Opinion in Microbiology* **34**, 53–59 (2016).

9. Supporting information

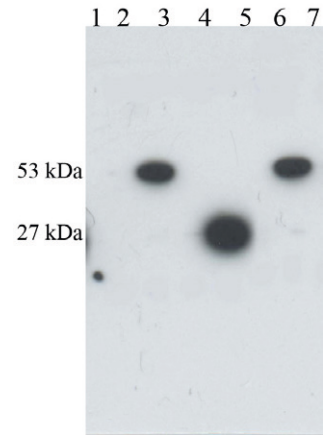

Figure S1: Western blot with cells grown in Xam1 with 2% glucose using Rabbit polyclonal GFP[1] antibody. Secondary antibody detection was done using the Amersham ECL kit. **1** Molecular weight ladder; **2** Xac *amy::gfp-minC;* **3** Xac *amy::gfp-minC* + arabinose[1]; **4** Xac ΔminC amy::gfp; **5** Xac ΔminC amy::gfp + arabinose[1]; **6** Xac ΔminC amy::*gfp-minC;* **7** Xac ΔminC amy::*gfp-minC* + arabinose[1];

[1]G1544 from SIGMA diluted 1:2500.

[2]0.05% arabinose during 1 h.

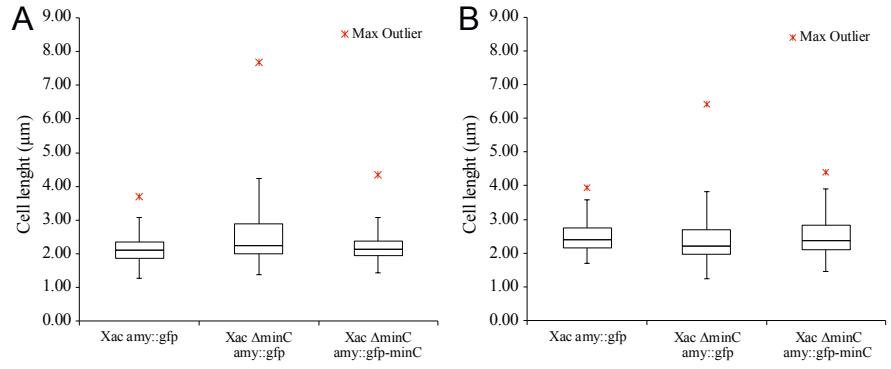

Figure S2: (A) Cell length of Xac *amy::gfp* (n = 1599), Xac Δ*minC amy::gfp* (n = 1114) and Xac Δ*minC amy::gfp-minC* (n = 1624), grown to exponential phase in Xam1 medium. **(B)** Cell length of Xac *amy::gfp* (n = 729), Xac Δ*minC amy::gfp* (n = 589) and Xac Δ*minC amy::gfp-minC* (n = 551), grown to exponential phase in NYGB medium. Both sets were measured automatically with Coli-Inspector, plugin for ObjectJ. Whiskers at the top represent the 1.5 interquartile range and whiskers at the bottom extend to the minimum value.

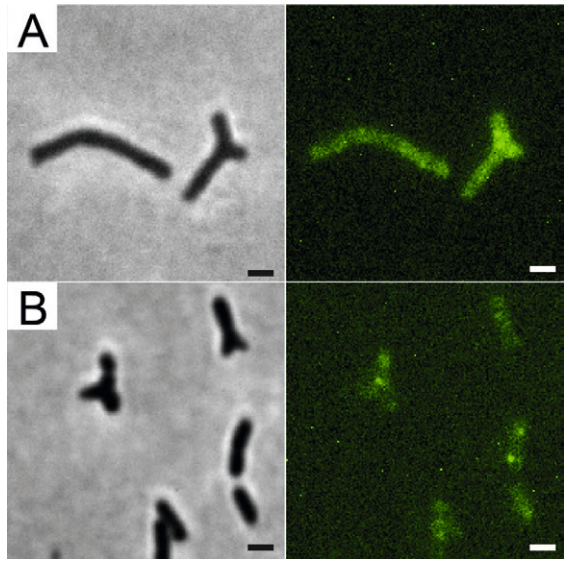

Figure S3: Xac Δ*minC amy::gfp* grown to exponential phase in NYGB medium diluted to Xam1 medium and then grown overnight. **(A)** without sodium pyruvate. **(B)** with 1% sodium pyruvate. Scale bar: 1 µM.

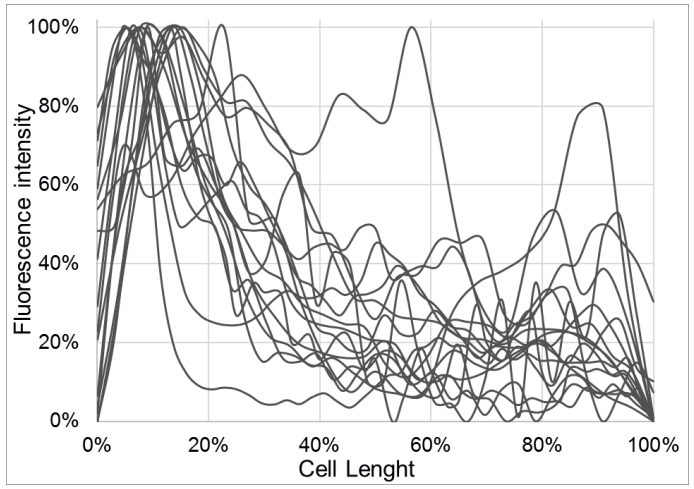

Figure S4: Line scans showing relative fluorescence intensity of FITC channel (GFP-MinC) along the central axis of Xac Δ*minC amy::gfp-minC* cells grown to exponential phase in Xam1 medium.

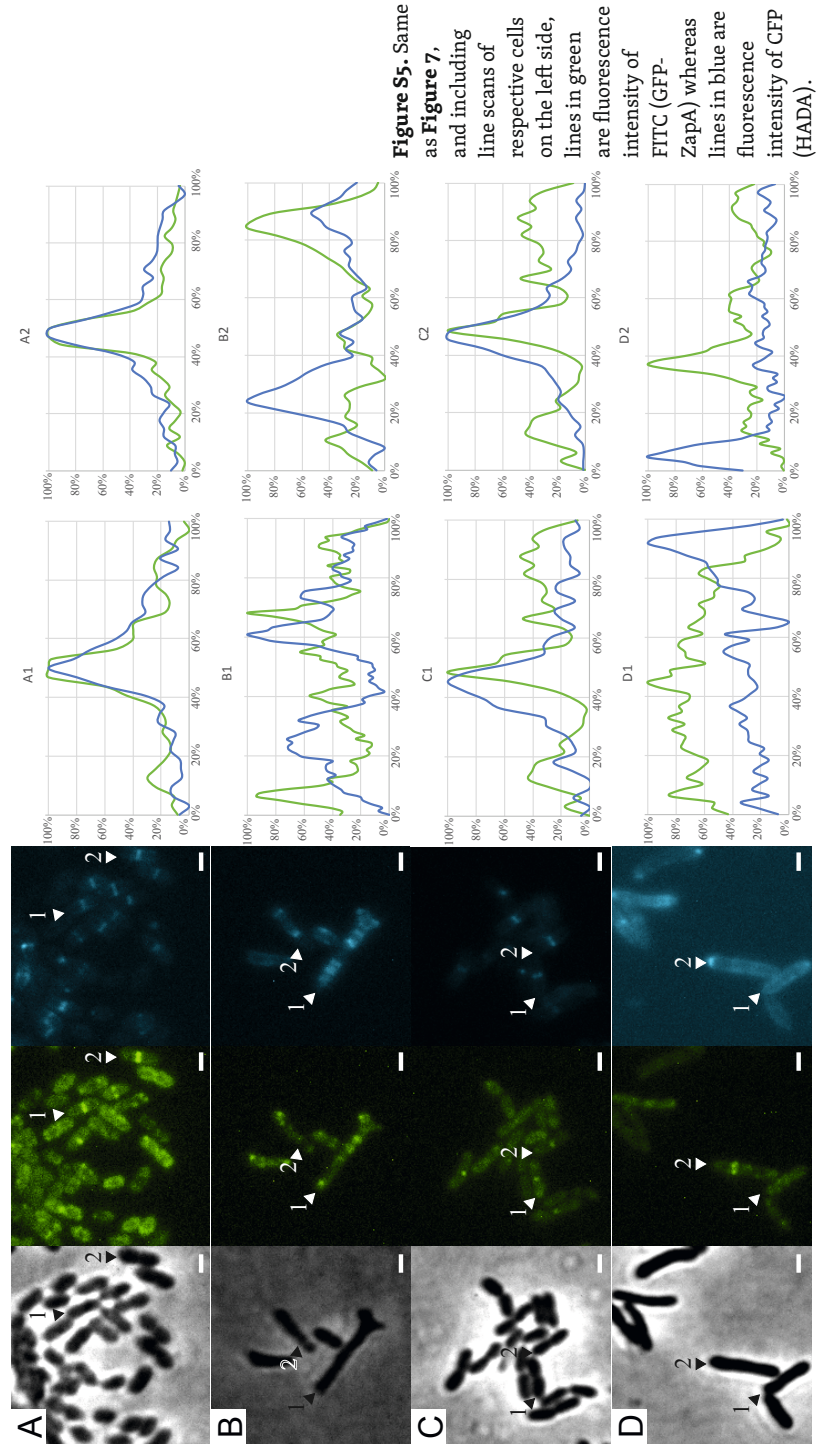

Figure S5. Same as **Figure 7**, and including line scans of respective cells on the left side, lines in green are fluorescence intensity of FITC (GFP-ZapA) whereas lines in blue are fluorescence intensity of CFP (HADA).

Table S1: Oligonucleotides used in this study.

Name	Sequence
pARAF	5'- AAAGAATTCGCATAATGTGCCTGTCAAATG
pARAR	5'- TTTAGATCTTTCCTCCTGCTAGCCCAAAAAAACG
minCF	5'- TAAGCGGCCGCGTGGCAAGTGTGAATGTGGATTTTG
201402minCR	5'- AAATCTAGATCAATCAAGCGCAGCGATCTTG
minC_pLAL1F	5'- AAAGAATTCACCATGGCAAGTGTGAATGTGGATTTTG
minC_pLAL1R	5'- AAAAAGCTTTCAATCAAGCGCAGCGATCTTG
minCupF	5'- AAAGGATCCGTATGACTGAGGTATCCCAACATGTC
minCupR	5'- AAATCTAGATGCCACAACTCAGCTCCCCGTCGATG
minCdownF	5'- AAATCTAGAGATTGACGCGGCCCAACCACAGAAATATTC
minCdownR	5'- AAAAAGCTTCAATGATGATCTGCAGGCGGTTCTTGG
minCupF (*Bam*HI)	5'- AAAGGATCCGTATGACTGAGGTATCCCAACATGTC
minCupR (*Xba*I)	5'- AAATCTAGATGCCACAACTCAGCTCCCCGTCGATG
minCdownF (*Xba*I)	5'- AAATCTAGAGATTGACGCGGCCCAACCACAGAAATATTC
minCdownR (*Hind*III)	5'- AAAAAGCTTCAATGATGATCTGCAGGCGGTTCTTGG

Video 1 can be downloaded at:
https://www.frontiersin.org/articles/10.3389/fmicb.2017.01352/full#supplementary-material

Chapter 5 — Summary

André S. G. Lorenzoni and Dirk-Jan Scheffers

Summary

Bacteria are the most ubiquitous organisms on Earth. In a human body, there are more bacterial cells than human cells (*1*). Among other functions, these microorganisms are responsible for fixation of nitrogen from the atmosphere in soils, which enables the survival of complex terrestrial life (i.e., plants and animals) (*2*). The metabolic diversity of bacteria has been harnessed for the synthesis of industrial compounds such as pharmaceuticals, food ingredients and additives, and biocatalysts (*3*). However, a small proportion of bacteria are pathogenic, causing damage to agriculture and humans (*4*). To combat these bacteria, humans have developed antibiotics and antimicrobials, which drastically reduced mortality from bacterial diseases and increased human life expectancy worldwide (*5*).

The widespread use of antibiotics stimulated antibiotic resistance (*6*), which has rapidly become a danger to public health. More than 700 000 human deaths worldwide a year are caused by antimicrobial resistance (*7*), and this figure is likely to increase in the future (*8*). Antibiotics and antimicrobial compounds such as copper are also used in agriculture to combat plant pathogens *(9–13)*. The use of antimicrobials in agriculture reduces the loss of crops due to field diseases and increases the yield of food production. However, increasing antimicrobial resistance in phytopathogens is also a threat to agriculture (*14*).

So far the discovery of antibiotics has managed to keep human pathogens under control (*15*). The discovery of new antibiotics is needed to avoid a widespread pandemic of antibiotic resistant bacteria (*16*). In a similar manner, new antimicrobials are also needed to combat plant diseases more effectively (**Chapter 1**). Once discovered and characterized for their mode of action, antimicrobial substances can be chemically modified to improve potency, stability, delivery, or pharmacokinetics. This strategy has resulted in the development of dozens of new clinically useful antibiotics (*17*).

The first experimental chapter of this thesis (**Chapter 2**) is about the screening of organometallic compounds, and characterization of the antimicrobial activity of the compound **7b-BF$_4$**. Those compounds were synthesized with the primary idea of developing gold-based anticancer drugs. **7b-BF$_4$** exhibited the highest antimicrobial activity against Gram-positive bacteria among the potential drugs screened. The compound was tested on two multidrug resistant bacteria, methicillin resistant *Staphylococcus aureus* and Vancomycin resistant *Enterococcus faecium*, and it was able to kill those multidrug resistant strains at the same concentration as drug sensitive strains. This suggested that **7b-BF$_4$** possesses a different mode of action when compared to the antibiotics to which those organisms are resistant.

Bacillus subtilis was used as a model organism to determine whether **7b-BF$_4$** disrupted the membrane permeability. Membrane permeability was investigated using a combination of the membrane permeable and membrane impermeable dyes (SYTO 9 and propidium iodide, respectively). This was followed by an investigation whether **7b-BF$_4$** disrupts the membrane potential in *B. subtilis* using the potentiometric probe DiSC$_3$. **7b-BF$_4$** does not disrupt membrane potential. The effect of this compound on the four major metabolic pathways (DNA, RNA, protein, and peptidoglycan synthesis) of *B. subtilis* was tested using precursors labelled with ^{3}H. **7b-BF$_4$** affected all the four pathways without indication of a pathway specific effect. **7b-BF$_4$** causes a sharp decrease in intracellular ATP concentration in *B. subtilis*, which is likely the reason the four metabolic pathways were affected. Development of resistance against **7b-BF$_4$** was stimulated in the lab growing *B. subtilis* under sublethal concentrations of the compound for an extended period of time, but resistance was not detected.

The results obtained in this chapter showed that **7b-BF$_4$** is a strong antimicrobial agent against Gram-positive bacteria. While the exact mode of action of this compound is still unknown, our work indicates that it is different from other known antibiotics. Our suggestions for further characterizing the mode of action of this compound in the future are: RNA sequencing of cells under stress caused by the compound; electron microscopy of cells in the presence of the compound, since the compound contains gold it should be possible to detect its localization; and further stimulation of resistant mutants followed by genomic analyses of detected mutants.

The second experimental report of this thesis (**Chapter 3**), presents an investigation into the mode of action of the chalcones **BC1** and **T9A**. Those chalcones were synthesized by our collaborators in Brazil, that have a particular interest in combating the Gram negative bacteria *Xanthomonas citri* subsp. *citri* (Xac), the agent of citrus canker (Ayusso

et al., in preparation). Nearly all citrus species are susceptible to citrus canker, and there are no effective ways of eliminating Xac from an infected plant, leading to the eradication of infected trees (*18*). Brazil is the biggest orange producer in the world and the orange industry is negatively affected by citrus canker (*19*).

Naturally occurring chalcones are usually not active against Gram negative bacteria (*20*, *21*), but those compounds can be chemically modified to target Gram negative bacteria (*22*, *23*). **T9A** was the result of a screening made by our colleagues, that synthesized chalchones with substituted by hydroxyl group (hydroxychalcones) (Ayusso *et al.*, in preparation). **T9A** was selected for this study because it was the most active drug on that screening (Ayusso *et al.*, in preparation). **BC1** is a methoxychalcone obtained from the molecular simplification of curcumin (*24*).

The effect of **BC1** and **T9A** on membrane permeability was tested using a combination of the membrane permeable and membrane impermeable dyes, in *B. subtilis* and Xac and **T9A** does not disrupt membrane permeability whereas **BC1** disrupts *B. subtilis* membranes and does not disrupt Xac membranes. The effect of **BC1** and **T9A** on four the major metabolic pathways (DNA, RNA, protein, and peptidoglycan synthesis) in *B. subtilis* and Xac, using the same precursors, labelled with ^{3}H. This chapter, to our knowledge, is the first report of metabolic pathways assays on Xac. We also tested the effect of **BC1** and **T9A** on intracellular ATP concentration in *B. subtilis* and Xac. Similarly to what was observed in chapter 2, the chalcones affected all the four macromolecular pathways. However, ATP concentration was not affected by the compounds in *B. subtilis* and little impact was observed in Xac. Fourier-transform infrared (FTIR) spectrophotometry with *B. subtilis* treated with the chalcones was consistent with membrane disruption by **BC1**, but inconclusive for **T9A**. FTIR was not successful in Xac due to the formation of xanthan gum and biofilms.

The data produced in this chapter do not allow us to draw a conclusion about a specific mode of action of the compounds tested. However, we were able to generate Xac strains with resistance to T9A and BC1, which opens the possibility to sequence and carry out genomic analyses to understand the mode of action of this compounds.

This chapter is followed by an appendix where our results on the mode of action of alkyl gallates against Xac are reported. Alkyl gallates

have been found to have activity against Xac, inactivating cells in the lab and preventing infection on citrus leaves (*25*). The antimicrobial activity of alkyl gallates was characterized in *B. subtilis*, because at that time, FtsZ from Xac had not been purified yet and membrane permeability assays were not available for Xac (*26*). This appendix contains my contributions to the work of our group on the characterization of the antimicrobial activity of alkyl gallates against Xac (*27*).

In this work we tested the activity of alkyl gallates on Xac membranes, which in combination with our colleagues' results, showed that the primary antimicrobial activity of alkyl gallates on Xac is on the membrane permeability. In an attempt to address the susceptibility to resistance, we tried to develop the resistance of Xac against heptyl gallate (the most effective alkyl gallate on pathogenicity test (*25*)). Xac developed resistance against our positive control kanamycin, but not against heptyl gallate in the same experimental setting. On the one hand, this result eliminated the possibility of sequencing and studying resistant mutants in order to further characterize the mode of action of the compound, on the other hand this is an indication that resistance against this compound is less likely to occur which increases its appeal as an antimicrobial agent. Additionally, the same setting can be used in future studies on mode of action of compounds against Xac.

The last experimental chapter of this thesis (**Chapter 4**) focuses on the cell biology of Xac. In this chapter we engineered a strain of Xac with the gene *minC* deleted. This gene encodes the MinC protein, part of the Min system that in Xac (as well as in the thoroughly studied bacteria *E. coli*) consists of the MinC, MinD, and MinE proteins (*28*). This system is responsible for the spatial regulation of cell division, ensuring that it happens at mid cell and not at a random site along the rod shaped bacteria (e.g. at the cell poles). In *E. coli* this is possible because MinC forms a complex with MinD, thereby preventing the Z-ring to assemble in its vicinity. MinE activity causes the MinCD complex to oscillate between cell poles, therefore FtsZ is driven away from the poles and assembles at mid cell (*29*).

We investigated cell division, chromosome segregation, and peptidoglycan incorporation in wild type and Δ*minC* mutants. The gene *minC* was deleted using allele exchange. Xac with *minC* deleted exhibited minicells, short filamentation, and branching. The *minC* gene was

complemented by integrating *gfp-minC* into the *amy* locus. Complemented Xac strains displayed a wild-type phenotype. In addition, GFP-MinC oscillated from pole to pole, similar to MinCD oscillations observed in *Escherichia coli* and more recently in *Synechococcus elongatus* (30) and *Vibrio cholerae* (31). Thus, oscillating MinC seems to be a common feature among bacteria with the *minE* gene. Further investigation of the branching phenotype revealed that, in branching cells nucleoid organization, divisome formation, and peptidoglycan incorporation were disrupted, and that peptidoglycan incorporation was uncoupled from divisome formation in branching cells. The branching was also nutrient dependent and was rescued in medium containing peptone.

With this thesis we attempted to open new possibilities for studying both the cell biology of Xac and the mode of action of antimicrobial compounds. The radiolabel assay to test specific metabolic pathways, fluorescence assays to test membrane permeability, membrane potential, and peptidoglycan incorporation, fluorescent protein fusions with ZapA, MinC, and ParB, and FtsZ assays used in this thesis are a fine addition to a tool set to test new antimicrobials with potential to combat citrus canker and other infections. Genomic analyses of resistant mutants and RNA sequencing of cells treated with compounds are possibilities to expand our tool set and to establish the mode of action of antimicrobial compounds in more detail.

Samenvatting

Bacteriën zijn de meest alomtegenwoordige organismen op aarde. In een menselijk lichaam zijn er meer bacteriële cellen dan menselijke cellen (1). Deze micro-organismen zijn, onder andere, verantwoordelijk voor de fixatie van stikstof uit de atmosfeer in de bodem, wat het overleven van complexe aardse levensvormen (d.w.z. planten en dieren) mogelijk maakt (2). De metabolische diversiteit van bacteriën wordt gebruikt voor de synthese van industriële verbindingen zoals farmaceutische producten, voedselingrediënten, additieven en biokatalysatoren (3). Sommige soorten bacteriën zijn echter pathogeen en veroorzaken schade aan de landbouwsector en de volksgezondheid (4). Om deze bacteriën te bestrijden, zijn er antibiotica en antimicrobiële middelen ontwikkeld. Deze middelen hebben de sterfte aan bacteriële ziekten drastisch verminderd en hebben wereldwijd de levensverwachting van mensen verhoogd (5).

Het wijdverbreide gebruik van antibiotica stimuleerde de ontwikkeling van antibioticaresistentie in bacteriën (6), die in een rap tempo een gevaar voor de volksgezondheid is geworden. Jaarlijks worden wereldwijd meer dan 700 000 menselijke sterfgevallen veroorzaakt door antimicrobiële resistentie (7), en dit cijfer zal in de toekomst waarschijnlijk toenemen (8). Antibiotica en antimicrobiële stoffen zoals koper worden ook in de landbouw gebruikt om plantpathogenen te bestrijden (9–13). Het gebruik van antimicrobiële middelen in de landbouw vermindert het verlies van gewassen als gevolg van veldziekten en verhoogt de opbrengst van voedselproductie. De concurrente ontwikkeling van antimicrobiële resistentie bij fytopathogenen vormt echter ook een bedreiging voor de landbouwsector (14).

Tot nu toe is de ontdekking van antibiotica er grotendeels in geslaagd om menselijke ziekteverwekkers onder controle te houden (15). Echter is de ontdekking van nieuwe antibiotica nodig om een wijdverspreide pandemie van antibioticaresistente bacteriën te voorkomen (16). Op vergelijkbare wijze zijn ook nieuwe antimicrobiële middelen nodig om plantenziekten beter te bestrijden (**Hoofdstuk 1**). Na ontdekking kunnen antimicrobiële stoffen chemisch worden gemodificeerd om de

potentie, stabiliteit, levering of farmacokinetiek te verbeteren. Deze strategie heeft geresulteerd in de ontwikkeling van tientallen nieuwe klinisch bruikbare antibiotica (17).

Het eerste experimentele hoofdstuk van dit proefschrift (**Hoofdstuk 2**) gaat over de antimicrobiële screening van organometallische verbindingen en de karakterisatie van de antimicrobiële activiteit van de verbinding **7b-BF4**. De verbindingen besproken in dit werk werden gesynthetiseerd met het doel om op goud gebaseerde middelen tegen kanker te ontwikkelen. **7b-BF4** vertoonde de hoogste antimicrobiële activiteit tegen Gram-positieve bacteriën onder de gescreende verbindingen. De verbinding **7b-BF4** werd getest op twee multiresistente bacteriën, methicilline-resistente *Staphylococcus aureus* en Vancomycineresistente *Enterococcus faecium* en het was in staat om die multi-geneesmiddelresistente stammen te doden bij dezelfde concentratie als geneesmiddel-gevoelige stammen. Dit suggereerde dat **7b-BF4** een ander werkingsmechanisme heeft vergeleken met de antibiotica waartegen deze organismen resistent zijn.

Bacillus subtilis werd gebruikt als model organisme om vast te stellen of verbinding **7b-BF4** de membraanpermeabiliteit van een organisme verstoord. Dit werd onderzocht met behulp van een combinatie van membraanpermeabele en membraanondoorlaatbare kleurstoffen (Respectievelijk SYTO 9 en propidiumjodide). Verbinding **7b-BF4** bleek de membraanpermeabiliteit van *B. subtilis* niet te verstoren. Vervolgens werd bekeken of het membraanpotentiaal van *B. subtilis* wordt verstoord door verbinding **7b-BF4** met behulp van de potentiometrische probe $DiSC_3$. Er is geen aanwijzing gevonden dat **7b-BF4** het membraanpotentiaal verstoord in *B. subtilis*. Het effect van verbinding **7b-BF4** op de vier belangrijkste metabole routes (DNA, RNA, eiwit en peptidoglycaan synthese) werd getest in *B. subtilis* met behulp van ^3H gelabelde metabole precursors. **7b-BF4** beïnvloedde alle vier de routes zonder indicatie van een pathway-specifiek effect. **7b-BF4** veroorzaakt een sterke afname van de intracellulaire ATP-concentratie in *B. subtilis*, wat waarschijnlijk de reden is dat de vier metabole routes worden beïnvloed. Ontwikkeling van resistentie tegen **7b-BF4** werd gestimuleerd door in het lab groeiende *B. subtilis* bij sub-letale concentraties van de verbinding gedurende een langere tijdsperiode te kweken, er werd echter geen ontwikkeling van resistentie gedetecteerd.

De resultaten die in dit hoofdstuk zijn verkregen, hebben aangetoond dat **7b-BF4** een sterk antimicrobieel middel tegen Gram-positieve bacteriën is. Hoewel de exacte werkingswijze van deze stof nog onbekend is, geeft ons werk aan dat het anders is dan de werkwijze van andere bekende antibiotica. Onze suggesties voor het verder karakteriseren van de werkingswijze van deze verbinding in de toekomst zijn: RNA-sequencing van cellen onder stress veroorzaakt door de verbinding; elektronenmicroscopie van cellen in de aanwezigheid van de verbinding, omdat de verbinding goud bevat, zou het mogelijk moeten zijn de lokalisatie in de cel ervan te detecteren; en verdere stimulatie van resistente mutanten gevolgd door genomische analyses van gedetecteerde mutanten.

Het tweede experimentele rapport van dit proefschrift (**Hoofdstuk 3**) presenteert een onderzoek naar de werkingswijze van de chalconen **BC1** en **T9A**. Deze chalconen werden gesynthetiseerd door onze medewerkers in Brazilië, die een bijzondere interesse hebben in het bestrijden van de Gram-negatieve bacterie *Xanthomonas citri* subsp. *citri* (Xac), de biologische agens die citruskanker veroorzaakt (Ayusso et al., in voorbereiding). Bijna alle citrus soorten zijn gevoelig voor citruskanker en er zijn geen effectieve manieren om Xac uit een geïnfecteerde plant te verwijderen, waardoor geïnfecteerde bomen gerooid moeten worden (18). Brazilië is de grootste sinaasappel producent ter wereld en de sinasappel industrie ondervind schade door citruskanker (19). Natuurlijk voorkomende chalconen zijn gewoonlijk niet actief tegen Gram-negatieve bacteriën (20, 21), maar deze verbindingen kunnen chemisch worden gemodificeerd om toch actief te worden tegen Gram-negatieve bacterien (22, 23). Verbinding **T9A** was het resultaat van een screening door onze collega's, die chalchonen met gesubstitueerde hydroxylgroepen (hydroxychalconen) synthetiseerden (Ayusso et al., In voorbereiding). Verbinding **T9A** werd geselecteerd voor deze studie omdat het de meest actieve verbinding in die screening was (Ayusso et al., In voorbereiding). Verbinding BC1 is een methoxychalcon verkregen uit de moleculaire versimpeling van curcumine (24).

Het effect van de verbindingen **BC1** en **T9A** op de membraanpermeabiliteit van *Bacillus subtilis* en Xac werd wederom getest met behulp van een combinatie van de membraanpermeabele en membraanondoorlaatbare kleurstoffen. Verbinding **T9A** verstoord de membraanpermeabiliteit niet in *B. subtilis* en Xac, terwijl verbinding **BC1** *B. subtilis*-membranen wel verstoort en Xac-membranen niet verstoort. Het effect van de verbindingen **BC1** en **T9A** op vier belangrijke metabole routes (DNA, RNA-, eiwit- en peptidoglycan-synthese) in *B. subtilis* en Xac, waarbij dezelfde ^{3}H gelabelde metabole precursors worden gebruikt. Dit hoofdstuk is, voor zover ons bekend, het eerste rapport van metabole route-assays op Xac. We hebben ook het effect van de verbindingen **BC1** en **T9A** op de intracellulaire ATP-concentratie in *B. subtilis* en Xac getest. Vergelijkbaar met wat in hoofdstuk 2 werd waargenomen, hadden de chalconen invloed op alle vier de macromoleculaire metabole routes. De ATP-concentratie werd echter niet beïnvloed door de verbindingen in *B. subtilis* en er werd weinig effect waargenomen in Xac. Fourier-transform infrarood (FT-IR) spectrofotometrie van met chalconen behandelde B. subtilis liet membraanverstoring zien door **BC1**, maar gaf geen doorslaggevend resultaat voor **T9A**. FT IR was niet succesvol in Xac omdat Xac xanthaangom bevat en biofilms maakt wat leidt tot een moeilijk te interpreteren FTIR spectrum.

De gegevens die in dit hoofdstuk worden geproduceerd, laten ons niet toe een conclusie te trekken over een specifieke werkingswijze van de geteste verbindingen. We waren echter wel in staat om Xac-stammen te genereren met resistentie tegen de verbindingen **T9A** en **BC1**, wat de mogelijkheid opent om genomische sequentie analyses uit te voeren om de werkingswijze van deze verbindingen te achterhalen.

Dit hoofdstuk wordt gevolgd door een appendix waarin onze resultaten van de werkingswijze van alkylgalaten tegen Xac worden vermeld. Alkylgalaten hebben activiteit tegen Xac, doden cellen in het laboratorium en voorkomen infectie op citrusbladeren (*25*). De antimicrobiële activiteit van alkylgalaten werd gekarakteriseerd in *B. subtilis,* omdat op dat moment FtsZ van Xac nog niet was gezuiverd en membraanpermeabiliteitsassays nog niet ontwikkeld waren voor Xac (*26*). Deze appendix bevat mijn bijdragen aan het werk van onze groep over de

karakterisering van de antimicrobiële activiteit van alkylgalaten tegen Xac (*27*).

Het laatste experimentele hoofdstuk van dit proefschrift (**Hoofdstuk 4**) richt zich op de celbiologie van Xac. In dit hoofdstuk ontwikkelden we een stam van Xac zonder het *minC*-gen Dit gen codeert voor het MinC-eiwit, onderdeel van het Min-systeem dat in Xac (evenals in de grondig bestudeerde bacterie *Escherichia coli*) bestaat uit de MinC-, MinD- en MinE-eiwitten (*28*). Dit systeem is verantwoordelijk voor de ruimtelijke regulatie van celdeling, ervoor zorgend dat dit gebeurt in het midden van de staafvormige cel en niet op een willekeurige plaats (bijvoorbeeld bij de celpolen). In *E. coli* is dit mogelijk omdat MinC een complex vormt met MinD, waardoor wordt voorkomen dat de Z-ring zich in de nabijheid daarvan assembleert. MinE-activiteit zorgt ervoor dat het MinCD-complex tussen de uiteinden van de cel oscilleert, met als gevolg dat de MinCD concentratie in het midden van de cel het laagst is en de Z-ring in het midden van de cel wordt gevormd (*29*).

We onderzochten celdeling, chromosoomsegregatie en incorporatie van peptidoglycaan in wild-type en Δ*minC*-mutanten. Het *minC*-gen werd verwijderd met behulp van allel-uitwisseling. Xac zonder het *minC*-gen vertoonde minicellen, korte filamentatie en vertakking. Het minC-gen werd gecomplementeerd door *gfp-minC* te integreren in de *amy*-locus. De gecomplementeerde Xac stammen vertoonden een wildtype fenotype. Bovendien oscilleerde GFP-MinC van pool tot pool, vergelijkbaar met MinCD-oscillaties waargenomen in *E.coli* en meer recentelijk in *Synechococcus elongatus* (*30*) en *Vibrio cholerae* (*31*). Hierdoor lijkt oscillerend MinC gekoppeld te zijn aan aanwezigheid van het *minE*-gen. Verder onderzoek van het vertakkende fenotype onthulde dat in de vertakkingscellen de nucleoïdeorganisatie, de vorming van divisomen en de incorporatie van peptidoglycanen waren verstoord, en dat de synthese van peptidoglycaan was losgekoppeld van divisoomvorming in vertakte cellen. Het vertakkingsfenotype was ook voedingsstof afhankelijk en werd niet gezien in medium dat pepton bevatte.

Met dit proefschrift hebben we geprobeerd nieuwe mogelijkheden te openen voor het bestuderen van zowel de celbiologie van Xac als de

werkingswijze van antimicrobiële verbindingen. De radiolabelassays om specifieke metabole routes te testen, fluorescentieassays voor het testen van membraanpermeabiliteit, membraanpotentiaal en peptidoglycaan-opname, fluorescente eiwitfusies met ZapA-, MinC- en ParB- en FtsZ-assays die in dit proefschrift worden gebruikt, vormen een prima aanvulling op een gereedschapskist die is ingesteld op het testen van nieuwe antimicrobiële stoffen met de potentie voor de bestrijding van citruskanker en andere infecties. Genomische analyses van resistente mutanten en RNA-sequencing van cellen die zijn behandeld met antimicrobiele verbindingen zijn mogelijk nodig om onze toolset uit te breiden en om de werkingswijze van die antimicrobiële verbindingen in meer detail vast te stellen.

References

1. R. Sender, S. Fuchs, R. Milo, Revised estimates for the number of human and bacteria cells in the body. *PLoS biology* **14**, e1002533 (2016).
2. P. M. Vitousek *et al.*, in *The Nitrogen Cycle at Regional to Global Scales*. (Springer, 2002), pp. 1–45.
3. T. Ishige, K. Honda, S. Shimizu, Whole organism biocatalysis. *Current opinion in chemical biology* **9**, 174–180 (2005).
4. M. McFall-Ngai, Adaptive immunity: care for the community. *Nature* **445**, 153 (2007).
5. D. Acemoglu, S. Johnson, Disease and development: the effect of life expectancy on economic growth. *Journal of political Economy* **115**, 925–985 (2007).
6. M. Barber, M. Rozwadowska-Dowzenko, Infection by penicillin-resistant staphylococci. *The Lancet* **252**, 641–644 (1948).
7. R. Kolter, G. P. van Wezel, Goodbye to brute force in antibiotic discovery. *Nat Microbiol* **1**, 15020 (2016).
8. M. E. de Kraker, A. J. Stewardson, S. Harbarth, Will 10 million people die a year due to antimicrobial resistance by 2050? *PLoS medicine* **13**, e1002184 (2016).
9. J. Taylor, C. Dudley, Seed treatment for the control of halo-blight of beans (Pseudomonas phaseolicola). *Annals of Applied Biology* **85**, 223–232 (1977).
10. J. Taylor, K. PHELPS, C. Dudley, Epidemiology and strategy for the control of halo-blight of beans. *Annals of Applied Biology* **93**, 167–172 (1979).
11. K. S. Park, Y. T. Kim, H. S. Kim, J. S. Cha, K. H. Park, Selection of the antibacterial agents for control against Pseudomonas syringae pv. syringae causing leaf spot disease on green pumpkin (Cucurbita moschata). *The Korean Journal of Pesticide Science* **19**, 119–124 (2015).
12. J. Loper *et al.*, Evaluation of streptomycin, oxytetracycline, and copper resistance of Erwinia amylovora isolated from pear orchards in Washington State. *Plant disease* **75**, 287–290 (1991).
13. S. S. Gnanamanickam, Biological control of bacterial blight of rice. *Biological control of rice diseases*, 67–78 (2009).
14. F. Behlau, B. I. Canteros, G. V. Minsavage, J. B. Jones, J. H. Graham, Molecular Characterization of Copper Resistance Genes from Xanthomonas citri subsp. citri and Xanthomonas alfalfae subsp. citrumelonis. *Applied and Environmental Microbiology* **77**, 4089–4096 (2011).
15. C. L. Ventola, The antibiotic resistance crisis: part 1: causes and threats. *Pharmacy and Therapeutics* **40**, 277 (2015).
16. G. M. Rossolini, F. Arena, P. Pecile, S. Pollini, Update on the antibiotic resistance crisis. *Current opinion in pharmacology* **18**, 56–60 (2014).
17. S. B. Singh, J. F. Barrett, Empirical antibacterial drug discovery—foundation in natural products. *Biochemical pharmacology* **71**, 1006–1015 (2006).
18. T. R. Gottwald, J. H. Graham, T. S. Schubert, Citrus canker: the pathogen and its impact. *Plant Health Progress* **10**, (2002).
19. M. F. Neves, V. G. Trombin, F. F. Lopes, R. Kalaki, P. Milan, in *The orange juice business*. (Wageningen Academic Publishers, 2012), pp. 23–24.
20. R.-I. Tsukiyama, H. Katsura, N. Tokuriki, M. J. A. a. a. c. Kobayashi, Antibacterial activity of licochalcone A against spore-forming bacteria. **46**, 1226–1230 (2002).
21. H. Haraguchi, K. Tanimoto, Y. Tamura, K. Mizutani, T. J. P. Kinoshita, Mode of antibacterial action of retrochalcones from Glycyrrhiza inflata. **48**, 125–129 (1998).
22. A.-M. Katsori, D. J. E. o. o. t. p. Hadjipavlou-Litina, Recent progress in therapeutic applications of chalcones. **21**, 1575–1596 (2011).
23. S. F. Nielsen, M. Larsen, T. Boesen, K. Schønning, H. J. J. o. m. c. Kromann, Cationic chalcone antibiotics. Design, synthesis, and mechanism of action. **48**, 2667–2677 (2005).
24. L. G. Morão *et al.*, A simplified curcumin targets the membrane of Bacillus subtilis. *MicrobiologyOpen*, e00683 (2018).
25. I. C. Silva *et al.*, Antibacterial activity of alkyl gallates against Xanthomonas citri subsp. citri. *Journal of Bacteriology* **195**, 85–94 (2013).
26. E. Król *et al.*, Antibacterial activity of alkyl gallates is a combination of direct targeting of FtsZ and permeabilization of bacterial membranes. *Frontiers in Microbiology* **6**, (2015).
27. M. M. Kopacz, A. S. Lorenzoni, C. R. Polaquini, L. O. Regasini, D. J. J. M. Scheffers, Purification and characterization of FtsZ from the citrus canker pathogen Xanthomonas citri subsp. citri. e00706 (2018).
28. A. S. Lorenzoni, G. C. Dantas, T. Bergsma, H. Ferreira, D.-J. Scheffers, Xanthomonas citri MinC Oscillates from Pole to Pole to Ensure Proper Cell Division and Shape. *Frontiers in microbiology* **8**, 1352 (2017).
29. V. W. Rowlett, W. Margolin, The bacterial Min system. *Current Biology* **23**, R553-R556 (2013).
30. J. S. MacCready, J. Schossau, K. W. Osteryoung, D. C. Ducat, Robust Min-system oscillation in the presence of internal photosynthetic membranes in cyanobacteria. *Molecular Microbiology*, (2016).
31. E. Galli *et al.*, Cell division licensing in the multi-chromosomal Vibrio cholerae bacterium. *Nature microbiology* **1**, 16094–16094 (2016).

Acknowledgments

DJ, thanks for all the help and time you dedicated to the completion of my thesis, especially when I needed it the most. Arnold, thanks for being the head of this amazing group where I met a lot of nice people.

Ewa, thanks for helping me on my first steps with my PhD. Abigail, it was good to have your company in the MLII lab. Danae, you were very helpful as a colleague especially when it came to microscope and image analysis. Ana, it was nice to have you around (especially finding chocolates and notes in my mailbox). Menno, Erik, and Aleksandra, it was nice to have you in the cell division group. Tessa, you were the best student I had during my PhD, thanks for the work in the lab. Yvonne, it was nice to cycle and explore the Dutch countryside with you. Fernando, thank you for bringing cookies and making funny jokes, you are a nice colleague even though you are brown. Cyrus, I enjoyed your company for playing volleyball, boxing, kayaking, and chitchatting. Ahsen, Amalina, Anarita, Carsten, Ciprian, Fabiola, Hyun Yong, Irfan, Max, Min, Sasha, and Reto, Adriaan, Anna, Ciska, and Ina, it was nice to meet you in Groningen. Anmara, Bea, Jeroen, Janny, and Greetje thanks for keeping the lab running.

A special thanks to my closest friends in Groningen, László, Marten, Niels & Paula, Riccardo, Sabrina, and Zsofi we are almost like a little family. Your company was very pleasant, but I also know that I can count on you in difficult moments. Our trips together will be always part of my best memories. I hope to see you again as often as possible in the future. Niels dank je wel voor de samenvatting.

Riccardo, my best friend in Groningen, it was amazing to have you around. We had a lot of nice memories, Kos, Berlin, and specially our trip to Italy. It was a refreshing break from the dark Groninger winter. Your family was very welcoming and made me feel at home in a moment that I missed so much. I was also going to mention the Toyota Hiace, but that is just a small toy compared to our last trip with the Volkswagen Crafter.

Parichita and Lúcia, it is motivating to know that the work from this thesis is going to be useful in your PhDs, and I thank you for that. I wish you a lot of success continuing this line of research.

Lovaine, foi muito bom saber que você continuou meu projeto de mestrado, repassar o conhecimento adquirido é gratificante.

Plinho, você foi um excelente orientador de mestrado. Obrigado por enviar a carta de recomendação para o DJ, mesmo querendo que eu fizesse doutorado no seu laboratório.

Manu, eu gostei muito que vieste nos visitar.

Zeide e Deda vocês são exemplos pra mim desde pequeno. Mesmo morando longe a influência de vocês faz parte desta tese. Estendo estes sentimentos a minha mãe e ao resto da minha família. Flávio e Vera, a presença de vocês facilitou muito a mudança de continente. Saber que a qualquer hora eu seria recebido na casa de vocês com a cama arrumada e comida gostosa é um conforto inestimável.

Stephanie, I wouldn't have made it so far without you, your input and example was really helpful for finishing this thesis. In the hardest moments of my PhD I almost regretted moving to Groningen. However, you were here to cheer me up and change my life forever. You contributed to my life in so many ways that is impossible to list half of them, but most importantly you helped me to make friends and be a better person.

Acknowledgments

A